541
S
14.GS:
CIR 541
c.2
Geol Survey

TRENCH COVERS TO MINIMIZE INFILTRATION AT WASTE DISPOSAL SITES

K. Cartwright
T. H. Larson
B. L. Herzog
T. M. Johnson
K. A. Albrecht
D. L. Moffett
D. A. Keefer
C. J. Stohr

LIBRARY
NOV 22 1989
IL STATE GEOLOGICAL SURVEY

Circular 541, 1988

(Prepared for U.S. Nuclear Regulatory Commission)
Department of Energy and Natural Resources
ILLINOIS STATE GEOLOGICAL SURVEY

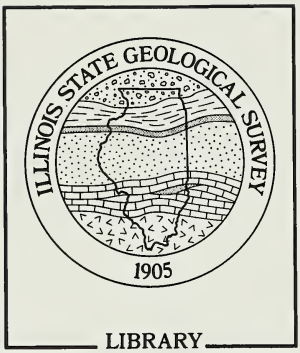

Graphic Artist: Barbara Stiff

ed by authority of the State of Illinois/1989/1200

ILLINOIS STATE GEOLOGICAL SURVEY
3 3051 00002 8583

TRENCH COVERS TO MINIMIZE INFILTRATION AT WASTE DISPOSAL SITES

K. Cartwright
T. H. Larson
B. L. Herzog
T. M. Johnson
K. A. Albrecht
D. L. Moffett
D. A. Keefer
C. J. Stohr

ILLINOIS STATE GEOLOGICAL SURVEY
Morris W. Leighton, Chief

Natural Resources Building
615 East Peabody Drive
Champaign, Illinois 61820

LIBRARY
NOV 22 1989
IL STATE GEOLOGICAL SURVEY

Circular 541, 1988

(Prepared for U.S. Nuclear Regulatory Commission)
Department of Energy and Natural Resources
ILLINOIS STATE GEOLOGICAL SURVEY

Digitized by the Internet Archive
in 2012 with funding from
University of Illinois Urbana-Champaign

http://archive.org/details/trenchcoverstomi541cart

TRENCH COVERS TO MINIMIZE INFILTRATION AT WASTE DISPOSAL SITES

K. Cartwright
T. H. Larson
B. L. Herzog
T. M. Johnson
K. A. Albrecht
D. L. Moffett
D. A. Keefer
C. J. Stohr

ILLINOIS STATE GEOLOGICAL SURVEY
Morris W. Leighton, Chief

Natural Resources Building
615 East Peabody Drive
Champaign, Illinois 61820

Circular 541, 1988

(Prepared for U.S. Nuclear Regulatory Commission)
Department of Energy and Natural Resources
ILLINOIS STATE GEOLOGICAL SURVEY

CONTENTS

ACKNOWLEDGMENTS AND FOREWORD vi
ABSTRACT 1
INTRODUCTION 1
Current Trench Cover Designs 2
Infiltration-Limiting Covers 4
Artificial Materials 5
Clay Seals 5
Layered Cover Designs 6
EVALUATION OF GEOLOGIC MATERIALS
IN EXPERIMENTAL COVER DESIGNS 9
Selection of Materials 9
Physical Properties of Materials 9
Particle Size 9
Clay Mineralogy 10
Engineering Properties of Materials 10
Classification 10
Moisture-Density Relationships 10
Dispersion Tests 10
Hydrologic Properties 11
Saturated Hydraulic Conductivity 11
Volumetric Moisture Content/Capillary Pressure Relationship 11
Unsaturated Hydraulic Conductivity 11
MATHEMATICAL MODELING OF MOISTURE MOVEMENT
THROUGH TRENCH COVERS 16
Basic Equations of Mathematical Models 16
Results of Simulations using MOMOLS 17
Results of Simulations using UNSAT2 18
Influence of Boundary Conditions 22
Simulation of Laboratory Column-Scale Experiments 22
Field-Scale Simulations 29
COLUMN STUDIES 37
Column Preparation 37
Results 39
Conclusions 41
CONSTRUCTION OF FIELD-SCALE EXPERIMENTAL
TRENCH COVERS 44
Designs 44
Site and Material Selection 44
Lower Layers 44
Upper Layers 45
Construction History 47
Preliminary Work 47
Placement of Lower Layers 47
Placement of Upper Layers 48
Seeding 49
Soil Compaction Performance 49
FIELD MONITORING OF EXPERIMENTAL PROTOTYPE COVERS 50
Phase One: July-November, 1983 50
Instrumentation 50
Results of Field Monitoring 52
Phase Two: May 1984-June 1986 55
Instrumentation 55
Volumetric Moisture Content 56
Gravimetric Moisture Content 56
Soil Tensions 60
Soil Temperatures 78
CONCLUSIONS 81
REFERENCES 82
APPENDIX: TENSIOMETRY 87

FIGURES

1	Locations of major low-level radioactive waste disposal sites in the United States	2
2	Design of an infiltration-limiting cover	4
3	Conceptual design of a completed low-level radioactive waste-disposal trench	6
4	Basic geologic environment for waste containers	7
5	Schematic diagram showing a wick layer around a burial trench	8
6	Particle-size analysis for soils	9
7,8	Results of compaction and saturated hydraulic conductivity tests	12
9	Soil-moisture retention curves for Peoria Loess, Fairgrange Till, and silty sand	12
10	Soil-moisture retention curves for Fairgrange Till using the pressure membrane extractor	12
11	Soil-moisture retention curves for samples from the experimental trench covers at the Sheffield study site	13
12	Primary wetting curves for soils used in MOMOLS	14
13	Hydraulic conductivity functions for soils used in MOMOLS	14
14	Hydraulic conductivity functions for soils used in UNSAT2 simulations	15
15	Hydraulic conductivity functions for soils taken from the experimental trench covers at the Sheffield study site	15
16	Total moisture entry into compacted Peoria Loess	18
17	Predicted advance of wetting front in compacted Peoria Loess	19
18	Redistribution after 4 hours of simulated rainfall in Peoria Loess	19
19	Predicted moisture redistribution in a 30-cm layer of Peoria Loess	20
20	Effect of coarse-grained gravel layer on moisture retention compared to moisture movement through a single layer of fine-grained material	20
21	Effect of medium sand layer on moisture retention compared to moisture movement through a single layer of fine-grained material	21
22	Influence of hydraulic conductivity ratio on storage efficiency	21
23	Cross section of simulated gamma column with superimposed finite element network	23
24,25	Predicted distribution of pressure head at selected times for Case 1 simulations	24
26	Predicted change in pressure head with time at various depths for Case 1 simulations	24
27,28	Predicted distribution of pressure head at a selected time for Case 2 simulations	25
29	Predicted change in pressure head with time for various depths for Case 2 simulations	26
30,31	Predicted distribution of pressure head and water content at selected times for Case 3 simulations	26
32	Predicted change in pressure head with time for various depths for Case 3 simulations	27
33,34	Predicted distribution of pressure head at selected times for Case 4 simulations	27
35	Predicted change in pressure head with time for various depths for Case 4 simulations	28
36,37	Predicted distribution of pressure head at selected times for Case 5 simulations	28
38	Predicted change in pressure head with time for various depths for Case 5 simulations	29
39	Cross section of hypothetical field-scale cover design	30
40	Cross section of one-half of symmetrical simulated field-scale cover with superimposed finite element network	30
41,42	Predicted distribution of pressure head and water content (Case 1)	31
43	Predicted distribution of pressure head at selected times (Case 2)	32
44,45	Predicted distribution of pressure head and water content at selected times (Case 2)	32
46	Initial distribution of total hydraulic head (Case 2)	33
47	Predicted distribution of hydraulic head after 162.5 hours (Case 2)	33
48	Predicted distribution of pressure head at selected times (Case 3)	33
49	Predicted distribution of hydraulic head after 382 hours (Case 2)	34
50	Predicted distribution of hydraulic head after 13.9 hours (Case 3)	34
51	Predicted distribution of pressure head at selected times (Case 4)	35
52	Predicted distribution of soil-water content at selected times (Case 4)	35
53,54	Predicted distribution of hydraulic head after 171 hours and 289 hours (Case 4)	36
55	Predicted changes in pressure head with time at selected positions (Case 4)	36

56	Diagram of gamma column used to determine moisture content and bulk density	39
57,58	Change in moisture content with time in laboratory soil column 1-A	40
59	Change in moisture content with time in laboratory soil column 1-C	42
60	Change in moisture content with time in laboratory soil column 1-D	42
61	Change in moisture content with time in laboratory soil column 3	43
62	Change in moisture content with time in laboratory soil column 4	43
63	Location of Sheffield study site	44
64a.	Plan view of experimental trench covers at the Sheffield study site	46
64b	Cross sections of the experimental trench covers at the Sheffield study site	46
65	Schematic diagram of tensiometer nest used in the Phase 1 monitoring program	50
66	Daily rainfall for July - November, 1983	52
67	Tensiometer readings for July 19 through November 16, 1983	53
68	Tensiometer readings plotted as moisture content	54
69	Cross-section of cover 1 depicting Phase 2 tensiometers and neutron-probe access tube	57
70	Cross-section of cover 2 depicting Phase 2 tensiometers and neutron-probe access tube	57
71	Cross-section of cover 3 depicting Phase 2 tensiometers and neutron-probe access tube	58
72	Cross-section of cover 4 depicting Phase 2 tensiometers and neutron-probe access tube	58
73	Volumetric moisture content within the experimental covers in 1984 and 1985	59
74	Mass wetness of samples from three covers collected in August 1984	60
75	Total head for 6 days during autumn, 1985	62
76	Volumetric moisture content on 6 days during autumn, 1985	63
77	Total head for 6 days during winter 1986	66
78	Volumetric moisture content on 6 days during winter 1986	67
79	Total head on 6 days during spring 1986	69
80	Volumetric moisture content for 6 days during spring 1986	70
81	Percent saturation for November 9 through December 9, 1986	72
82	Rate of moisture movement into the lower layers of covers 1, 2, and 3 for the period November 9 through December 9, 1985	73
83	Moisture content for the period May 10 through May 29, 1986	75
84	Moisture content for the period May 10 through May 29, 1986	77
85	Average daily soil temperatures are plotted for 6 days during winter 1986	79
86	Average daily soil temperatures and average daily air temperature for the period May 10 through May 29, 1986.	80
87	Original tensiometer design using ⅞-inch ceramic cup and rigid ½-inch plastic pipe	86
88	Modified tensiometer design utilizing small ceramic cup and 1/16-inch tubing	86
89	Final tensiometer design features intermediate-sized ceramic cups and nylon tubing	88

TABLES

1	Characteristics of current trench covers in the United States	3
2	Procedures used in tests of soils	10
3	Summary of physical properties of materials used in laboratory experiments	11
4	Absorption coefficients	37
5	Moisture content and density of samples taken of laboratory columns	38
6	Moisture and time measurements in laboratory columns	41
7	Characteristics of materials used in experimental trench covers	45
8	Characteristics of Typar(R) polypropylene filter fabric	45
9	Water content and degree of compaction of each trench cover	48
10	Phase 1 tensiometer installation data	51
11	Rainfall near Sheffield, Illinois during Autumn 1985	61
12	Precipitation near Sheffield, Illinois during Winter, 1986	65
13	Total monthly rainfall near Sheffield, Illinois during Spring, 1986	68
14	Average rate of moisture movement across coarse grained-fine grained interface	74
15	Performance ranking of experimental trench covers	81

FOREWORD

This report was prepared as an account of work sponsored by the U.S. Nuclear Regulatory Commission (U.S. NRC), an agency of the United States Government, under grant no. FIN B6965. This report was completed in the fall of 1986 and originally published by the U.S. NRC in the winter of 1987. No major technical changes have been made to this edition of the report, although modifications in presentation were necessary to meet the standards for an Illinois State Geological Survey Circular. Furthermore, units of measure and technical terminology have been made consistent throughout the text and figures. The modifications did not influence data interpretation.

ACKNOWLEDGMENTS

We are grateful to James A. Shaffner, Project Officer for the Nuclear Regulatory Commission, who gave us guidance and support during this study; to Henry J. H. Harris, who designed the gamma-ray attenuation unit and provided instruction in its use; to Walter J. Morse, Anthony G. Devine, Stephen J. Klein, Wen-June Su, Paul B. DuMontelle, Leon R. Follmer and others who conducted field and laboratory tests to determine the properties of the materials; and to Richard W. Healy, M. Peter deVries, and others of the U.S. Geological Survey for their advice and assistance during the field monitoring phase of this study. Special thanks are due to Edna Yeargin and Linda Cunningham for their assistance in preparing this manuscript. The computer program MOMOLS was developed by Stuart A. Rojstaczer as part of the original research of this project.

We dedicate this volume to David Lee Moffett (1959-1986), who was a key member of our monitoring team, having designed and installed most of the field instrumentation (Appendix). The ultimate success of this project is due largely to David's expertise, inventiveness and energy.

ABSTRACT

We have investigated methods to limit infiltration through trench covers by reviewing current practices, testing geologic materials, simulating selected cover designs, and designing, constructing, and monitoring four field-scale experimental covers. We conclude that multi-layered soil covers are superior to single-layered covers. Laboratory and computer simulations indicate that a wick effect can be established by placing a fine-grained layer over a coarse-grained layer, thereby delaying and possibly reducing moisture infiltration through the entire cover. Field experiments indicate that the wick effect does occur under certain circumstances; but a potentially more important feature of the layered cover design is the ability of the coarse-grained layer to remove moisture from the system through drain tiles.

INTRODUCTION

The United States has 11 major shallow land burial sites for low-level radioactive wastes (fig. 1). Five are operated by the U.S. Department of Energy (DOE) and six are commercial sites. Of these, two DOE and four commercial sites are located in the humid eastern part of the country (fig. 1); tritium migration has been observed at all six eastern sites. The probable cause of migration is infiltration of precipitation through trench covers (Battelle, 1976). The reduction of infiltration at low-level radioactive waste disposal sites appears essential to proper management in humid regions.

The trench covers at sites in the humid eastern part of the United States have not prevented tritium migration. In addition, migration of other radionuclides has been reported at the West Valley, Maxey Flats, and Oak Ridge sites (Battelle, 1976). Barnwell was the last humid site to report tritium migration, which only occurred beneath the trenches. It is one of two sites using compacted clay for trench covers and has the thickest covers of any of the six sites.

The reported cases of radionuclide movement have been attributed to excess percolation of precipitation through the trench covers. Commonly, the trench cover and the waste-filled trench are more permeable than the original materials into which the trenches were excavated. Consequently, despite compaction efforts, water can accumulate in the trenches. This phenomenon has been called the "bathtub effect." Even where water does not accumulate in the trenches, it provides a mechanism for transport of radionuclides. Such has occurred at Oak Ridge (Duguid, 1976) and at Maxey Flats (Meyer and O'Connell, 1973). In addition, trenches can become so full that contaminated water seeps over the top, as has occurred at West Valley (Kelleher, 1979). Erosion of trench covers can contribute to such problems.

Because of the failure of present cover practices to prevent radionuclide migration into groundwater at low-level radioactive waste disposal sites, Murphy and Holter (1980) concluded that "effective management of surface water, through the application of improved capping techniques and surface water diversion, is a major factor in determining the success of operators in preventing water infiltration into burial trenches." Recognizing this problem, the federal government now requires that "covers must be designed to minimize, to the extent practicable, water infiltration, to direct percolating or surface water away from the disposed waste, and to resist degradation by surface geologic processes and biotic activity" (10CFR, part 61, sec 51).

Our research specifically investigates the need to minimize infiltration through trench covers. This document constitutes the final report for the research project: A Study of Trench Covers to Minimize Infiltration at Waste Disposal Sites. The objectives of this program were (1) to provide basic information on the characteristics of materials that might be used in construction of waste trench covers, (2) to study the interaction of these materials which will limit water from precipitation infiltrating through the wastes, and (3) to test under field conditions the most promising trench cover designs. In order to provide an overall perspective on this research, we have summarized the results of Task I—A Review of Present Practices and Annotated Bibliography (Herzog et al., 1982), and Task II—Laboratory Evaluation and Computer Modeling of Trench Cover Designs (Johnson et al., 1983). On the basis of these results, we designed and constructed four field-scale prototype trench covers.

Results of an extensive literature review (Herzog et al., 1982) are summarized in the first section of this report. The discussion of layered cover designs is of particular importance because it is the basis for our subsequent studies of layered systems.

Materials testing proceeded in three phases: generic cover materials, specific materials available in the vicinity of the field site, and samples collected from the prototype trench covers. Results of basic tests as well as some properties derived from them are summarized in the section, Evaluation of Geologic Materials.

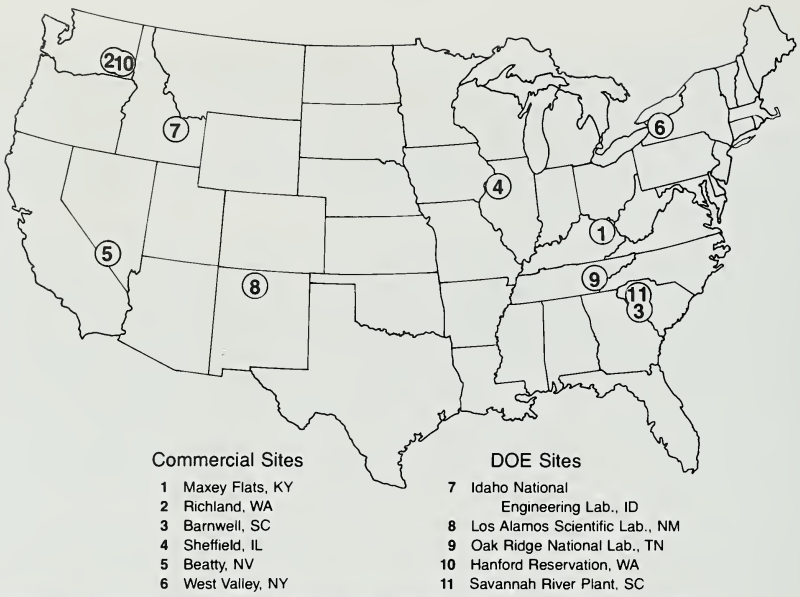

Figure 1 Locations of major low-level radioactive waste disposal sites in the United States.

Computer and laboratory modeling of layered systems described in the sections, Mathematical Modeling and Column Studies, are discussed in more detail by Johnson et al. (1983). Field-scale designs (Construction of Trench Covers section) were based on the results of the modeling studies, but do not duplicate the modeled conditions. Knowledge acquired in all phases of the investigation was used in the designs. The basic layered-system concept was shown by the modeling to be workable; however, results of materials testing and conclusions of the modeling led us to choose different materials for the field experiment. The final designs also included drains within the coarse-grained layers, a feature derived from our literature review (Dragonette et al., 1979).

The Field Monitoring section and the Appendix provide descriptions and a preliminary analysis of our experimental cover monitoring program. Data are presented in various forms to provide both an overview of long-term cover response as well as detailed analysis of specific events. Based on our field experience, we present conclusions concerning the effectiveness of layered designs of trench covers.

Current Trench Cover Designs

Trench covers at all of the existing sites have basically the same design: material is excavated from the trenches, mounded to a minimum depth of 1 to 3 meters, then seeded for erosion control. At sites in the humid regions, covers are compacted by heavy earth-moving equipment or by temporarily placing excavated material from other trenches on the mounds. The covers at the Barnwell and Maxey Flats sites and on the more recent trenches at the Sheffield site incorporate clay obtained from local sources.

Table 1 summarizes the characteristics of trench covers at the major low-level waste disposal sites.

A literature search was made for information about low-level waste-disposal sites outside the United States. Few documents were located, and those that were indicate that, outside the United States, shallow land burial is not often used because of the shortage of land. The one exception

is Canada, where five sites currently hold significant amounts of low-level waste: the Whiteshell Nuclear Waste Establishment in southeastern Manitoba, the Chalk River Nuclear Laboratories in east-central Ontario, the Bruce Nuclear Power Development in southwestern Ontario, the Gentilly Nuclear Power Development in southern Quebec, and a refinery of Eldorado Nuclear Limited on the north shore of Lake Ontario (Cherry et al., 1979). At Whiteshell, burial trenches are covered with compacted, excavated fill composed mainly of clay and till (Cherry et al., 1973). No descriptions of the trench covers at the other sites were found.

Table 1. Characteristics of current trench covers in the United States[a]

Site	Type of final cover	Thickness of final cover
Barnwell, South Carolina	0.6 m clay between waste and ground surface; additional mounded cover	3 m cover at center line; 1.5 m at trench edge
Beatty, Nevada	Excavated earth fill; no compaction; stones on top	Minimum 2 m total; mounded 0.6 m above grade
Maxey Flats, Kentucky	1 m compacted clay; mounded; reseeded	1 m cover; mounded 0.6 m above grade
Richland, Washington	Excavated earth fill; no compaction	Minimum 2 m total; mounded 1 m above grade
Sheffield, Illinois	Compacted clay cover; surface reseeded	Minimum of 1 m final cover; mounded
West Valley, New York	Excavated earth fill (re-worked till)[b]; compacted topsoil added	Minimum of 3 m cover; mounded 1.5 m minimum above grade
Hanford, Washington	Excavated fill of gravel, fine sand and silt to surface[c]; mounded as necessary	Minimum 2.5 m total, or that needed to reduce dose to less than 1 mR/hr at surface
Idaho National Engineering Lab, Idaho	Excavated soil fill; reseeded	Minimum 1 m to ground surface
Los Alamos Scientific Lab, New Mexico	Excavated tuff and soil fill[d]; compacted by heavy earth-moving equipment	Minimum 1.5 m total cover with mounding to 0.5-1 m above grade
Oak Ridge National Lab, Tennessee	Excavated material to ground surface; few experimentally sealed[e]; reseeded	Minimum 1 m to ground surface
Savannah River Plant, South Carolina	Excavated fill to ground surface; mounded as necessary	Minimum of 1.2 m cover, or that needed to reduce dose to less than 6 mR/hr at surface

[a]adapted from table 24-5, Battelle, 1976.
[b]from Prudic and Randall, 1979.
[c]from Barraclough et al., 1979.
[d]from National Research Council, 1976.
[e]experimental seals were a mixture of soil and bentonite (Webster 1979).

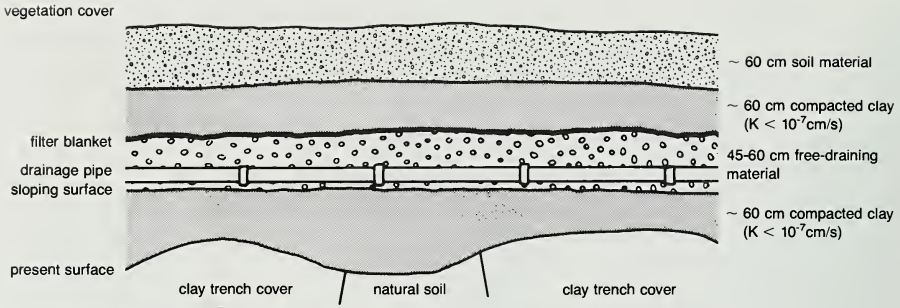

Figure 2 Design of an infiltration-limiting cover (after Dragonette et al., 1979).

Infiltration-Limiting Covers

Many factors affect the performance of a cover. The most important is the choice of material. Two general types of infiltration-limiting covers have been proposed (Herzog et al., 1982): covers of manufactured materials such as concrete, asphalt, and plastic membranes, and covers composed of natural materials such as clay barriers or layered soils. Increasing the thickness of existing covers has also been suggested; however, this may not sufficiently limit infiltration in humid regions (Lutton et al., 1979; Fenn et al., 1975).

Other factors contributing to cover performance include method and degree of compaction, erosion, waste composition, and waste stability. The method and degree of compaction of the cover material influences both the hydraulic conductivity and strength of the final cover (U.S. GAO, 1976; Brunner, 1972; Klein et al., 1982). Erosion of trench covers can also contribute to cover failure. For erosion control, individual trench covers are superior to a single cover over the entire site, as Kelleher determined in a study of the low-level radioactive waste disposal site at West Valley, New York (1979). For the purpose of limiting infiltration, however, a single site cover is thought to be more effective (Dragonette et al., 1979); this is illustrated in figure 2. The slope of the final cover surface has an important effect on surface-water drainage, and as a result, on both erosion and infiltration. In their study of improvements in trench cover practices at low-level radioactive waste disposal sites, SCS Engineers (1978) suggested that the uppermost 1 meter of all trenches should be filled with excavated material and covered with a compacted, sloped mound to reduce infiltration and the effects of waste decomposition and differential settlement. The optimal slope is suggested to be 5 percent.

The U.S. Government Accounting Office (1976) reported that to compact material, it must be no thicker than 90 cm (3 feet). Attempts to compact a thicker sequence produces a hard crust over softer material. Brunner and Keller (1972) state that in sanitary landfills the cover must be compacted in 15 cm (6-inch) layers. Matuszek et al. (1979) suggest that cover specifications should be tailored to the individual site based on the permeability of the cover material and predictions of the amount of waste compaction.

Differential settlement of the waste and overlying of the overlying cover is an unavoidable consequence of current waste-disposal practices. The factors that contribute to settlement include decomposition of degradable wastes, collapse of waste containers, settlement of uncompacted backfill and waste, and piping of backfill and cover material into open voids within the trench. Differential settlement is the most common mechanism of trench cover failure. Design of a trench cover to withstand differential settlement and still function effectively is extremely difficult. Investigations of the ability of various trench-cover designs to resist settlement are currently underway at the University of Arizona (Nowatzki and McGray, 1983). In our investigations, we assume that the waste is stable and differential settlement does not occur.

- **Artificial Materials**

Numerous nonsoil materials can be used to construct an "impermeable" cover (SCS Engineers, 1978; Lutton et al., 1979; Herzog et al., 1982). These materials include concrete or cement, asphaltics, soil cement, and synthetic polymeric membranes. SCS Engineers (1979) compared the advantages, disadvantages, expected longevity, and cost of these alternatives. Most were expensive and all had problems related to climate, chemical degradation, and/or installation.

Relatively few examples exist which utilize such materials in final covers at actual disposal sites. At the Idaho and Hanford sites, concrete and asphalt and plastic membranes are used in storage schemes for transuranic wastes. The wastes are placed on a concrete or asphalt pad and are covered with a membrane and earth to permit easy retrieval. Concrete was used to separate alpha-contaminated wastes from beta-contaminated wastes at Oak Ridge burial grounds 3, 4, and 5 (Oakes and Shank, 1979); this practice has been discontinued. Arora (1980) concluded that the use of rigid barriers, such as concrete, concrete asphalt, soil cement, and metallic sheets is largely precluded by the persistent settlement observed in many trenches.

Plastic membranes have been used at sanitary landfills primarily as a remedial measure for groundwater contamination (Farb, 1978; Tolman et al., 1980). Plastic membranes were installed in 1980 over 8 hectares (20 acres) of the closed Maxey Flats, Kentucky, low-level radioactive waste disposal site to reduce the significant amounts of infiltration and leachate generation that occurred with native clay covers. Preliminary results suggest significant reductions in infiltration at each site. There are no data, however, on the long-term effectiveness of such covers or their ability to withstand differential settlement of the waste.

- **Clay Seals**

Clays currently used in trench covers are generally native soils of low hydraulic conductivity. For a clay cover to be effective, the U.S. EPA (Lutton et al., 1979) has recommended a minimum of 15 cm (6 inches) of clay with a hydraulic conductivity no more than 1×10^{-7} cm/sec. Although Maxey Flats and Barnwell both used clay covers, both have reported tritium migration. SCS Engineers (1978) noted that a plastic liner or soil sealants could be used to enhance a clay cover.

Bentonite, which is primarily montmorillonite clay, is commonly used as a soil sealant in clay liners because of its swelling properties and very low hydraulic conductivity. Most sources that deal with clay barriers suggest that bentonite is superior to other clays. The EPA (1978) reported, however, that kaolinite and illite are superior to montmorillonite for resisting shrink/swell desiccation and cracking. The use of bentonite in soil covers for a radioactive waste disposal site in South Carolina was examined by Hawkins and Horton (1967). Their experiments indicated that a 2.5 cm (1-inch) layer of bentonite overlain by 60 cm (2 feet) of topsoil to protect the bentonite layer during dry periods was sufficient to prevent infiltration. Caution must be taken, however, to prevent growth of deep-rooted plants on covers.

Volclay Soil Labs (1975) suggests that bentonite should be sandwiched between soil layers, at least in sanitary landfills, because contact between the waste and bentonite may cause shrinkage of the clay minerals. This would not cause difficulty at low-level radioactive waste sites, where filling the top meter of the trenches with excavated earth is common practice. A bentonite layer and soil cover could be added over existing trench covers. Das and Dakshinamurti (1975) have shown that the addition of bentonite to a soil can also significantly decrease the infiltration rate. Arora (1980) also claimed that mixing bentonite with water-soluble polyacrylates will increase bentonite's soil-sealing capabilities.

Bentonite covers are not yet in widespread use. The few experimentally sealed trenches at Oak Ridge (table 1) use a thin layer of a native shale and bentonite (Webster, 1979; Arora, 1980). These experimental covers are being assessed for long-term effectiveness as a function of the type of bentonite used, preparation of the substrate, design and control of the sealing operation, and follow-up maintenance.

SCS Engineers (1978) suggest that an effective trench cover design should incorporate a clay or membrane barrier. Their design differs from other clay designs because it incorporates an upper gravel layer to direct water laterally away from the trench (fig. 3). Although this design is not currently in use, a modified design using compacted clay covered by freely draining sand has been approved for use at a sanitary landfill located in an environmentally sensitive site in Florida (Nelson et al., 1980). It will be many years however, before the performance of this cover will be known.

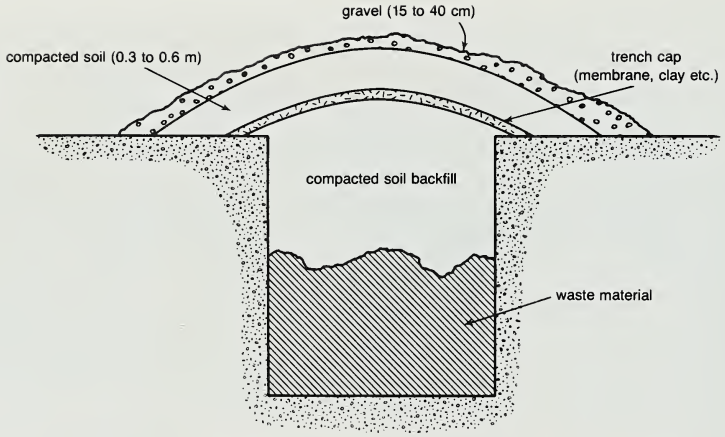

Figure 3 Conceptual design of a completed low-level radioactive waste-disposal trench (after SCS Engineers, 1978).

• Layered Cover Designs

Layered soil covers designed to limit infiltration by retaining water in a fine-grained layer overlying a coarse-textured layer were first proposed by Corey and Horton (1969). They referred to the water retention phenomenon as the "wick effect." Based on the findings of Alway and McDole (1917), Eagleman and Jamison (1962), and others that soil above a sand layer held more water than soil without the sand layer, Corey and Horton proposed that a sloping layer of gravel be used to divert water around burial trenches containing solid radioactive waste. They conducted laboratory experiments and computer simulations to determine the influence of an underlying gravel lens on volumetric moisture content and flow paths.

Their first experiment, which consisted of infiltration through columns of unsaturated sandy loam or sandy clay soil overlying gravel, indicated that the volumetric moisture content of the soil layer increased and that breakthrough into the gravel did not occur until the overlying soil was saturated. Upon rewetting after a period of drainage, the soil layer was found to retain more water than that produced by most precipitation events. In a second experiment, the flow paths of water near a gravel lens were traced with dye in a laboratory model. Flow patterns indicated that a gravel lens diverts water laterally if the overlying soil is unsaturated.

In summary, Corey and Horton showed that an underlying gravel layer can significantly increase the water-retention of the overlying soil and they suggest that "water does not flow through the gravel until the (overlying soil) . . . becomes saturated" (1969, p. 21). They also noted the ability of layered soil to temporarily store increased quantities of infiltration, which must be diverted around the gravel and underlying waste between infiltration events to prevent leaching of the waste. However, in simulations of prolonged infiltration, lateral flow through the soil overlying the sloping gravel layer was not sufficient to prevent the predicted buildup of a saturated zone in a soil overlying even the 2-meter-wide (6.5 ft) sloping barrier. Therefore, they concluded that the lateral distance over which water can be diverted would not be sufficient to protect a sizeable waste container.

In 1977, Frind et al. reexamined the use of the wick effect in the design of waste-storage facilities (fig. 4). They used a transient, saturated-unsaturated, finite-element flow model, much more flexible and sophisticated than the model used by Corey and Horton, to simulate soil-water pressure and flow for various storm conditions in a small laboratory-scale system. In their simulations, Frind et al. evaluated the effects of several factors on the performance of a layered cover including soil types, interface slope, thickness of the upper wick layer, infiltration rate, and

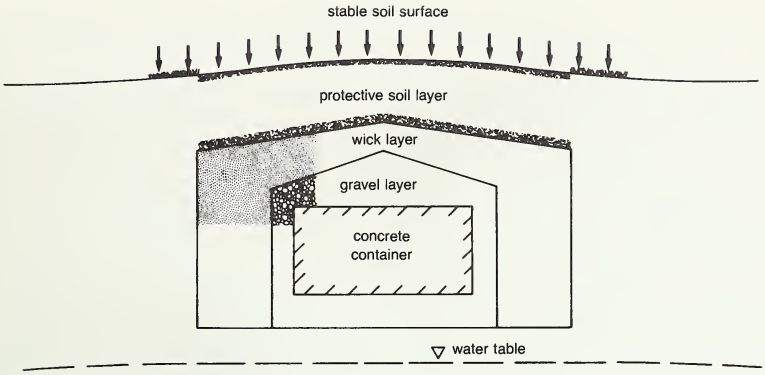

Figure 4 Basic geologic environment for waste containers (after Frind et al., 1977).

cumulative volume of infiltration. Design criteria were discussed regarding the use of stable soils to maintain dry conditions within underlying waste containers over long periods of time to minimize leaching of the waste.

Frind et al. (1977, p. 3.135-3.136) discussed the physical basis for the wick effect and its use in a layered cover system:

> The hydraulic properties of partially saturated porous media responsible for the wick effect are the relationships between volumetric moisture content and pressure head and those between volumetric moisture content and hydraulic conductivity.
>
> At a particular pressure head, all pores which are sufficiently small to exert a capillary pressure equal to or greater in magnitude than the applied pressure will be filled with water; therefore, a fine-grained soil will contain more water than a coarse-grained soil at an equal (negative) pressure. In draining an initially saturated soil, the largest pores will drain first, and as the pressure decreases, progressively smaller pores will drain. Similarly, in wetting a dry soil, the smallest pores will fill first, followed by progressively larger pores.
>
> If the two soils are in contact at a common interface, and the pressure is allowed to increase at this interface, the volumetric moisture content of the sand will increase as progressively larger pores are filled. This will be accompanied by an increase in the hydraulic conductivity of the sand. The gravel, having predominantly large pores, will remain in a relatively dry condition and its hydraulic conductivity will remain low until the pressure approaches zero. A sloping interface should result in lateral hydraulic gradients in the sand layer which would tend to divert water horizontally.
>
> The extent to which the water can be diverted while maintaining a negative pressure at the sand-gravel interface will depend upon several factors including the reach of the interface, the magnitude of the lateral hydraulic gradient, the hydraulic conductivity and thickness of the fine layer, the degree of contrast in the pressure head-volumetric moisture content curves of the coarse and fine layers, as well as rainfall intensity and duration. A fully designed system would require complete optimization of these factors.

The results of their simulations indicate that the wick effect is potentially useful in the design of waste-storage facilities. Under certain conditions, water is theoretically capable of being retained within and diverted laterally through a wick layer overlying a suitably shaped gravel layer. They found that system failure for a wick 3 m (10 ft) in width could be related to a critical volume of

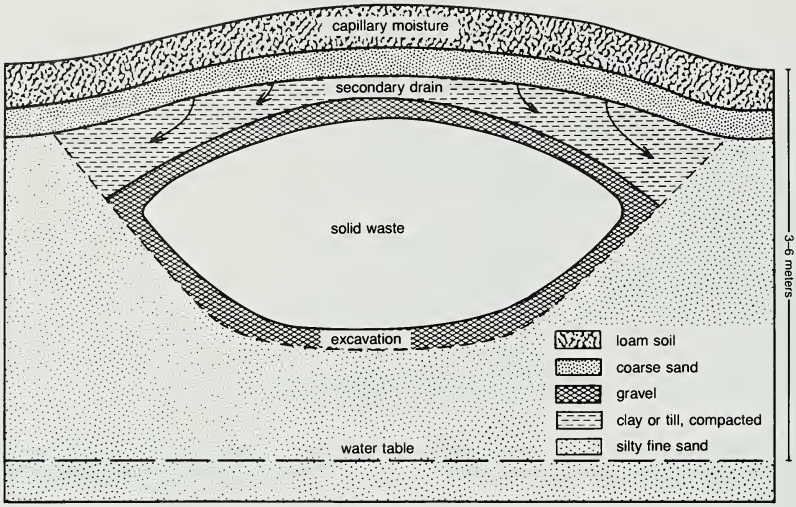

Figure 5 Schematic diagram showing a wick layer around a burial trench (after Cherry et al., 1973).

cumulative infiltration, but changes in the slope of the interface and/or wick thickness could significantly improve system performance. They do indicate, however, that prior to the development of design criteria, problems related to the construction and long-term integrity of the system should be investigated.

Cherry et al. (1973) tested a similar system (fig. 5) at Chalk River, Canada. Recent reports (personal communication) indicate that the system failed, probably due to quality control problems during construction.

Although layered-soil covers have been proposed to limit infiltration at disposal sites, and mathematical modeling has been used to determine the effectiveness of this type of cover, experimental verification of proposed designs has been limited almost exclusively to laboratory-scale experiments (Corey and Horton, 1969; Lindsay et al., 1979). The only documented field-scale experiments of the effectiveness of a layered-soil cover were described by Rancon (1980). In those experiments, a trench approximately 2 m (6.5 ft) wide, 4 m (13 ft) long, and 2 m deep was excavated and backfilled with coarse gravel, the upper surface of which sloped toward the sides of the trench. The gravel was overlain by a 1-m (3-ft) layer of fine-grained soil which also sloped toward and overlapped the sides of the trench.

Moisture movement into the trench was studied using neutron moisture probes inserted into access tubes in the trench and in the surrounding soils. The volumetric moisture content of the materials within the trench and in the surrounding soil was measured periodically throughout a one-year seasonal cycle between 1973 and 1974. During this time, wetting fronts resulting from heavy rainstorms were observed to significantly increase the volumetric moisture content of the surrounding soil profile to depths of more than 3 m (10 ft). In the trench, the volumetric moisture content of the upper fine-grained layer increased; however, there was no noticeable moisture movement into the underlying gravel, which remained essentially dry. In the second phase of the experiment, water was sprayed onto the surface of the trench cover. During infiltration, the downward movement of the wetting front ceased when the interface was reached, while the volumetric moisture content of the upper layer decreased. Since there was no apparent movement of water into the underlying gravel, Rancon concluded that water must have drained laterally above the interface.

EVALUATION OF GEOLOGIC MATERIALS IN EXPERIMENTAL COVER DESIGNS

Selection of Materials

The geologic materials selected for laboratory testing and computer modeling to determine their potential for use in field-scale, experimental trench covers included glacial till, loess (windblown silt), and sand and gravel. Fine-grained glacial till and loess are common materials in Illinois and are likely to be used in the construction of either landfill covers or liners.

Initial laboratory tests were conducted to characterize these materials prior to their incorporation in preliminary models of moisture movement through hypothetical cover designs and to determine significant characteristics for the design and construction of the experimental field-scale covers. Test procedures are listed in table 2. The materials tested initially included the Fairgrange Till of late Wisconsinan age, which is widespread in central Illinois, and the Peoria Loess, also of late Wisconsinan age, and widespread throughout Illinois. Permeable sand and gravel materials tested initially were outwash materials from a gravel pit near Champaign.

The actual materials used to construct the experimental covers consisted of Tiskilwa Till, Peoria Loess, and pea gravel. Tiskilwa Till, which is found near the study site, and Fairgrange Till are genetically related and have similar physical properties. Peoria Loess has been used as cover material at the Sheffield disposal site.

Physical Properties of Materials

- **Particle Size**

Results of particle-size analysis for Peoria Loess, Fairgrange and Tiskilwa Tills, silty sand (HT-1), and pea gravel are depicted in figure 6. Peoria Loess consists of 1 to 6 percent sand, 80 to 88 percent silt, 10 to 20 percent clay-sized particles, and about 1 percent gravel-sized materials, generally carbonate concretions or fossils. Fairgrange Till, classified texturally as a loam till, has a gravel content of about 4 percent based on the total weight of the sample. The fine (<2 mm) fraction averages 32 percent sand, 38 percent silt, and 30 percent clay. Tiskilwa Till has a similar textural composition.

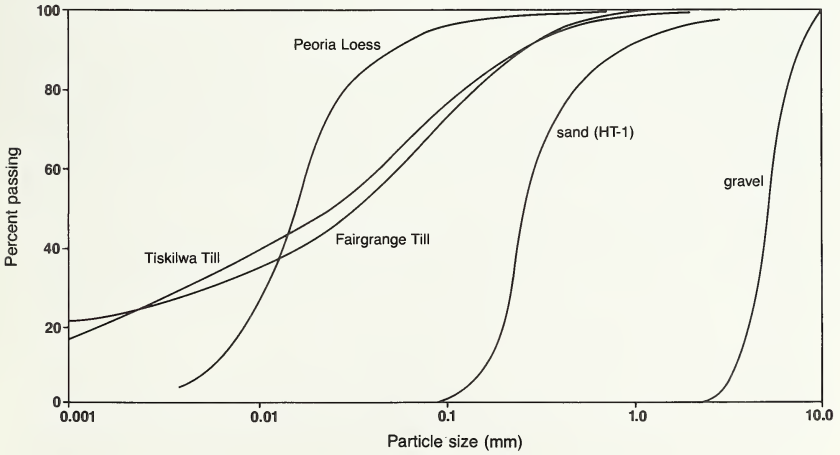

Figure 6 Particle-size analysis for soils used in computer models and the experimental trench covers.

Table 2. Procedures used in tests of soils from the field study site near Sheffield, Illinois

Test or Classification	Procedure
Description of Soils	ASTM[a] D-2488
Classification of Soils	ASTM D-2487
Water Content Determination	ASTM D-2216
Specific Gravity Determination	ASTM D-854
Particle-Size Analysis	ASTM D-422 and ISGS Sedigraph Procedure
Dry Preparation of Soil Samples	ASTM D-421
Wet Preparation of Soil Samples	ASTM D-2217
Liquid Limit Determination	ASTM D-423
Plastic Limit Determination	ASTM D-424
Shrinkage Factor Determination	ASTM D-427
Linear Shrinkage Determination	No standard
Standard Proctor Compaction Test	ASTM D-698
Pinhole Test for Dispersive Soils	USDA, Soil Conservation Service[b]
Natural Bulk Density	No standard
Natural Dry Density	No standard
Pocket Penetration	No standard
Torvane Shear	No standard

[a]ASTM - American Society for Testing and Materials, 1979.
[b]Sherard et al. 1976.

- **Clay Mineralogy**

Peoria Loess contains a characteristically high percentage of expandable (montmorillonitic) clay minerals, ranging from 30 to 50 percent of the clay minerals present. The remainder is predominantly illite; kaolinite and chlorite constitute only about 5 percent. Quartz is the predominant nonclay mineral in the loess.

The Fairgrange Till consists of approximately 9 percent expandable clay minerals, 72 percent illite, and 19 percent kaolinite plus chlorite.

Engineering Properties of Materials

- **Classification**

The loess was found to be nonplastic and classified NP. Liquid limits are within a 4 percent range. The loess has a higher shrinkage factor and a lower shrinkage ratio than the till. The liquid and plastic limits of the Fairgrange and Tiskilwa Tills are nearly identical. These materials are both classified as CL, moderately plastic. The shrinkage limits of both tills are also nearly the same. These results are presented in table 3.

- **Moisture-Density Relationships**

The maximum achievable dry density for the loess was 1.71 to 1.75 g/cm^3 (107 to 109.5 pcf) at an optimum gravimetric moisture content of 12.7 to 15.2 percent. The dry density of the loess was significantly less than that of the tills. The maximum achievable dry density of the till materials ranged from 1.96 to 2.00 g/cm^3 (122.4 to 125.0 pcf) at optimum gravimetric moisture contents of 10.0 to 12.5 percent. These results are presented in table 3.

- **Dispersion Tests**

An important issue regarding the stability of trench covers is their susceptibility to internal erosion or piping. Piping occurs when erosion of materials takes place underground. Highly susceptible materials are those considered to be naturally dispersive. The identification of materials susceptible to piping can be accomplished using the U.S. Soil Conservation Service pinhole test (Sherard et al., 1976). Results of pinhole tests performed on soil materials used in the laboratory experiments

Table 3. Summary of physical properties of geologic materials used in initial laboratory experiments

Material	Source	Classification	Liquid limit (%)	Plastic limit (%)	Plasticity Index (%)	[a]Shrinkage factor (%)	[a]Shrinkage ratio	Pinhole classification	Specific gravity	Compaction Test[d] Optimum gravimetric moisture content (%)	Compaction Test[d] Maximum dry density (pcf)	Compaction Test[d] Maximum dry density (g/cm^3)
Tiskilwa Till	trench cover	CL	24.5	14.3	10.2	10.2	2.00	low erosion susceptibility	2.72[b]	10.0	122.4	1.96
Loess	trench cover	NP	20.4	----	----	16.0	1.76	high erosion susceptibility	2.62[b]	12.7	109.5	1.75
Fairgrange Till	landfill, De Witt County	CL	25.8	14.8	11.0	12.4	2.01	--	2.71[c]	12.5	125.0	2.00
Loess	outcrop, St. Clair County	NP	24.64	----	----	----	----	--	2.71[c]	15.2	107.0	1.71

[a]Determined by ASTM D-427
[b]Determined by ASTM D-854
[c]Determined from shrinkage limit test
[d]Average of two or more samples; ASTM D-698 (Standard Proctor)

and field-scale covers are shown in table 3. Data from the pinhole test indicate that the glacial till (Tiskilwa Till) used in the field-scale trench covers has a low susceptibility to erosion; whereas loess used in the covers has a high susceptibility to erosion.

Hydrologic Properties

- **Saturated Hydraulic Conductivity**

The relation between compaction gravimetric moisture content, density, and saturated hydraulic conductivity for Peoria Loess and Fairgrange Till is shown in figures 7 and 8. Much lower values of saturated hydraulic conductivity were observed for samples compacted at gravimetric moisture contents above optimum than for samples compacted at gravimetric moisture contents below optimum.

- **Volumetric Moisture Content/Capillary Pressure Relationship**

Desaturation tests were conducted to determine the soil-moisture characteristic curve for each material, using Tempe cells or a pressure membrane extractor. Soil-moisture characteristic curves for samples of Fairgrange Till, Peoria Loess, and silty sand are shown in figure 9. Figure 10 extends the curve out to three bars for the Fairgrange Till with data from the pressure membrane extractor. Figure 11 presents soil-moisture characteristic curves for undisturbed samples of compacted Peoria Loess, compacted Tiskilwa Till, and gravel from the experimental trench covers at the field study site.

- **Unsaturated Hydraulic Conductivity**

In the equations used to model unsaturated flow, curves describing $\psi(\theta)$ and $K(\theta)$ must generally be defined for each porous material. The measurement of volumetric moisture content as a function of pressure head, $\psi(\theta)$, which reflects pore-size distribution, is a relatively straightforward procedure; however, the hydraulic conductivity function $K(\theta)$ is very difficult to measure directly. For this reason, $K(\theta)$ has been calculated from the $\psi(\theta)$ curves using the methods of Mualem (1978), Green and Corey (1971), and Van Genuchten (1980). The first two of these different methods were prescribed as input to the two numerical models, MOMOLS and UNSAT2, described in the section, Mathematical Modeling, in this report.

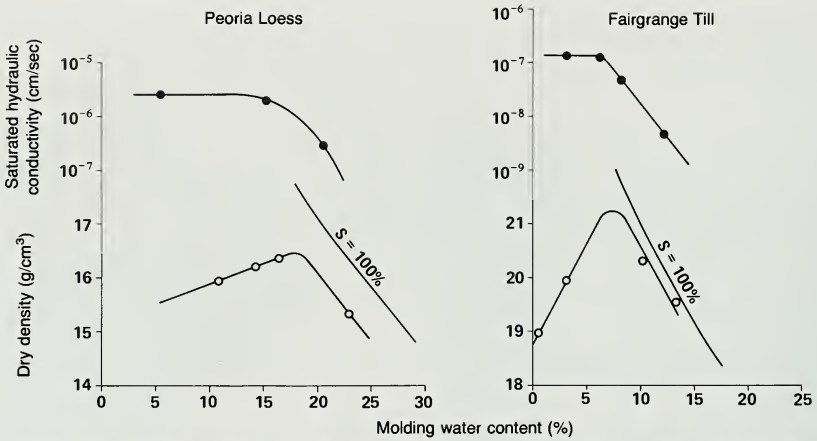

Figure 7 and **Figure 8** Results of compaction and saturated hydraulic conductivity tests for Peoria Loess (left) and Fairgrange Till (right) showing decreases in hydraulic conductivity for samples compacted at water contents greater than optimum.

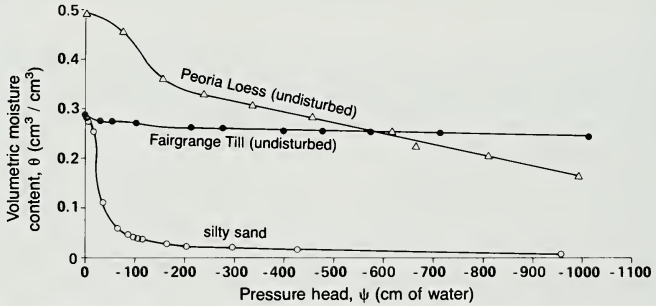

Figure 9 Soil-moisture retention curves for undisturbed samples of Peoria Loess, Fairgrange Till, and silty sand.

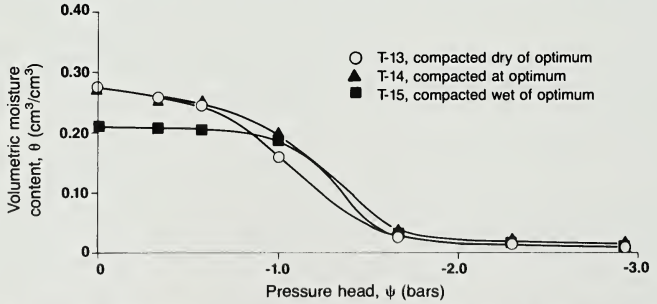

Figure 10 Soil-moisture retention curves for samples of compacted Fairgrange Till using the pressure membrane extractor.

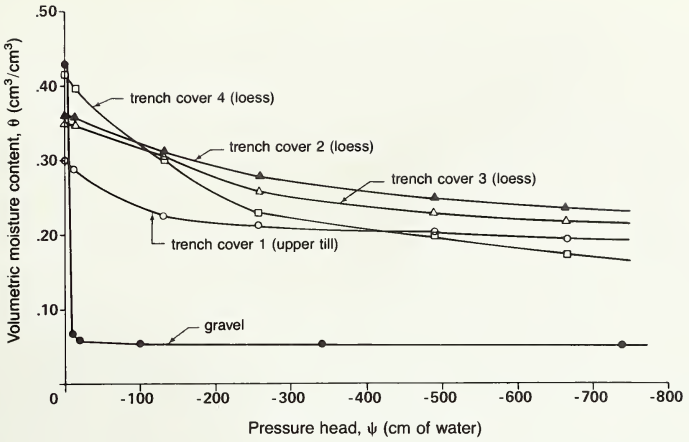

Figure 11 Soil-moisture retention curves for samples of compacted loess and till and gravel from the experimental trench covers at the Sheffield study site.

In the one-dimensional finite difference model of moisture movement (MOMOLS) used in this study, the equation of Mualem (1978) is used to calculate $K(\theta)$. Soil moisture characteristic curves used as input for MOMOLS are shown in figure 12. Resulting hydraulic conductivity functions are depicted in figure 13.

The method of Green and Corey (1971) was used to describe the $K(\theta)$ relationship used in two-dimensional simulations of moisture movement using UNSAT2. This procedure utilizes the soil-moisture characteristic curve and a value for saturated hydraulic conductivity. Figure 14 depicts these hydraulic conductivity functions.

We chose Van Genuchten's (1980) method for calculating $K(\theta)$ from soil moisture retention curves from materials used in our experimental field covers (fig. 11). Resulting hydraulic conductivity functions are depicted in figure 15.

In these calculations pressure head and hydraulic conductivity are assumed to be single-valued functions of θ. In fact, natural soils show hysteresis in both the $\psi(\theta)$ and $K(\theta)$ relationships. However, these calculations neglect hysteretic effects.

In this study, the range of pressure heads investigated was limited to between 0 and –1000 cm of water. This is the practical limit of in situ measurements using ceramic-cup tensiometers installed in the experimental trench covers.

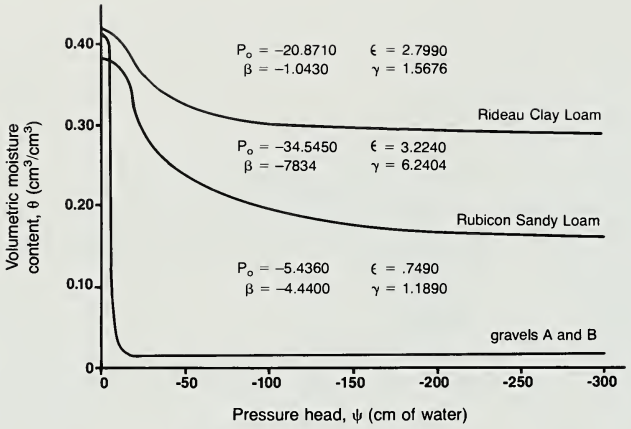

Figure 12 Primary wetting curves for soils used in MOMOLS one-dimensional simulations.

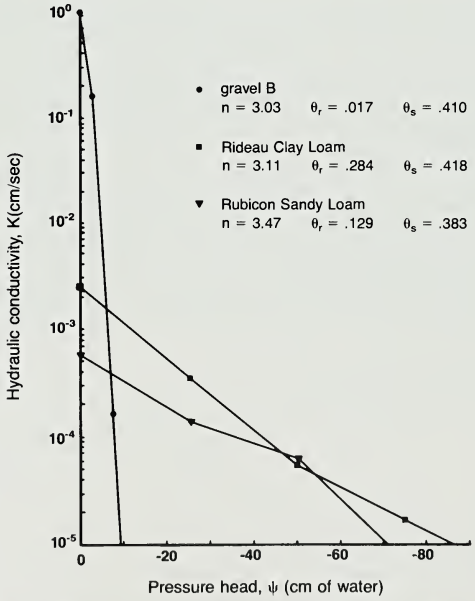

Figure 13 Hydraulic conductivity functions for soils used in MOMOLS one-dimensional simulations.

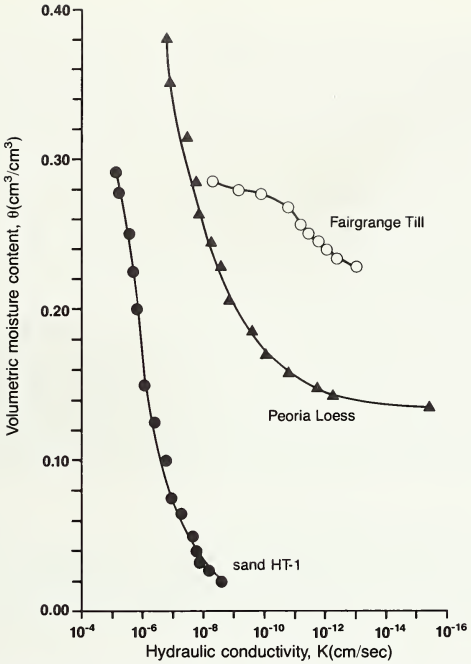

Figure 14 Hydraulic conductivity functions for soils used in UNSAT2 simulations, calculated using Green and Corey's (1971) method.

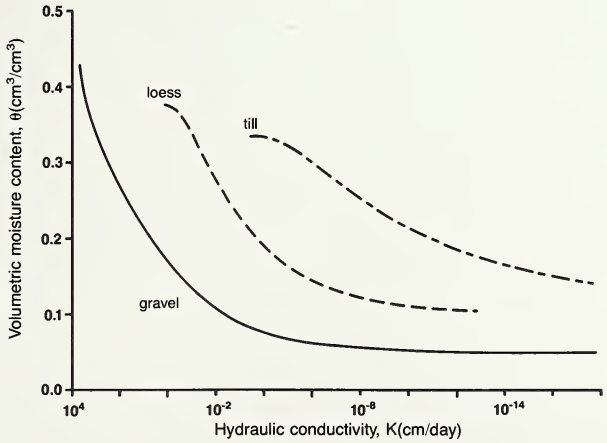

Figure 15 Hydraulic conductivity functions for undisturbed samples of soils taken from the experimental trench covers at the Sheffield study site. Calculated using Van Genuchten's (1980) method.

MATHEMATICAL MODELING OF MOISTURE MOVEMENT

The evaluation of alternative cover designs to limit the infiltration of moisture into waste-disposal trenches involves the use of predictive techniques. Predictive mathematical models have been developed to describe the flow of moisture through variably saturated porous materials. Using specified boundary conditions and the predicted relationship between K and θ for each material, a mathematical model can simulate the flow of moisture through individual materials and layered combinations of materials.

In our study, models of moisture flow were calibrated and verified using laboratory column and field experiments. The selection of materials used in alternative cover designs was based on the behavior of these materials in column experiments and in numerical simulations. In the initial stages, one-dimensional models were used to evaluate many different layered systems. More sophisticated, multidimensional models were later used to test selected cover designs under a variety of simulated field conditions.

Basic Equations of Mathematical Models

The flow of water through porous materials is described using Darcy's law, which can be stated in generalized form:

$$q = -K\nabla H \qquad [1]$$

where q is the flux (positive downward), H is the hydraulic head, and K is the hydraulic conductivity (the measure of the ability of the material to transmit fluid). The hydraulic head consists of the pressure head, ψ, and the gravitational head, z (equal to elevation):

$$H = \psi - z \qquad [2]$$

For unsaturated flow, $\psi < 0$; whereas for saturated flow, $\psi > 0$.

Under saturated conditions the hydraulic conductivity, K, depends on the internal geometry of the porous medium and on the properties of the fluid. For a given saturated, homogeneous material, K is a constant. For unsaturated flow, the hydraulic conductivity of a given material is a function of volumetric moisture content, θ. For an unsaturated homogeneous material, Darcy's law thus becomes

$$q = -K(\theta)\nabla H \qquad [3]$$

The hydraulic conductivity decreases rapidly as θ decreases. This decrease in conductivity is caused by a reduction in water-filled pore space; the large pores with the greatest ability to transmit fluid are the first to empty.

Applying continuity, we obtain the general equation describing flow in unsaturated, rigid porous media:

$$\frac{\partial\theta}{\partial t} = \nabla \cdot [K(\theta)\nabla H] \qquad [4]$$

or, expanding H:

$$\frac{\partial\theta}{\partial t} = \nabla \cdot [K(\theta)\nabla(\psi - z)] \qquad [5]$$

By introducing the diffusivity, D, equation 5 can be rewritten with θ as the sole dependent variable:

$$\frac{\partial\theta}{\partial t} = \nabla \cdot [D(\theta)\nabla\theta] - \frac{\partial K(\theta)}{\partial z} \qquad [6]$$

where $D(\theta) = K(\theta)\frac{\partial\psi}{\partial\theta}$

By introducing the specific moisture capacity, C, equation 5 can be rewritten with ψ as the sole dependent variable:

$$C(\psi)\frac{\partial\psi}{\partial t} = \nabla \cdot [K(\psi)\nabla\psi] - \frac{\partial K(\psi)}{\partial z} \qquad [7]$$

where $C = \frac{\partial\theta}{\partial\psi}$

Either equation 6 or 7 may be used to describe flow of fluid through unsaturated materials. Equation 7 is more versatile since it can also be used to describe flow through saturated media. It is also preferred because it can automatically handle layered systems with different soil moisture characteristics.

Results of Simulations using MOMOLS

For the simulation of one-dimensional moisture flow a finite difference approximation of Richard's equation describing unsaturated flow through homogeneous materials was incorporated into the program MOMOLS (Moisture Movement in Layered Soils) developed by Rojstaczer (1981). Nodal spacing in this program is constant, and a fully implicit scheme is used to evaluate the spatial and time derivatives. Required data in MOMOLS include data from the $\psi(\theta)$ relationship in the form of the equation by King (1965). The $K(\psi)$ relationship is calculated in MOMOLS using the method of Mualem (1978).

Rojstaczer (1981) used the computer program MOMOLS to simulate one-dimensional, vertical moisture movement through a layered column of fine- or medium-textured soil underlain by coarse gravel. The soils overlying the gravel at a depth of 24 cm consisted of either the Rideau Clay Loam or the Rubicon Sandy Loam described by Topp (1969). The behavior of two different hypothetical types of coarse gravel was also simulated. The two gravel layers (gravels A and B) were assumed to have identical characteristics except that the saturated hydraulic conductivity of gravel A was 10 cm/s; whereas gravel B had a hydraulic conductivity of 1 cm/s. Soil moisture retention curves and calculated hydraulic conductivity functions for these materials are illustrated in figures 12 and 13 (Evaluation of Geologic Materials section).

Simulations were made of three basic cases characterized by different surface boundary conditions. Moisture movement in response to steady rainfall was simulated using a constant flux boundary condition at the surface (Case 1). In Case 2, the effects of moisture redistribution after a period of constant rainfall were investigated. A constant pressure head of zero at the surface was used in Case 3 to simulate constant ponding. In all cases, the boundary condition at the bottom of the column was held constant at a pressure head of –300 cm. According to Rojstaczer (1981):

> The ability of the coarse, unsaturated material to impede moisture movement was clearly shown in the simulations. In all simulations progress of the moisture front temporarily or permanently ceased once the interface was reached. The lack of moisture movement across the interface caused pressure potentials and volumetric moisture contents to build in the overlying layer. Pressure and moisture build-up continued until either a static pressure profile was established (and all moisture movement ceased) or interfacial pressures achieved a critical maximum value, ψ_c. If ψ_c was reached at the interface, the moisture front rapidly progressed into the coarse layer. The rapid infiltration into the gravel depleted moisture storage at and directly above the interface and as a result pressures at the interface quickly dropped from ψ_c to a value which was more or less maintained throughout the rest of the simulation.
>
> The critical pressure, ψ_c, necessary to allow moisture movement across the interface was less than zero in all but two simulations. Deviations from zero were greater than could be attributed to computational error. In all simulations the value of ψ_c was found to be a function of two factors, the rate at which moisture and pressure build-up was occurring in the overlying layer and the conductivity of the underlying gravel. The dependence of ψ_c on these factors can be easily shown in a case by case analysis of the simulations.

During laboratory evaluation of materials, it was observed that compacting soils with different gravimetric moisture contents resulted in much different saturated hydraulic conductivities (figs. 7 and 8). One-dimensional simulations were carried out using MOMOLS and the physical characteristics associated with soils compacted wet and dry of optimum to determine the effects on infiltration. Moisture retention curves for the compacted loess, and sand and gravel used in these simulations are shown in figures 9 and 10 in the section, Evaluation of Geologic Materials. Simulations were limited to one- and two-layer systems. Subjects that were investigated include moisture entry into the top layer, moisture redistribution in the top layer, and the influence of the second layer on moisture breakthrough from the first.

Figures 16 and 17 summarize the results of simulations performed to identify the factors influencing moisture entry (infiltration) into the surface layer. Higher values of initial capillary pressure result in greater moisture entry (fig. 16). Although the hydraulic conductivity of the soil is lower when the capillary pressure is higher, the potential infiltration rate is much higher. Moisture entry is also influenced by the compaction volumetric moisture content when fine-grained soils are used in the surface layer. In soils compacted wet of optimum volumetric moisture content, there is a much lower moisture entry and a much slower rate of moisture front advance (fig. 17) than in soils

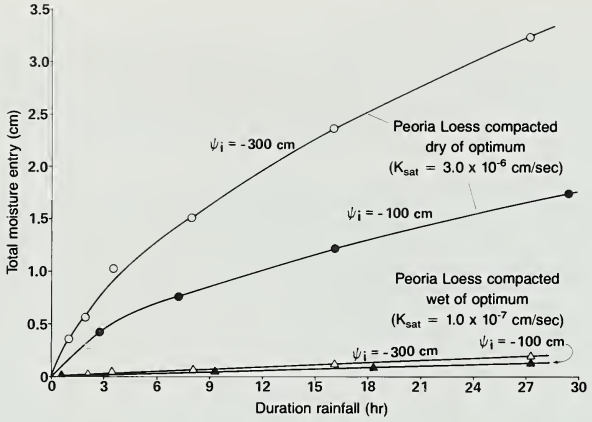

Figure 16 Total moisture entry into samples of compacted Peoria Loess under differing initial conditions. Higher moisture entry (and storage capacity) is primarily the result of the greater hydraulic conductivity of samples compacted dry of optimum.

compacted dry of optimum. This effect is partly related to differences in hydraulic conductivity; soils compacted wet of optimum exhibit much lower values of saturated hydraulic conductivity than those compacted dry of optimum.

Moisture redistribution was investigated by changing the surface boundary condition from a constant head to a constant surface flux equal to zero. Figure 18 shows the predicted moisture redistribution after a 4-hour rain for a surface soil compacted dry of optimum. After rainfall, the moisture front advanced deeper into the soil compacted dry of optimum (about 11 cm as compared to only 4 cm for the soil compacted wet of optimum). Moisture redistribution in the soil compacted wet of optimum showed progressive advance of the moisture front and eventually some percolation through the 30-cm layer. Figure 19 shows the moisture front advance for a more complex rainfall sequence—4 hours of rain followed by 50 hours of dry weather, then another 4 hours of rain. For a soil compacted dry of optimum, the moisture front advance is much deeper after the second rain.

If the texture of the second layer is much coarser than the fine-grained top layer, moisture will build up in the top layer before entering the second layer. The volumetric moisture content in a layer of compacted Peoria Loess overlying a coarse gravel builds up significantly prior to breakthrough after 2600 hours of continued surface ponding (fig. 20). For comparison, changes in the volumetric moisture content in a single layer of Peoria Loess are also shown. Figure 21 illustrates the more limited moisture retention that occurs in compacted Peoria Loess overlying medium sand. The adjacent example of a single layer of loess illustrates an almost negligible difference between the layered and nonlayered cases.

Key factors in the establishment of a wicking system are contrasting pore sizes combined with high values of capillary pressure. In our work, we have found a useful indicator of the wicking potential of a two-layer system to be the conductivity ratio, defined as the saturated hydraulic conductivity value of the lower layer divided by the value of the upper layer. As an example, figure 22 shows the relationship between conductivity ratio and the storage efficiency of the top layer. For the materials we investigated, large conductivity ratios suggest major differences in the pore sizes of the soils, and hence, indirectly imply good wicking potential. This may not be true for all materials, especially those in which individual grains or clods may behave as separate systems under certain pressure conditions.

Results of Simulations using UNSAT2

The two-dimensional finite element model, UNSAT2, developed by Neuman (1973) and Neuman et al. (1975), was used to simulate moisture movement through laboratory columns and field-scale

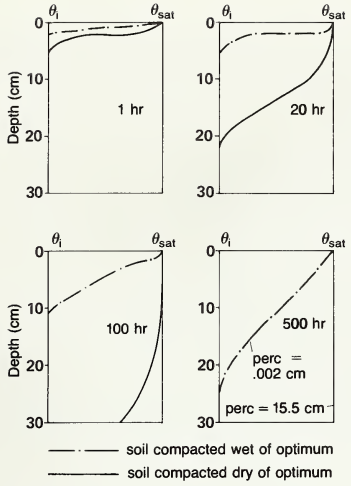

Figure 17 Predicted advance of wetting front in compacted Peoria Loess with constant pressure head = 0 at surface.

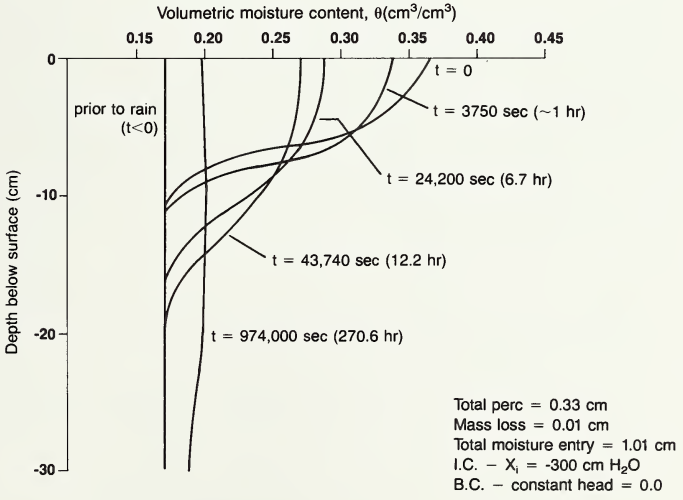

Figure 18 Redistribution after 4 hours of simulated rainfall in Peoria Loess compacted dry of optimum.

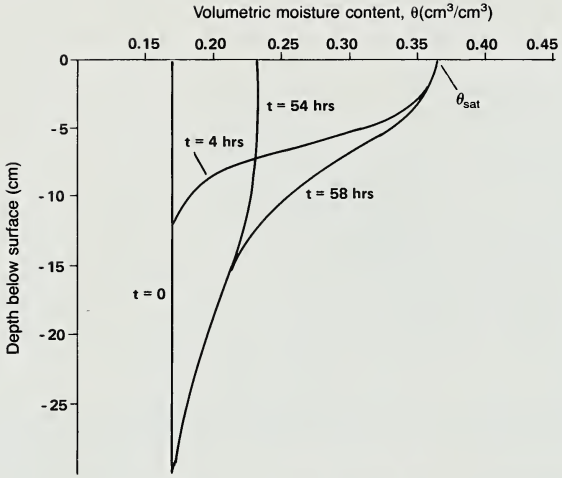

Figure 19 Predicted moisture redistribution in a 30-cm layer of Peoria Loess (P-6) compacted dry of optimum. The simulated rainfall sequence consists of 4 hours of rain, followed by 50 hours of redistribution, followed by 4 hours of rain. Initial conditions consist of a constant pressure head of –300 cm.

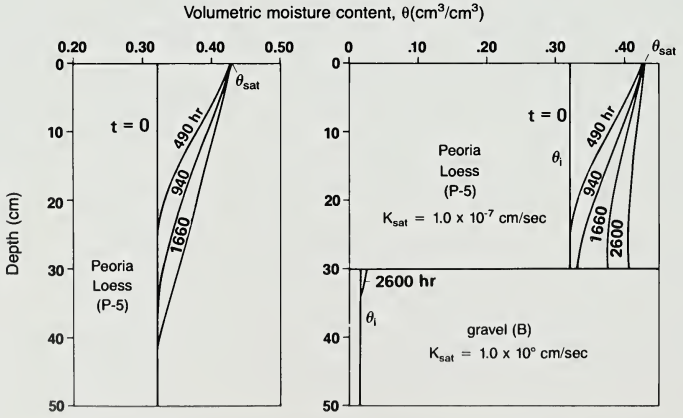

Figure 20 Effect of coarse-grained gravel layer on moisture retention in the overlying fine-grained material compared to moisture movement through a single layer of fine-grained material.

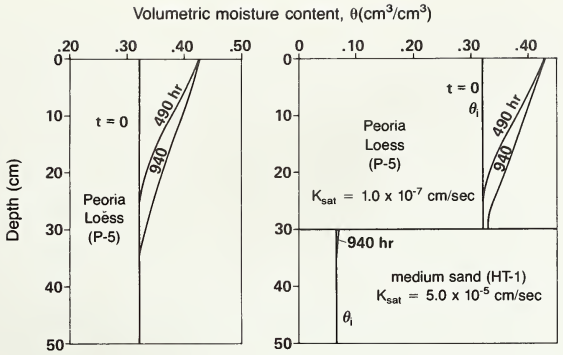

Figure 21 Effect of medium and layer on moisture retention in the overlying fine-grained material compared to moisture movement through a single layer of fine-grained material.

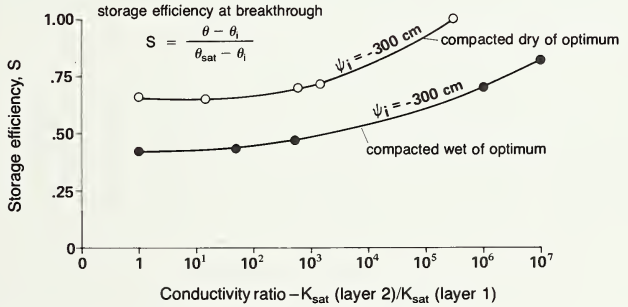

Figure 22 Influence of hydraulic conductivity ratio on the storage efficiency of the top layer of two-layered system.

cover designs. The model uses a Galerkin-type, finite-element method to simulate two-dimensional, nonsteady flow of water in incompressible, saturated-unsaturated soils; evaporation and water uptake by roots are also considered. Theoretical development of the model is presented by Neuman et al. (1975), and the results of verification with field measurements and comparison with the results obtained by a finite difference technique are described in Feddes et al. (1975). A user's guide including documentation and example problems was published by Davis and Neuman (1983).

Two types of problems were studied. The first involved the simulation of moisture movement through a system designed to the scale of the laboratory gamma column described later in this report. The primary purpose of these simulations was to attempt to calibrate and verify the model for the particular soils and boundary conditions used in this study. The second type of problem involved the simulation of infiltration and two-dimensional moisture movement through a field-scale design of a sloping, layered cover.

- **Influence of Boundary Conditions**

UNSAT2 incorporates several possible types of boundary conditions—including evaporation and infiltration boundaries and water uptake by roots—in addition to those of constant total head (h), constant pressure head (ψ) or constant flux (Q). In the simulations described here, boundary conditions at the surface included continuous rainfall (constant surface flux, Q) and continuous ponding (constant pressure head, $\psi = 0$). At the bottom, boundary conditions consisted of either a constant pressure head, $\psi = 0$ (water table), a prescribed constant negative pressure (tension), or a seepage face. The sides of both the column and field-scale simulations are no-flow boundaries.

Along soil-air interfaces (in the absence of ponding) the soil can lose water to the atmosphere by evaporation or gain water by infiltration. While the maximum possible rate of evaporation depends only on atmospheric conditions, the actual flux across the soil surface is limited by the ability of the soil to transmit water from below. Similarly, if the intensity of rainfall exceeds the infiltration capacity of the soil, surface-water runoff will occur and the actual flux depends on antecedent moisture conditions in the soil.

A seepage face is an atmospheric boundary at which water seeps out from the saturated part of an exposed face. Pressure head along the seepage face must be zero (atmospheric pressure). The extent of the seepage face varies with time. Such a condition conceivably might represent conditions at the bottom of a landfill cover if the waste remains unsaturated, and if drains or sumps maintain atmospheric pressure. In the simulations with a seepage face at the bottom, the unsaturated part of the boundary is a prescribed flux boundary ($Q = 0$); when saturated, it is treated as a prescribed pressure head boundary with $\psi = 0$.

As in the previous simulations, the infiltration rate resulting from a constant surface-flux boundary condition is substantially lower than that for continuous surface ponding with a constant pressure head, $\psi = 0$. The latter appears to best represent conditions during an actual storm when the infiltration rate typically decreases asymptotically to approximately the saturated hydraulic conductivity of the upper layer as the surface soil becomes saturated.

- **Simulation of Laboratory Column-Scale Experiments**

A soil column 29 cm long and 8 cm wide was chosen to simulate laboratory column experiments. In most simulations, the column consisted of 11 cm of Peoria Loess overlain by 9 cm of a medium sand, which was overlain by 9 cm of Peoria Loess. Physical and hydraulic properties of these materials are recorded in the section, Evaluation of Geologic Materials, in this report. The configuration of the finite element network is shown in figure 23. For all simulations, the sides of the column were considered no-flow boundaries and all but the top and bottom nodes had initial pressure heads of -100 cm. Only boundary conditions at the top and bottom of the column were changed between simulations to allow better comparison of results.

Case 1 The first case involved a single thick layer of loess, under conditions of constant ponding at the surface and a constant pressure head of -100 cm at the bottom of the column. Figures 24 and 25 show pressure head and volumetric moisture content profiles at several times. Pressure head and volumetric moisture content increase with depth smoothly and rapidly. Figure 26 shows pressure head as a function of time for various depths within the one-layer column; steady state conditions occur rapidly and smoothly.

Case 2 Subsequent cases involved three-layer columns with layers of loess above and below a layer of sand. In the second case, the boundary conditions remained the same as for Case 1. Figures 27 and 28 show pressure head and volumetric moisture content distributions at various times. Initially, the pressure head decreased in the loess below the sand. The minimum value was reached at about 14 hours. As time progressed, the pressure head throughout the sand increased until it reached a constant value equal to the pressure head at the top of the sand. The pressure head in the upper loess layers was similar to the upper portion of the single layer as modeled in Case 1. Volumetric moisture content of the two loess layers was similar to the upper and lower portions of the Case 1 model. An abrupt change occurred in the volumetric moisture content at the sand-loess interfaces. The volumetric moisture content of the sand slowly increased with time—first at the top, then gradually throughout, until a constant value was reached. Figure 29 shows the change in pressure head at various depths in the column with time. Steady-state pressures in the upper layer were higher than in the upper portion of the single-layer column;

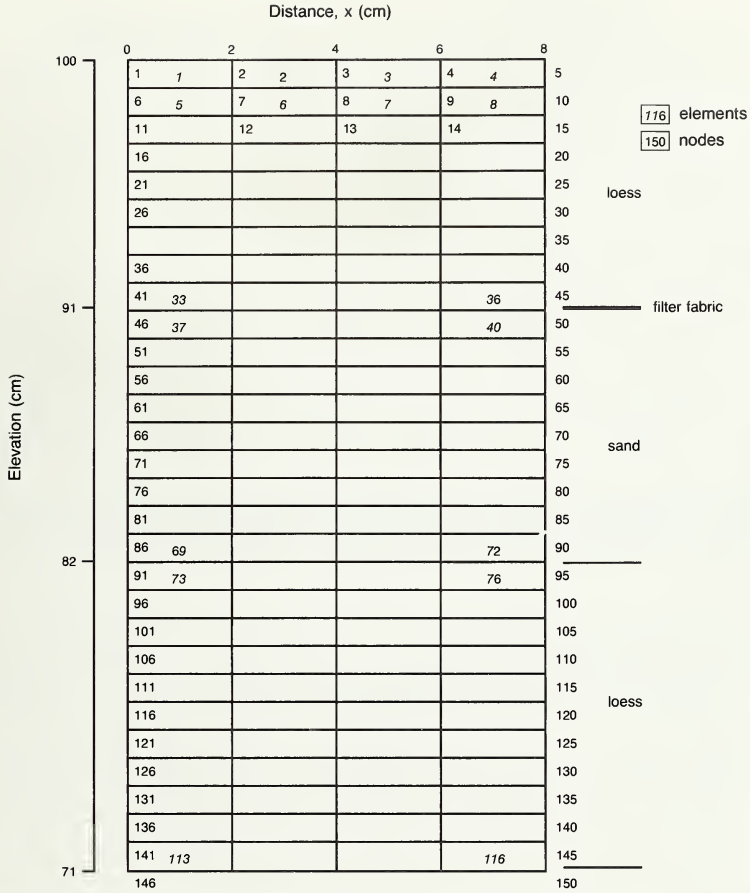

Figure 23 Cross section of simulated gamma column with superimposed finite element network.

however, the increase in pressure head in the lower loess layer occurred later than in the lower loess in the one-layer case.

Case 3 Case 3 was identical to Case 2, except that the lower boundary was assumed to have a constant pressure head of zero to simulate saturated conditions in the waste below the cover. Figures 30 and 31 show the pressure head and volumetric moisture content profiles for various times. Profiles in the upper loess were similar for Cases 2 and 3 for the first 110 hours. Over longer periods, saturation was achieved more rapidly in Case 3, in which a water table was simulated at the bottom. When the base of the cover was saturated, pressure heads approached zero and volumetric moisture contents approached saturation much faster than they did in Case

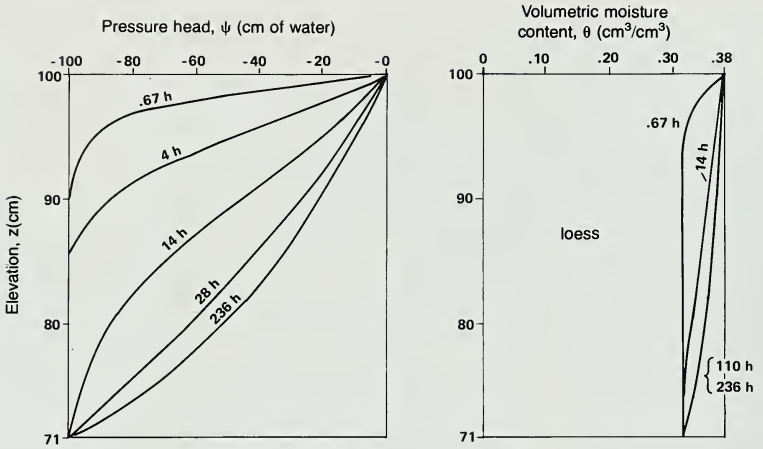

Figure 24 and **Figure 25** Predicted distribution of pressure head (left) and volumetric moisture content (right) at selected times for Case 1 simulations consisting of a one-layer cover of Peoria Loess under conditions of constant surface ponding and constant pressure head = –100 cm of water at the bottom.

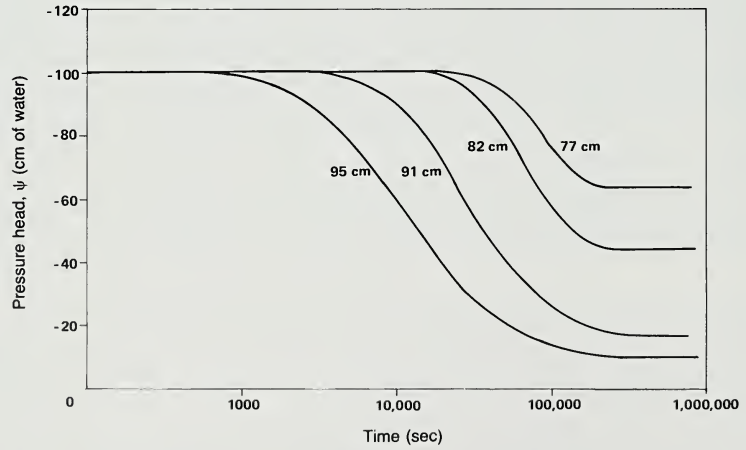

Figure 26 Predicted change in pressure head with time at various depths for Case 1 simulations consisting of a one-layer column of Peoria Loess under conditions of constant ponding at the surface and constant pressure head = – 100 cm of water at the bottom.

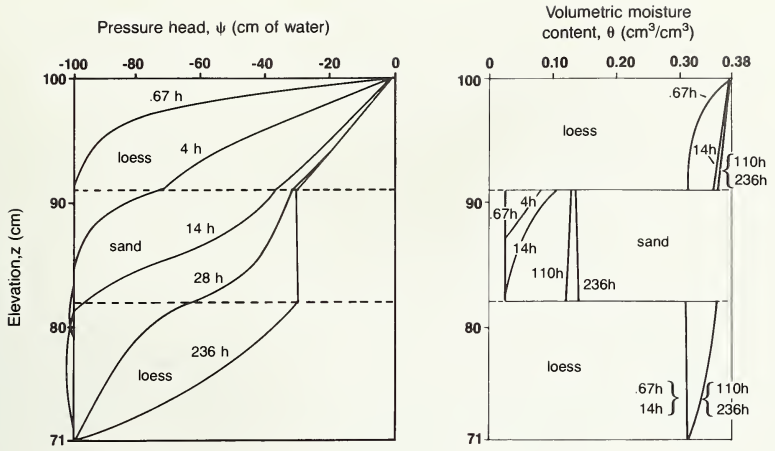

Figure 27 and **Figure 28** Predicted distribution of pressure head (left) and volumetric moisture content (right) at selected times for Case 2 simulations consisting of a three-layer column under conditions of constant ponding at the surface and constant pressure head = – 100 cm of water at the bottom.

2. By the end of the simulation, the lower loess and bottom half of the sand were saturated, showing that the column became saturated from the bottom up. Figure 32 shows the change in pressure head with time. Pressure heads in the upper loess and at the upper interface were nearly identical to those in Case 2 for approximately the first 4000 seconds. Pressure head increased significantly throughout the column between 10,000 and 20,000 seconds.

Case 4 In the fourth case, the bottom of the column was modeled as a seepage face. We believe that this case may best represent actual conditions. The results of this simulation are shown in figures 33 to 35. The response of this system differed from that observed in Cases 2 and 3. For approximately the first 28 hours, the results of this simulation and those for Case 2 were very similar in the upper loess and sand, and the pressure heads in the lower loess were greater in Case 4 with a seepage face. By the end of the simulation—when the bottom was saturated—the profile was virtually identical to that of the water table case (Case 3). These observations also generally held true for the volumetric moisture content profiles. The change in pressure head with time (fig. 35) was similar to that for Case 1 for all but the lower loess during the first 100,000 seconds. Final equilibrium pressures were similar to those in Case 3.

Case 5 In the final case, the bottom boundary was the same as in Case 2, but a constant surface flux equal to the saturated hydraulic conductivity of the loess (2×10^{-4} cm/s) was assumed. The results are shown in figures 36 to 38. As the simulation progressed, the increases in both pressure head and volumetric moisture content were constant with depth throughout the upper loess. The lower loess and interface experienced a decrease in pressure head for about the first 200,000 seconds. Subsequently, pressure head increased throughout the column. Volumetric moisture content and pressure head throughout the column were less than that observed in the case of a constant pressure head of zero at the surface. Little change was noted in the volumetric moisture content of the sand and lower loess. Pressure heads did not change rapidly at any point in the column until after 200,000 seconds.

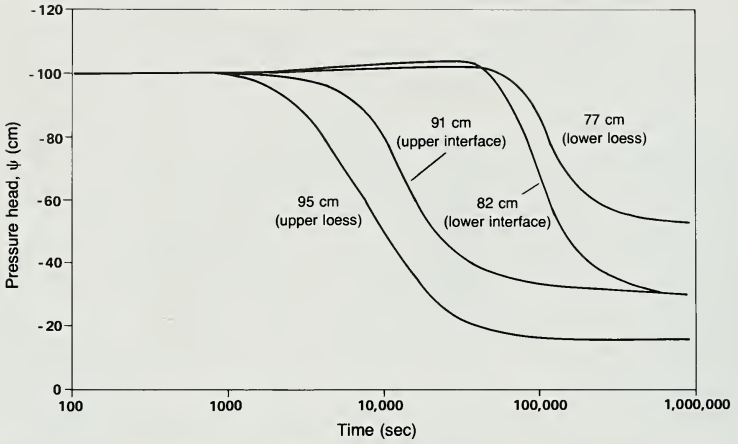

Figure 29 Predicted change in pressure head with time for various depths for Case 2 simulations consisting of a three-layer column under conditions of constant ponding at the surface and constant pressured head = –100 cm at the bottom

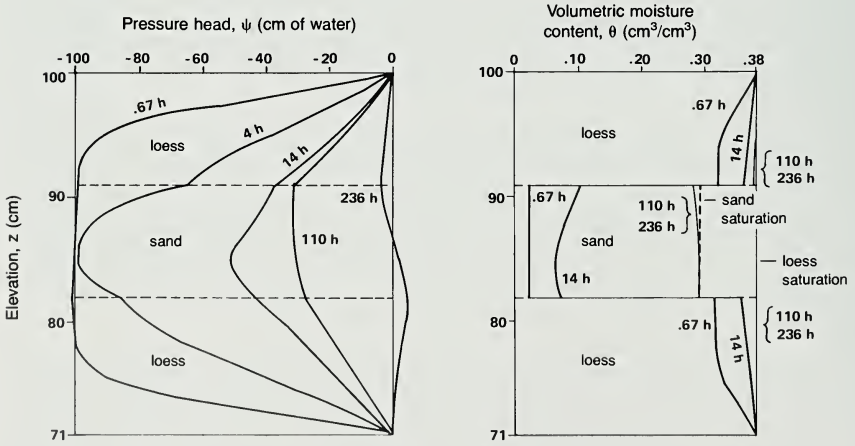

Figure 30 and **Figure 31** Predicted distribution of pressure head (left) and volumetric moisture content (right) at selected times for Case 3 simulations consisting of a three-layer column under conditions of constant ponding at the surface and constant pressure head = 0 (water table) at the bottom.

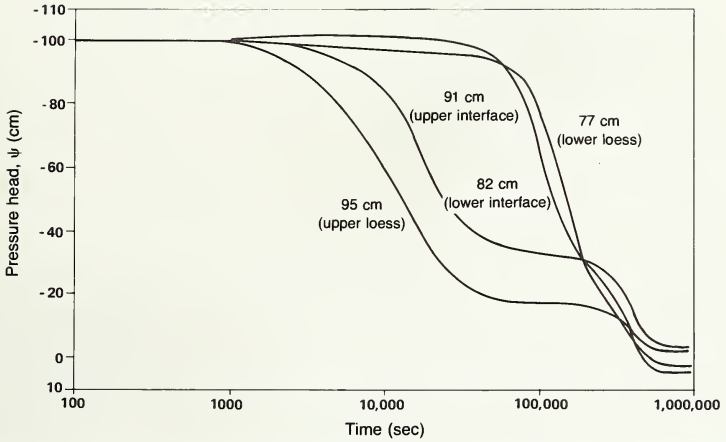

Figure 32 Predicted change in pressure head with time for various depths for Case 3 simulations consisting of a three-layer column under conditions of constant ponding at the surface and constant pressure head = 0 (water table) at the bottom.

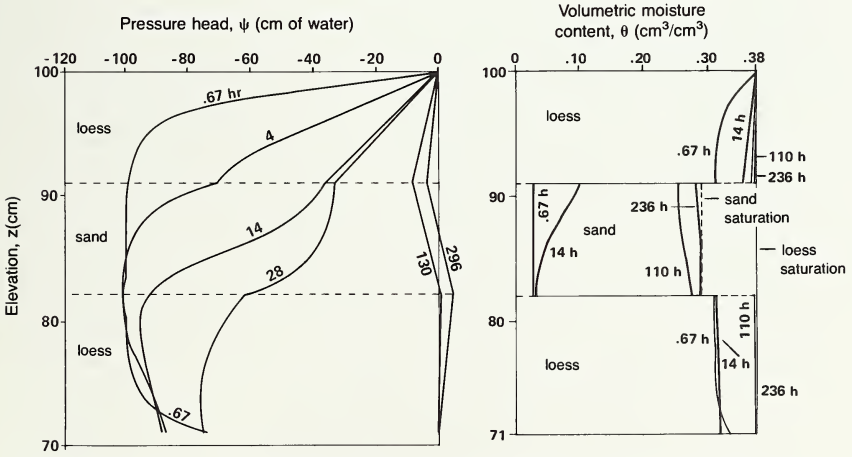

Figure 33 and **Figure 34** Predicted distribution of pressure head (left) and water content (right) at selected times for Case 4 simulations consisting of a three-layer column under conditions of constant ponding at the surface and a seepage face at the bottom.

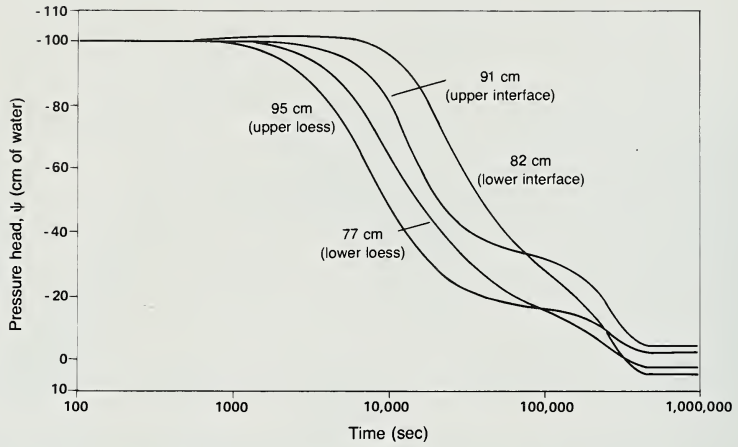

Figure 35 Predicted change in pressure head with time for various depths for Case 4 simulations consisting of a three-layer column under conditions of constant ponding at the surface and a seepage face at the bottom.

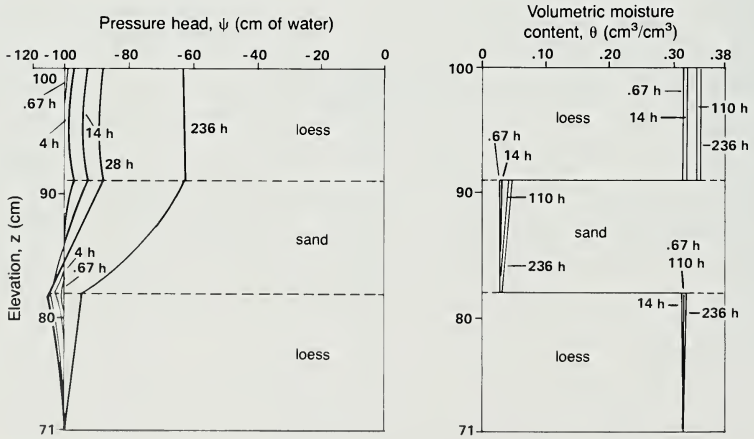

Figure 36 and **Figure 37** Predicted distribution of pressure head (left) and volumetric moisture content (right) at selected times for Case 5 simulations consisting of a three-layer column under conditions of constant surface discharge equal to the saturated hydraulic conductivity of the loess and constant pressure head = −100 cm of water at the bottom.

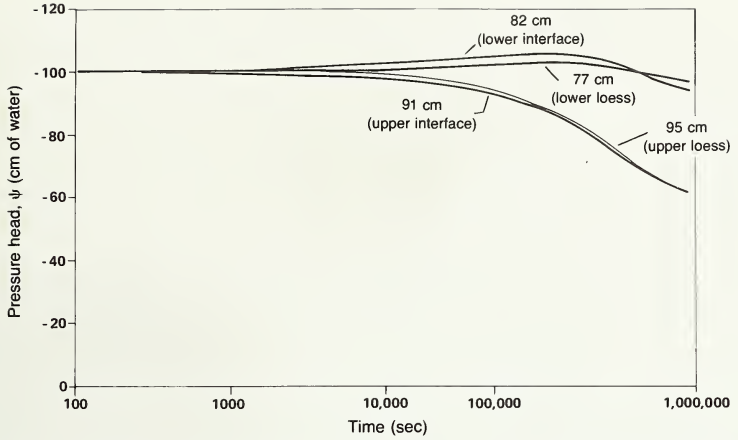

Figure 38 Predicted change in pressure head with time for various depths for Case 5 simulations consisting of a three-layer column under conditions of constant discharge at the surface equal to the saturated conductivity of the loess and constant pressure head = –100 cm of water at the bottom.

• Field-Scale Simulations

Infiltration and moisture movement through a hypothetical field-scale layered cover were simulated using UNSAT2. The particular design chosen initially for modeling (fig. 39) consists of three layers, each 60 cm thick. For comparison, a single fine-textured layer cover 180 cm thick was also simulated (Case 1). The cover was assumed to be 6 m wide with a 5-percent slope of each layer from the center to the sides. This was the approximate configuration of the covers being tested in the field. Because the hypothetical cover in figure 39 is symmetrical, moisture movement through only half of the cover was modeled.

Figure 40 is a cross section of the sloping cover and superimposed finite element network used in the simulations. The sides of the cover were assumed in all simulations to be no-flow boundaries. A constant pressure head of zero, indicating continual ponding, was imposed on the surface of the cover, while the boundary condition at the bottom varied in each case. Initial conditions within the cover consisted of a constant pressure head of –100 cm in each case described here. The materials used in the field-scale cover simulations consisted of compacted Peoria Loess (P-2) and gravel (B). The desaturation moisture-retention curves for each material are presented in figure 9; figure 10 illustrates the relationship between hydraulic conductivity and degree of saturation calculated by the method of Green and Corey (1971). The effects of hysteresis were not included in these simulations.

The magnitude of the first time-step in these calculations, $\delta t'$, was 1 hour; subsequent time-steps increased gradually to a maximum of 3 hours. Within each time-step, iterations were controlled with a convergence criterion of 1 cm maximum change in pressure head.

Case 1 Infiltration into a single-layer cover of compacted loess was simulated for a period of 297 hours of constant surface ponding. A constant pressure head of – 110 cm was maintained at the bottom of the cover corresponding to its elevation above an arbitrary datum x, and all interior nodes were assigned an initial pressure head of – 100 cm.

The wetting front in the single layer case propagated uniformly through the cover until steady-state conditions were attained. The vertical distribution of pressure head with depth at various times is shown in figure 41 at a position 100 cm from the left edge of the cover. The vertical

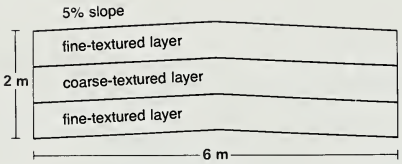

Figure 39 Cross section of hypothetical field-scale cover design.

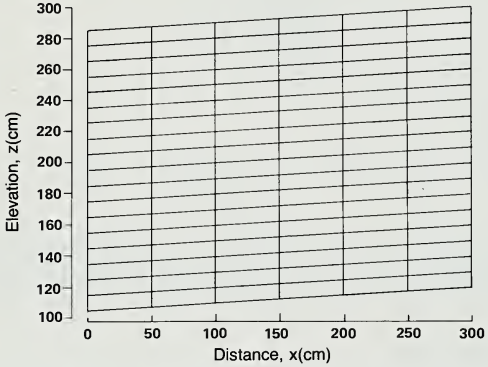

Figure 40 Cross section of one-half of symmetrical simulated field-scale cover with superimposed finite element network.

change in volumetric moisture content with time at the same location is shown in figure 42. After 297 hours the wetting front had penetrated to a depth of more than 140 cm in this part of the single-layer cover.

Case 2 The introduction of a coarse-grained, unsaturated layer between two layers of loess had a significant effect on infiltration and moisture movement in the cover. Simulations in Case 2 utilized the same boundary conditions as in Case 1; however, the cover in Case 2 consisted of 60-cm layers of loess overlying gravel, which in turn overlay loess.

As the one-dimensional simulations using MOMOLS indicated, moisture movement in the loess overlying the gravel temporarily ceased once the interface was reached. The lack of moisture movement across the interface caused pressure heads and volumetric moisture contents to build up in the overlying layer; pressure heads and volumetric moisture contents increased until the interfacial pressure reached a critical maximum value, ψ_c. If ψ_c was reached at the interface, the wetting front progressed rapidly into and through the coarse layer. In the one-dimensional simulations it was found that rapid infiltration into the gravel layer depleted moisture at and directly above the interface, and as a result, pressure heads at the interface dropped quickly from ψ_c to a value that was more or less maintained for the remainder of the simulation. In the two-dimensional simulation, however, pressure heads at the interface did not drop appreciably following moisture breakthrough, but remained virtually constant at the interface and in the underlying gravel.

The effects of a layered cover on infiltration are illustrated in figure 43, in which the predicted distribution of pressure head at selected times in the three-layer cover is compared to that predicted for the single layer cover of Case 1. Boundary conditions were the same in both cases. Especially

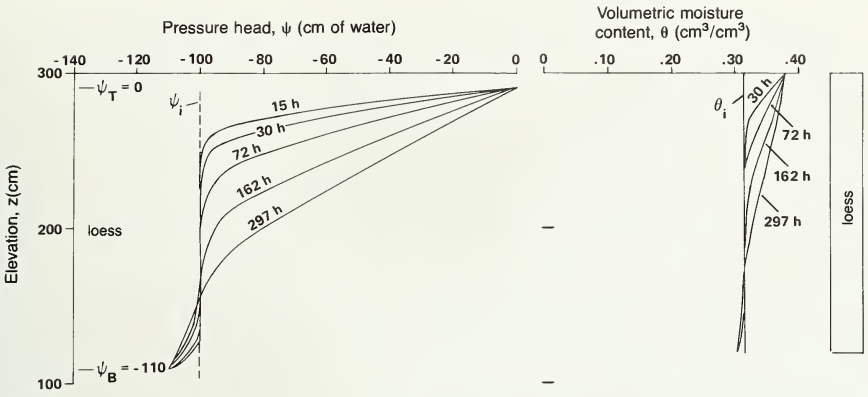

Figure 41 and **Figure 42** Predicted distribution of pressure head (left) and volumetric moisture content (right) at selected times in a one-layer cover of Peoria Loess at x = 100 cm under conditions of constant surface ponding and constant pressure head = –z at the bottom (Case 1).

noticeable is an increase corresponding to the rise in pressure head above the gravel layer and lack of movement into the gravel for more than 162 hours of ponding. Also apparent is the further decrease in pressure head below the gravel in response to the initial gradient applied to the system and the lack of moisture movement from the gravel into the underlying layer. Following breakthrough, however, the moisture front progressed much more rapidly through the gravel than in the one-layer case because of the higher degree of saturation in the upper layer of the three-layer case.

The predicted vertical distributions of pressure head and volumetric moisture content at several selected times are presented in figures 44 and 45 for the column of nodes at the position x = 100 cm in the cover (fig. 40). Moisture breakthrough into the gravel layer occurred quite suddenly after approximately 180 hours of moisture buildup in the overlying layer. By 382 hours, pressure heads in the gravel layer had increased substantially and the overlying loess was nearly saturated; however, the volumetric moisture content of the gravel was still very low. Pressure heads in the loess beneath the gravel began to increase after 382 hours.

The simulated layered cover system had a slope of 5 percent. The effects of this slope on moisture flow are illustrated in figures 45–47, which show the predicted distribution of total hydraulic head in the cover. Initial hydraulic head conditions at the onset of ponding at the surface are shown in figure 46, where the initial gradient associated with the assumption of a constant initial pressure head for the entire system is apparent. After 162.5 hours (fig. 47), the head distribution indicated the buildup in pressure head and volumetric moisture content above the gravel layer; the vertical gradient in total head at the interface is significant. In response to the slope of the cover, a lateral component of flow developed in both the upper and lower loess layers. Although the loess was still unsaturated, some of the moisture that had built up in the upper layer of loess began to move laterally through the loess above the gravel and stopped at the no-flow boundary along the edge of the cover. Possibly, this lateral infiltration may be directed off the surface of the waste through the edge of the cover.

The breakthrough of the moisture front into the gravel is shown in figure 49, which presents the total predicted hydraulic head distribution in the cover after 382 hours of surface ponding. The maximum vertical head gradient was now at the base of the gravel, and no lateral flow occurred in the loess overlying the gravel following breakthrough. Moisture movement into the upper loess and gravel became nearly vertical. Lateral flow of moisture is still apparent in the lower layer of loess into which the wetting front had not yet progressed.

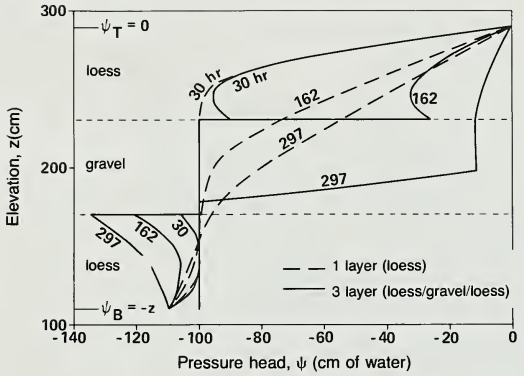

Figure 43 Comparison of predicted distribution of pressure head at selected times in a one-layer cover of Peoria Loess and in a three-layer cover of Peoria Loess, gravel and Peoria Loess at x = 100 cm under conditions of constant ponding at the surface and constant pressure head = –z at the bottom (Case 2).

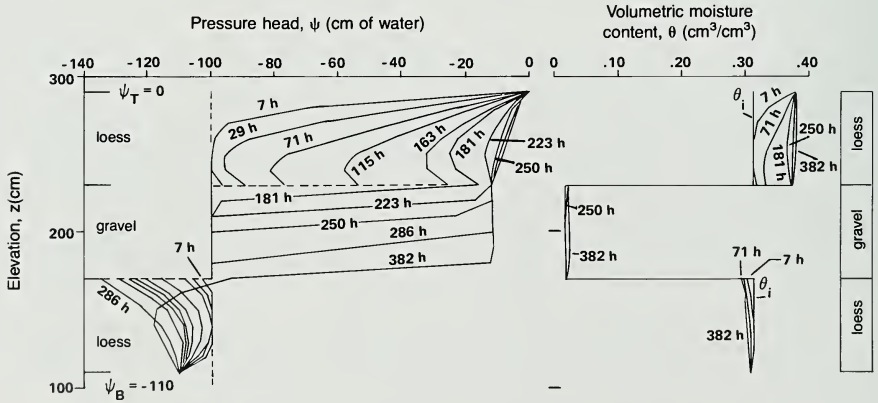

Figure 44 and **Figure 45** Predicted distribution of pressure head (left) and volumetric moisture content (right) at selected times in the three-layer cover at x = 100 cm under conditions of constant ponding at the surface and constant pressure head = –z at the bottom (Case 2).

Case 3 The system modeled in Case 3 is identical to that in Case 2 except for the boundary condition at the bottom of the cover. In Case 3 the pressure head of zero was held constant at the bottom of the three-layer cover. This corresponded to saturated conditions in the waste beneath the cover.

Given the initial conditions, the principal effect of this boundary condition was that significant upward flow of moisture into the lower layer of loess occurred in response to pressure head gradients. Figure 48 illustrates the predicted vertical pressure head distribution at 14 and 139 hours

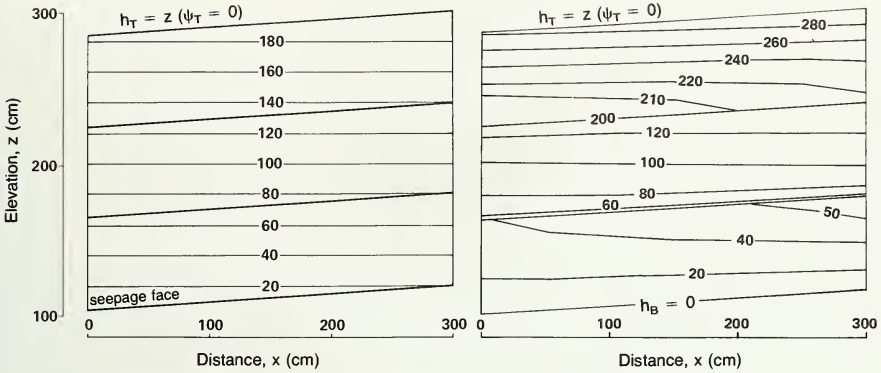

Figure 46 *left* Initial distribution of total hydraulic head (cm) in the three-layer cover corresponding to a constant pressure head = –z at the bottom (Case 2).

Figure 47 *right* Predicted distribution of hydraulic head (cm) in the three-layer cover under conditions of constant surface ponding and constant pressure head = –z at the bottom after 162.5 hours (Case 2).

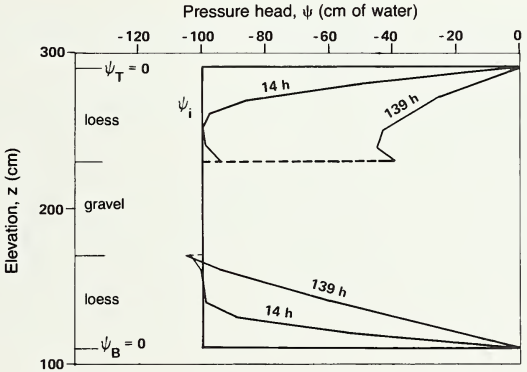

Figure 48 Predicted distribution of pressure head at selected times in the three-layer cover at x = 100 cm under conditions of constant ponding at the surface and constant pressure head = 0 (water table) at the bottom (Case 3).

for the column of nodes at x = 100 cm. As shown in the previous cases, however, the gravel layer formed a temporary barrier to moisture flow because of contrasts in unsaturated hydraulic conductivity with that of the overlying fine-grained layer. In Case 3, the same phenomenon occurred, limiting the upward flow of moisture from the water table. Figure 50 shows the total head distribution in the cover after 13.9 hours. As expected, the wetting front had not progressed very far below the surface; although, the upward flow from the saturated base of the cover into the loess was readily apparent. This upward flow also resulted in a significant lateral component of flow toward the edge

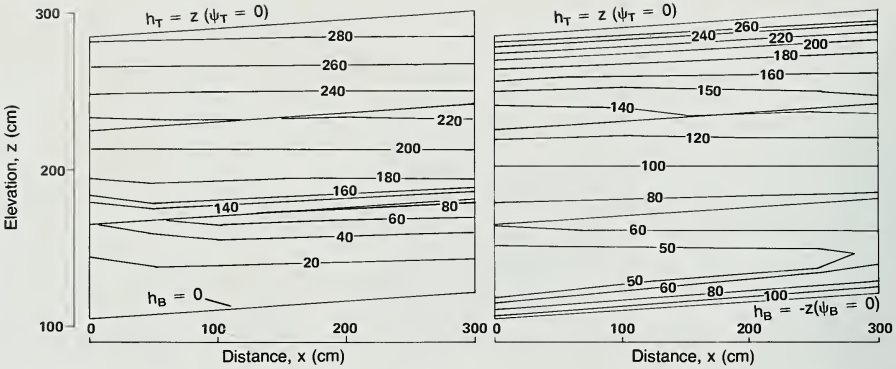

Figure 49 *left* Predicted distribution of hydraulic head (cm) after 382 hours in the three-layer cover under conditions of constant surface ponding and constant pressure head = –z at the bottom (Case 2).

Figure 50 *right* Predicted distribution of hydraulic head after 13.9 hours in the three-layer cover under conditions of constant ponding at the surface and constant pressure head = 0 (water table) at the bottom (Case 3).

of the cover, partly because of the downward gradient initially imposed on the system. The onset of lateral flow in the loess overlying the gravel was also already evident after 13.9 hours.

Case 4 Case 4 incorporates a seepage-face boundary at the bottom of the three-layer cover. As indicated previously, the seepage face behaves as a no-flow boundary as long as the boundary remains unsaturated; however, once the boundary is saturated, seepage occurs in response to hydraulic gradients and atmospheric conditions.

Figures 51 and 52 illustrate predicted vertical distributions of pressure head and volumetric moisture content at selected times for the column of nodes at the center of the cover at x = 300 cm. These results are quite similar to those for Cases 2 and 3 in the upper two layers. However, the seepage face at the bottom of the cover in Case 4 was initially unsaturated, and thus a no-flow boundary. Pressure head in the bottom layer, was initially assumed to be –100 cm throughout; it attained a steady-state distribution until the wetting front reached it after approximately 286 hours. As in Case 2, the pressure head in the gravel attained a relatively constant value (ψ_c) equal to that at the interface with the overlying loess. The volumetric moisture content of the gravel remained quite low, however, and increased significantly only after the wetting front had penetrated the entire system.

Figures 53 and 54 show the distribution of total hydraulic head after 171 and 289 hours in the three-layer cover with a seepage face at the bottom. After 171 hours (fig. 53), the total head distribution showed conditions immediately prior to moisture breakthrough into the gravel layer. Sharp vertical gradients were evident at the interface of the upper loess and the gravel. As in Cases 2 and 3, there was a lateral, downslope component of moisture flow in the loess overlying the gravel prior to moisture breakthrough. There was also a noticeable lateral gradient in the bottom layer because of the slope and no-flow nature of the unsaturated seepage boundary. Figure 54 shows the predicted distribution of total head after 289 hours. The moisture front had penetrated the gravel layer. Lateral flow was no longer noticeable in the loess overlying the gravel; however, some apparent lateral flow occurred within the gravel layers and in the underlying loess.

Figure 55 shows the predicted changes in pressure head as a function of time at four positions within the cover system in Case 4. Pressure heads increased steadily, corresponding to increasing volumetric moisture content in the upper layer of loess, approaching zero pressure 10 cm below the surface. At the interface between the upper loess and the gravel, pressure head began to rise after 1 hour and increased rapidly after about 30 hours. When the pressure head increased to

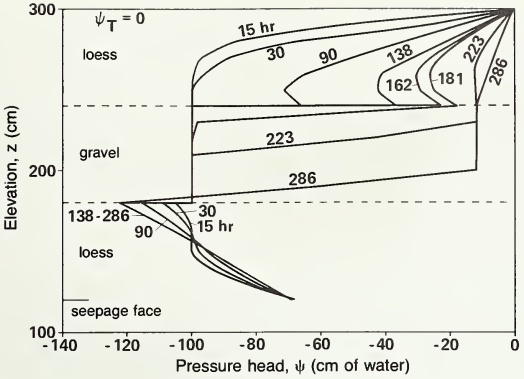

Figure 51 Predicted distribution of pressure head at selected times in the three-layer cover at x = 300 cm under conditions of constant ponding at the surface and a seepage face at the bottom (Case 4).

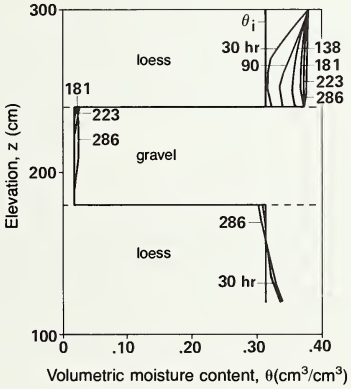

Figure 52 Predicted distribution of soil-water content at selected times in the three-layer cover at x = 300 cm under conditions of constant ponding at the surface and seepage face at the bottom (Case 4).

approximately 12 cm (ψ_c), moisture broke through into the gravel; the pressure head at the interface remained constant during the rest of the simulation. In the gravel, 10 cm below the interface, the pressure head remained at the initial pressure of –100 cm until the moisture front passed after approximately 170 hours, and the pressure head increased rapidly to that measured at the interface above. Subsequently, the pressure head in the gravel also remained constant throughout the rest of the simulation. Conversely, the pressure head at the interface of the gravel and the underlying loess decreased steadily after about 1 hour in response to redistribution of moisture resulting from the imposed initial condition of a constant pressure head of –100 cm to a steady-state distribution of no-flow.

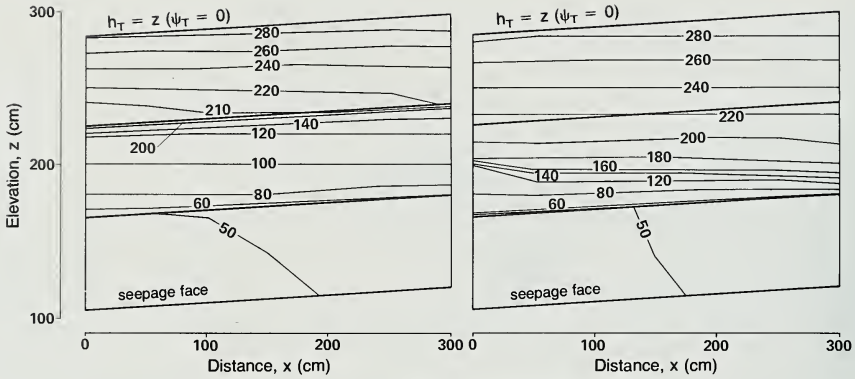

Figure 53 and **Figure 54** Predicted distribution of hydraulic head (cm) after 171 hours (left) and 289 hours (right) in the three-layer cover under conditions of constant ponding at the surface and a seepage face at the bottom (Case 4).

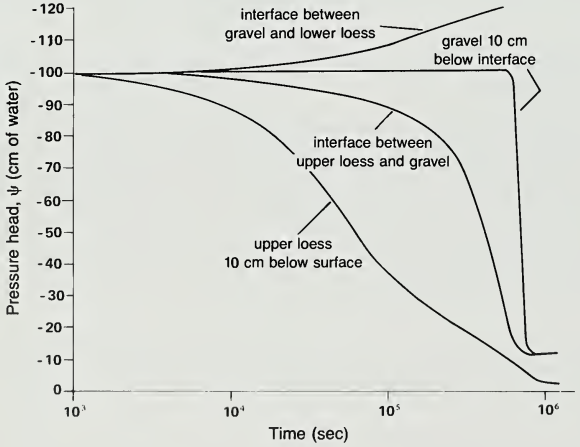

Figure 55 Predicted changes in pressure head with time at selected positions in the three-layer cover under conditions of constant ponding at the surface and a seepage face at the bottom (Case 4).

COLUMN STUDIES

Laboratory columns were constructed to further investigate cover performance. Design of the laboratory tests were suggested by computer simulations of columns using UNSAT2. The UNSAT2 simulations used sand as a coarse-textured soil and loess as a fine-textured soil. Boundary conditions included no-flow boundaries at the sides; constant ponding at the upper boundary; and several different conditions at the lower boundary. In the laboratory tests, we chose one set of boundary conditions and varied the composition of the layers. Boundary conditions were designed to be most similar to Case 4 of the computer simulations: constant ponding at the surface and freely draining (seepage force) bottom surface. We believe the bottom boundary represented realistic field conditions. The top boundary, although not realistic, was a practical means of providing a driving force for the experiment.

The laboratory test designs were also suggested by field designs. We chose materials and layering sequences to be as similar to field conditions as possible, considering the extreme reduction in scale required for column experiments. Hence, the laboratory columns did not duplicate either computer simulations or field experiments, but had characteristics of both. Within the limited scope of their design, they provided insight into some processes at work in trench covers. Because only one-dimensional flow could be considered, results only suggested possible field performance.

Soil moisture and density of the laboratory columns were measured using a dual-energy gamma-ray absorption device. This device permitted the nondestructive measurement of moisture and density as the experiment progressed. Dual-energy gamma ray adsorption devices have long been used in experiments of this type. Instrumentation and methodology were based on previous experiments by Ferraz and Mansell (1979) and Nofziger and Swartzendruber (1974). In Task II Report of this project, Johnson, et al. (1983) discussed our apparatus, methods, and preliminary results.

Our system utilized two colinear sources (300 mCi each of cesium-137 and americium-241) to produce a single, 1-cm-diameter beam of gamma energy (fig. 56). Prior to these runs, the system was calibrated and correction factors were determined for errors associated with high-energy interference in the low-energy band (Nofziger and Swartzendruber, 1974), dead-time resolution (Fritten, 1969), and systematic drift (Santo and Tsuji, 1977). Absorption coefficients determined for each material are listed in table 4.

Column Preparation

Laboratory soil columns were constructed to simulate field-scale trench covers. The same materials and layering scheme used in the field were used in the laboratory. The vertical scale was reduced in the laboratory experiments in order to facilitate construction; however, the layering proportions were not changed. The laboratory columns were prepared by compacting the soil materials into stackable, rectangular plexiglas molds. Each segment was 14.0 cm high and 7.1 cm along the inside axis parallel to the gamma beam. Columns of either four or seven segments were used in these experiments.

The column molds were filled in 2.5- to 5.0-cm lifts, which were compacted using a square-ended spring compactor having a spring tension of either 4.36 or 8.72 kg. The surface of each lift was scarified before the next lift was added. A small piece of geofabric was placed at the interface between soil types (fig. 56). This ensured separation of materials and prevented piping of the

Table 4. Absorption coefficients for test materials.

Material	Cesium absorption coefficient (cm/gm)	Americium absorption coefficient (cm/gm)
Water	0.0846837	0.1993545
Loess	0.0778150	0.4429088
Gravel	0.0816232	0.4540794
Till	0.0792380	0.4492152

Table 5. Moisture content and density of samples taken during construction and dismantling of laboratory columns

Column	Material	Construction			Dismantling		
		Moisture content (gm/gm)	Moisture content (cm^3/cm^3)	Dry density $(lb/ft)^3$	Moisture content (gm/gm)	Moisture content (cm^3/cm^3)	Dry density $(lb/ft)^3$
1-A	Loess	0.124	0.190	95.4	0.287	0.420	91.1
	Gravel	0.005	0.009	109.1	—	—	—
	Till	0.110	0.172	102.9	0.157	0.283	112.9
1-B	Loess	0.109	0.168	96.1	0.274	0.416	94.8
	Gravel	0.003	0.005	100.6	—	—	—
	Till	0.106	0.168	98.7	0.188	0.324	108.0
1-C	Loess	0.150	0.238	98.9	0.244	0.385	98.9
	Gravel	0.007	0.011	103.0	—	—	—
	Till	0.146	0.274	117.2	0.158	0.283	112.1
1-D	Loess	0.141	0.227	103.6	0.271	0.384	88.3
	Gravel	0.003	0.006	103.9	—	—	—
	Till	0.123	0.213	114.8	0.145	0.267	115.6
3	Till	0.132	0.260	122.7	0.131	0.243	120.2
	Gravel	0.002	0.003	107.2	—	—	—
	Till	0.135	0.258	119.8	0.131	0.260	126.5
4	Loess	0.125	0.196	97.9	0.198	0.324	102.3
	Gravel	0.001	0.002	100.2	—	—	—
	Till	0.120	0.236	122.8	0.118	0.235	124.5
Modified proctor	Loess	0.13	0.23	108.5			
	Till	0.11	0.21	121.8			

highly dispersive loess. The columns were built on a perforated metal baseplate, which allowed drainage to be collected.

Samples of the column materials were collected at measured intervals during both construction and dismantling of the columns. These samples were used to determine volumetric moisture content and density of the materials and check the validity of the calculations made using the gamma-ray device. The measured values of density and moisture content are tabulated in table 5. The listed values represent averages of several samples from the specified material layer. The maximum density and optimum moisture content as determined by the Modified Proctor Test are also listed for the till and loess. These standard values can be compared to those produced in column construction. Since the compaction methods were different from those used in the test, any comparison can only be approximate.

In this sequence, columns 1-A, 1-B, 1-C, and 1-D all had similar layering, but column 1-D was shorter than the others. Column 4, which corresponded to field cover 3, differed from columns 1-A, 1-B, and 1-C in the proportion of loess to gravel; half the gravel was replaced by loess. The till layers in columns 1-A and 1-B were constructed from till that was crushed while wet. The rest of the till layers were constructed using till that had been crushed and sieved after having been dried. This difference in construction technique resulted in a significant difference in initial density with the dry-crushed till having a much higher density. This difference also carried over to the final results. The columns that had low initial density showed a large increase in both volumetric moisture content and density. Those that began with a high initial density exhibited only small increases in volumetric moisture content and density, and some showed a slight decrease in volumetric moisture content.

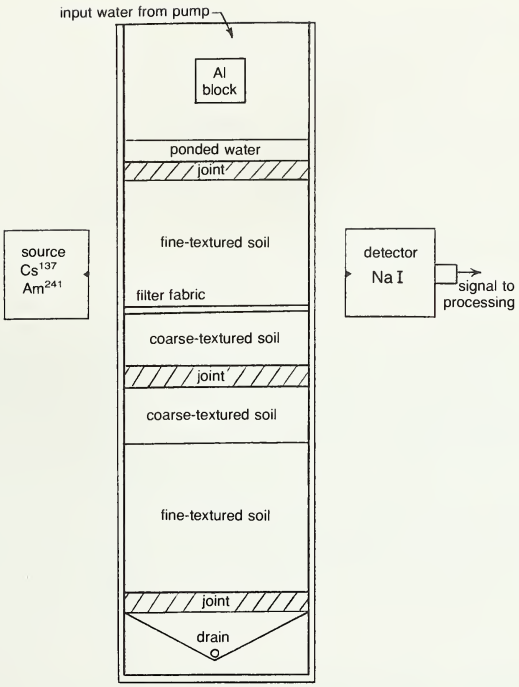

Figure 56 Diagram of gamma column used to simultaneously determine moisture content and bulk density.

Results

The change in calculated volumetric moisture content with time for each column is plotted in figures 57 to 62. Values plotted for each material indicate changes at representative locations in the column. Initial values were adjusted to correspond to measured volumetric moisture contents determined gravimetrically during column construction. Subsequent values indicate the relative change from this initial value. The final volumetric moisture contents determined during the dismantling of the columns are also plotted, thus providing a check on the accuracy of the gamma-ray determinations.

The final error in the loess, defined as the difference between the actual final measured volumetric moisture content and that indicated by gamma-ray determination, was 9.4 percent, which was acceptably within the sensitivity of the instrument. The error in the till was independent of the error in the loess and averaged 20 percent. This relatively large error was consistently positive, possibly indicating that the absorption coefficients for the till were incorrect. Fortunately, accurate determination of moisture changes in the till were not as critical to the experiment as accurate determinations in the loess. Although refinement of the till analysis would probably result in more accurate values, these errors were within acceptable limits.

Columns having loess as an upper layer all showed an immediate rise in volumetric moisture content in the loess with a sharp peak followed by a leveling off of volumetric moisture content at a somewhat higher value. In these columns, moisture was also detected moving into the gravel below, after delays of various lengths of time.

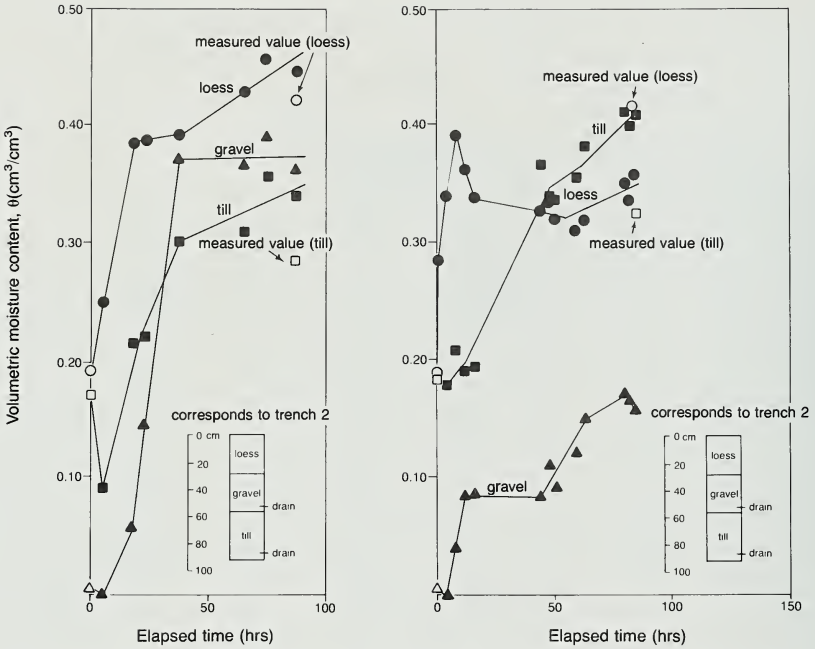

Figure 57 and **Figure 58** Change in moisture content with time in laboratory soil columns 1-A (left) and 1-B (right) under conditions of constant ponding at the surface.

One column had till as the upper layer. In column 3, very little change in moisture was detected in the upper layer over a period of more than 650 hours of constant ponding. During this period, no moisture was detected in the gravel, which was also observed to be dry when the column was dismantled. Although the results from column 3 showed the extremely low permeability of the till, they could not be used to test the wick effect. We could not determine if moisture was held in the upper layer because of the gravel, or if it was just moving very slowly.

The five columns that had loess as an upper layer could be used, however, to test the wick effect. The amount of time to reach peak volumetric moisture content in the loess and initial moisture increase was determined for each of these columns. These measurements were imprecise as a result of the occasionally long time interval between gamma-beam scans of the columns. Therefore, the median time between the first record of either the peak or initial moisture increase and the preceding measurement was used as the accepted value. These data are presented in table 6. A composite measurement, the delay, is also included in table 6. The delay is the time difference between the time to peak moisture in the loess and the time to initial moisture increase in the gravel below. A negative value implies that moisture began to move into the gravel before the peak was reached in the loess above. In column 1-C, no delay could be determined because of the imprecision in the measurements.

The correlation between the thickness of the upper layers and the initial moisture entry into the gravel is weak ($r = 0.39$) indicating that the delay was not caused by an increase in thickness. In fact, the correlation between the delay and thickness is even weaker ($r = 0.19$). The delay was also not dependent on the initial volumetric moisture content of the loess ($r = 0.32$). However, a correlation ($r = 0.63$) does exist between the delay and the initial density of the loess.

Table 6. Moisture and time measurements in laboratory columns.

Column	Time to peak moisture in loess (hr)	Time to initial moisture increase in gravel (hr)	Delay (hr)
1-A	17.5	11.5	–6
1-B	8	6	–2
1-C	6	6	0
1-D	4	14	10
4	4	20.5	14.5

A secondary objective of this experiment was the study of drains. The drainage system at the base of the gravel layer was an important component of our field experiment since, even if a wick effect were established, moisture would eventually enter the gravel. With drains, moisture would be removed before it could penetrate the lower soil layer. Ultimately, some moisture entry into the lower soil layer would be unavoidable and is acceptable because it would prevent dehydration fractures. For the drain system to function, the gravel must be nearly saturated at the level of the drain. Therefore, we sought a soil layer system in which moisture would pond at the base of the gravel, so that it could be removed by the drain.

Qualitative observations made during the experimental procedure provided insight into this problem. Of the five columns in which moisture entered the gravel, only one (1-A) failed to drain water from the base of the gravel. Significantly, the density of the till in this column was much lower than that in any of the others. This was also one of the two columns in which the wet-crush method of preparing the till sample was utilized. This indicated that the ponding phenomenon was also related to density, and therefore hydraulic conductivities.

Conclusions

Laboratory soil columns provided useful information and insights into possible performance of field experiments. Density of compacted materials was apparently important; increased density resulted in lower permeability and lower saturated hydraulic conductivity.

Moisture movement through compacted till layers was very slow; we could not detect any moisture movement into gravel below the till in column 3. This suggested that long monitoring periods will be required for larger field experiments before results will become available.

Moisture moved rapidly through compacted loess layers. Investigation of the wick effect using loess and gravel layers was not effective. We believe that the wick effect was established for short periods in some of our columns. However, the loess became saturated so rapidly that it was difficult to clearly detect delay of moisture movement into the gravel below. Less severe upper boundary conditions (such as constant small flux) might have produced more conclusive results.

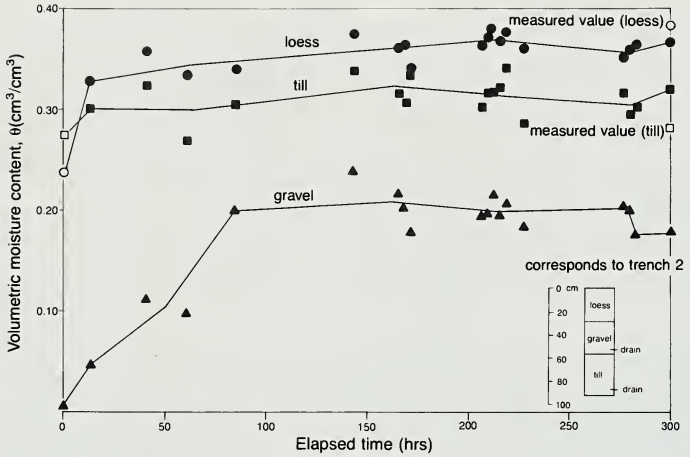

Figure 59 Change in moisture content with time in laboratory soil column 1-C under conditions of constant ponding at the surface. This column corresponds to trench cover 2 at the Sheffield study site.

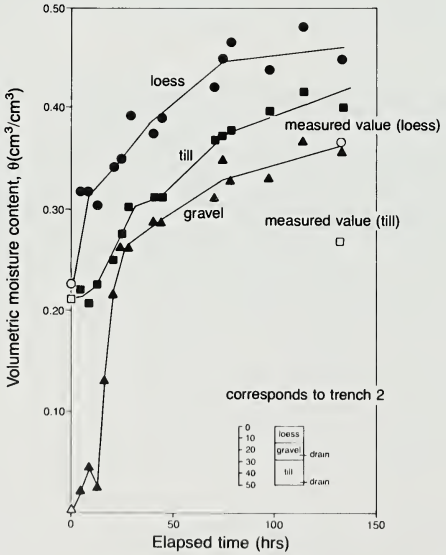

Figure 60 Change in moisture content with time in laboratory soil column 1-D under conditions of constant ponding at the surface. This column corresponds to trench cover 2 at the Sheffield study site.

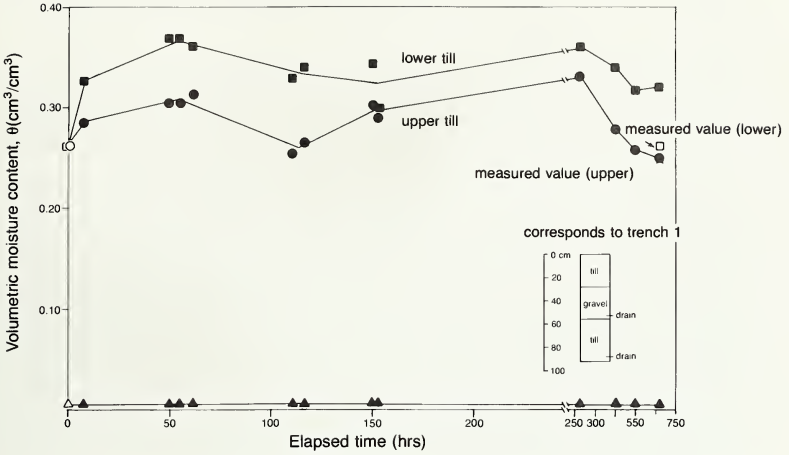

Figure 61 Change in moisture content with time in laboratory soil column 3 under conditions of constant ponding at the surface. This column corresponds to trench cover 1 at the Sheffield study site.

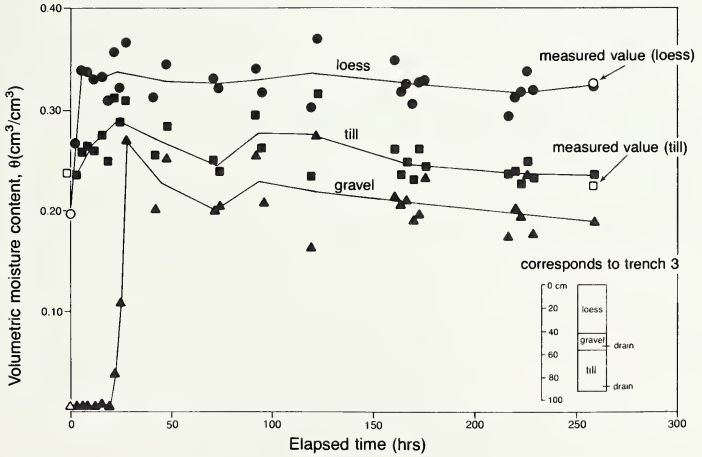

Figure 62 Change in moisture content with time in laboratory soil column 4 under conditions of constant ponding at the surface. This column corresponds to trench cover 3 at the Sheffield study site.

CONSTRUCTION OF FIELD-SCALE EXPERIMENTAL TRENCH COVERS

Designs

• Site and Material Selection

Based on the results of laboratory tests and computer modeling, four layered-soil cover designs were selected for field-scale tests in experimental trenches at the Sheffield, Illinois study site (fig. 63). Construction of the experimental trench covers began in December 1982 and was completed in July 1983. The approximately 1-hectare (2.5 acre) study site in Bureau County is located adjacent to the Sheffield low-level radioactive waste-disposal site.

The selection of geologic materials for detailed laboratory testing, computer simulation, and ultimately, for use in experimental trench covers was based on similarity to materials already tested and actually present near the study site. These geologic materials included Peoria Loess, a windblown silt common in Illinois and present at the study site; it has been used in covers at the adjacent Sheffield waste-disposal site. The fine-grained, Wisconsinan Tiskilwa Till, hauled to the study site from a borrow pit near Tiskilwa 30 km away, is genetically related to and has physical properties similar to the Fairgrange Till included in the preliminary laboratory tests and computer simulations. The coarse-grained material used in the trench covers was commercial river-run pea gravel. Characteristics of the earth materials used in construction of the experimental trench covers are listed in table 7 and in the section, Evaluation of Geologic Materials of this report.

• Lower Layers

The four experimental, layered-soil trench covers were approximately 6 m (20 ft) wide and 15 m (50 ft) long. Each cover was installed within a shallow trench excavated to a depth of 90 cm (3 ft).

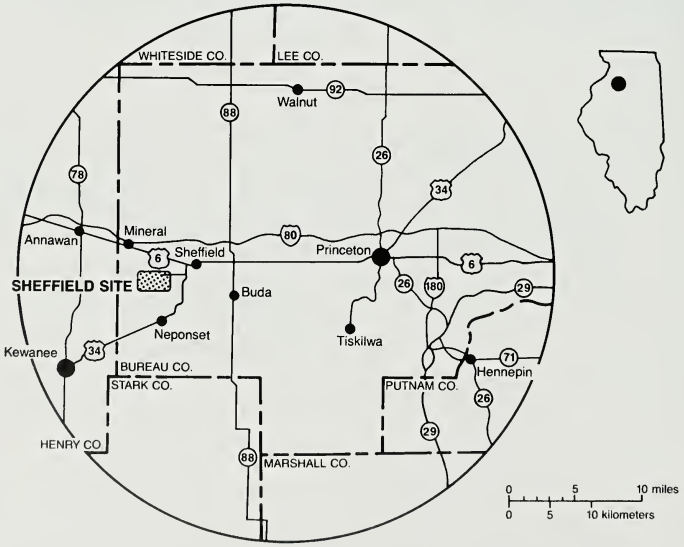

Figure 63 Location of Sheffield study site.

Table 7. Characteristics of earth materials used in field-scale experimental trench covers

	Saturated hydraulic conductivity (cm/sec)[a]	Compaction test[b]		
		Optimum gravimetric moisture content (%)	Maximum dry density (pcf)	(g/cm^3)
Loess	1.5×10^{-5}	12.7	109.2	1.75
Gravel	5.5×10^{-2}	---	---	---
Tiskilwa Till	4.0×10^{-9}	10.3	123.0	1.97

[a]determined from laboratory tests.
[b]determined by ASTM D-698; average of 3 samples.

The width and thickness of the experimental covers were virtually identical to those used in the two-dimensional, field-scale simulations. Figure 64 presents both a plan view and cross sections of each experimental trench cover. The base of each trench sloped 5 percent toward the center and 5 percent longitudinally (toward the north) so that water penetrating the cover could be collected in a longitudinal drain. The bottom of each trench was lined with impermeable PVC plastic (geomembrane) to prevent moisture movement into or out of the surrounding soils. Polypropylene geofabric was used above and below the plastic liner to protect the liner during construction. Physical properties of the geofabric are listed in table 8. A 30-cm (1-ft) layer of pea gravel with drains simulated stable waste and constituted a base for the overlying trench cover. Geofabric separated the gravel from the overlying compacted soil.

Table 8. Characteristics of Typar(R) polypropylene filter fabric used in field-scale covers and in laboratory, column experiments (data supplied by manufacturer)

Thickness	0.33 mm (0.013 in.)
Approximate pore size	0.3 mm
Hydraulic conductivity	3×10^{-2} cm/sec

A 60 to 75 cm (2 to 2.5 ft) thick basal layer of Tiskilwa Till, compacted 2 percent wet of optimum, overlay the gravel in each trench. Compacting till at a gravimetric moisture content wet of optimum should further decrease its hydraulic conductivity. The upper surface of the basal till layers was made to coincide with the natural ground surface. The plastic liner that covered the bottom of the trenches was also brought around the sides of the trenches and wrapped back into the covers. In covers with intermediate gravel layers (see below), the liner was brought outside (above) the gravel and terminated above the lateral drain (fig. 64). In the cover without an intermediate gravel layer, the liner was folded back onto the surface of the till and terminated about 30 cm (1 ft) from the edge.

- **Upper Layers**

In cover 1, a middle layer of pea gravel 60 cm (2 ft) thick was placed above the basal till. Geofabric was used above the gravel to maintain the interface with the overlying fine-grained material. The top layer, 60 cm (2 ft) of Tiskilwa Till, was compacted 2 percent dry of optimum to increase its capacity to store water for subsequent evapotranspiration.

Cover 2 was designed to test the importance of the contrast in hydraulic conductivity between the upper, fine-grained layer and the intermediate, coarse-grained layer. In this cover, Peoria Loess, compacted 2 percent dry of optimum substituted for the Tiskilwa Till used in the upper layer of cover 1. The loess/gravel sequence provided a saturated hydraulic conductivity contrast of approximately 10^3 cm/sec, while the till/gravel sequence provided a contrast of at least 10^5 cm/sec.

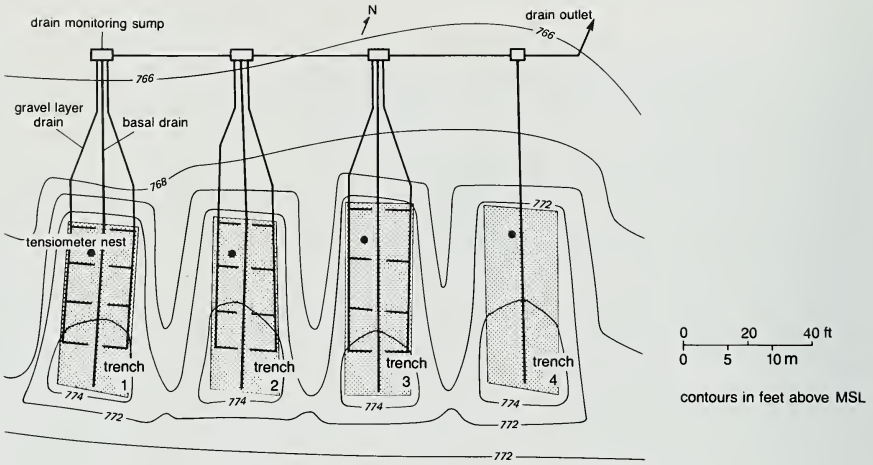

Figure 64a Plan view of experimental trench covers at the Sheffield study site.

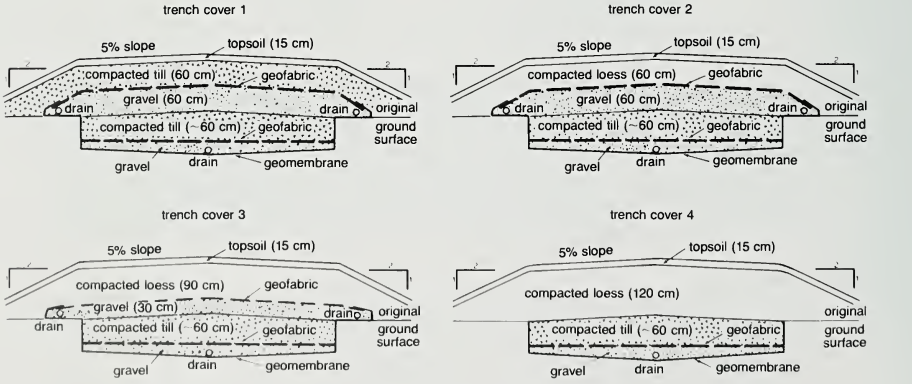

Figure 64b Cross sections of each of the experimental trench covers at the Sheffield study site.

The effects associated with varying the thickness of the upper two layers were studied in cover 3. Cover 3 was the same composition as cover 2 (loess over gravel over till), but the gravel layer was reduced to 30 cm (1 ft) and the loess increased to 90 cm (3 ft) in thickness.

Cover 4 was used to compare the proposed layered design to currently used single-layer designs. Similar to existing covers at the Sheffield radioactive waste site, Cover 4 was modeled after the newer covers at the Barnwell, South Carolina site. It consisted of 1.2 m (4 ft) of compacted Peoria Loess over 60 cm (2 ft) of compacted Tiskilwa Till without an intermediate gravel layer.

All layers as well as the ground surface sloped laterally 5 percent from the center of the cover and 5 percent longitudinally (to the north). The layers built above ground surface continued to slope to a point above the edge of the trench. Gravel layers extended 30 to 60 cm (1 to 2 ft) onto the ground surface covering lateral drains. Sides of all other upper layers sloped down to the ground at a 2:1 pitch on east and west sides (fig. 72) and at 3:1 pitch on north and south sides.

The 15-cm (6-in.) layer of topsoil placed over each cover as a rooting medium was seeded with a mixture of grasses, mainly fescue (Kentucky No. 31) with small amounts of rye grass (Balboa) and timothy. The fescue was chosen because root penetration is typically only 8 to 10 cm (3 to 4 in.) deep and maximum growth is limited to 30 to 45 cm (12 to 18 in.) high.

Construction History

- **Preliminary Work** (December 22-31, 1982, and March 14-16, 1983)

Construction of the field-scale, experimental trench covers began December 22, 1982, with the removal and stockpiling of topsoil from the site. Drainage lines and drain sump boxes for each trench were then installed. The drainage pipe consisted of corrugated polyethylene tubing 10.2 cm (4 in.) in diameter. Nonperforated drainage pipe connected the perforated drain at the base within each trench with each monitoring sump box. The sump boxes were connected by perforated drain piping, which ultimately discharged into a low area north of the site. Due to the shallow water table at the site, groundwater began to enter the drainage system and discharge almost immediately. Excavation of the four trenches using a large backhoe was completed by December 31, 1982. At that time seepage of groundwater into trench 4 was also observed. Construction was stopped shortly afterward for the winter.

Construction resumed March 14, 1983, with the placement of geofabrics and the plastic liner in the bottom of each trench. Due to the cold weather, some difficulty was encountered while attempting to glue the seams in the plastic liner, and several seams had to be reglued. Difficulty was also found in connecting the drain in each trench through the plastic liner with the drain pipe heading to the sump boxes.

- **Placement of Lower Layers** (March 17-May 9, 1983)

Following placement of the drain, gravel layer, and overlying geofabric in the bottom of each trench began delivery of till (Tiskilwa Till) from a borrow pit near Tiskilwa, Illinois, approximately 33 km (20 mi) east of the site. Compacted till, placed in five or six thin lifts, constituted the basal layer of each of the four experimental trench covers. Due to the dense nature of the extremely hard glacial till, great difficulty was encountered in breaking down the relatively large pieces of till prior to placement and compaction. A garden tractor equipped with a rototiller was used to prepare the till that was being stockpiled at the construction site. Placement of the first lifts of till upon the geofabric and underlying gravel in the trenches began April 21, 1983. In general, each lift of till was approximately 20 cm (8 in.) thick prior to compaction. Compaction was accomplished using 545-kg (1200-lb) portable vibratory compactors. Following compaction, the thickness of each lift was approximately 8 to 10 cm (3 to 4 in). The density and gravimetric moisture content of each compacted lift were checked at several locations immediately following placement using both a nuclear moisture/density meter and the balloon density test. Subsequent lifts were emplaced only after acceptance of the previous lift by the supervising engineer. Except for the interface between the first two lifts in each trench cover, the surface of each lift was scarified prior to placement and compaction of the next lift. In order to protect the underlying geofabric, the first lift of till was not scarified. An evaluation of compaction performance follows this section of the report.

In order to further reduce hydraulic conductivity, the basal layer of glacial till in each trench was compacted at a gravimetric moisture content slightly (approximately 2%) wet of the optimum

Table 9. Average gravimetric moisture content and degree of compaction of upper and lower layers in each trench cover based on combined results of balloon density test and nuclear moisture-density meter (percent compaction refers to density achieved compared to maximum density from Standard Proctor Test)

	Materials	Gravimetric moisture content (%)	Degree of compaction (%)
Cover 1			
Upper layer	till	13.5	99.0
Lower layer	till	11.7	99.1
Cover 2			
Upper layer	loess	14.1	94.9
Lower layer	till	11.4	96.1
Cover 3			
Upper layer	loess	14.2	95.6
Lower layer	till	11.6	96.5
Cover 4			
Upper layer	loess	10.1	97.6
Lower layer	till	11.4	95.7

gravimetric moisture content determined in Proctor Compaction tests. The natural gravimetric moisture content of the till, however, was generally very similar to the optimum gravimetric moisture content—approximately 10.8 to 11.3 percent by weight. Therefore, water was added to the till prior to placement in the trench. By May 9, the basal layer of till had been placed in all four trenches. The surface of the till layer in each trench was also graded to provide 5 percent slopes toward the edges and north end of each trench.

• **Placement of Upper Layers** (May 10-June 8, 1983)
The loess used in the construction of trench covers 2, 3, and 4 was obtained from a borrow pit 1 km (0.6 mi) east of the site. The natural gravimetric moisture content of the loess delivered to the construction site was approximately 16 percent by weight, somewhat greater than the optimum gravimetric moisture content of approximately 13 percent determined in laboratory tests. The upper layer of loess or till in each trench cover was designed to be compacted at a gravimetric moisture content slightly (2 percent) dry of optimum to increase the capacity to store water for subsequent evapotranspiration. It was therefore necessary to dry the loess stockpiled at the site prior to placement and compaction. Despite periods of warm sunny weather, the silty loess proved difficult to dry out rapidly. Therefore, several lifts of loess with a gravimetric moisture content approximately equal to optimum were accepted during construction.

On May 10, placement and compaction of the upper layer of loess began on trench cover 4, which does not have an intermediate gravel layer. Concurrently, the intermediate gravel layer drainage system consisting of perforated, corrugated drainage pipe wrapped in geofabric was installed directly on the till surface in trench cover 3. The drain system was then covered with 30 cm (1 ft) of gravel, the surface of which was then graded and overlain by geofabric. The first lift of compacted loess was then placed on the gravel layer in cover 3 on May 11.

For several days after May 11, construction was halted because periodic rain made it difficult to dry the loess prior to compaction. Following the layout of the drain pipe system, a 61-cm (2-ft) layer of gravel was placed in cover 2, then graded and covered with geofabric. The gravimetric moisture content of the uppermost lifts of loess in trench covers 3 and 4 was found to be somewhat high—14 to 15 percent. After remixing and additional drying of the most recent lifts, the trench covers were recompacted and accepted with a gravimetric moisture content of approximately 13 percent. The first lift of loess was then placed on trench cover 2.

A 61-cm (2-ft) layer of gravel was next placed on trench cover 1. Following the placement of geofabric, the first lift of glacial till was compacted in trench cover 1. The gravimetric moisture content of the till which had been stockpiled at the contruction site was approximately 11 percent,

slightly less than optimum. It was decided that this gravimetric moisture content would be acceptable if a density greater than 90 percent of maximum Proctor density could be achieved. Compaction of subsequent lifts of loess in each of the other three trenches also proceeded. Because of difficulty in drying the loess, however, the gravimetric moisture content had to be monitored closely. After testing, several lifts of loess were rejected and had to be remixed, allowed to dry, and recompacted.

The upper layer of till in trench cover 1 was completed on May 26, and after several days of wet weather, the upper layer of loess in trench cover 4 was completed on June 7. A 15-cm (6-in.) layer of topsoil was then added to the surface of trench covers 1 and 4. By June 9, the upper layers of loess in trench covers 2 and 3 were completed and 15 cm (6 in.) of topsoil was applied. Topsoil was then spread over the remainder of the site area and the surface graded.

- **Seeding** (October, 1983)

Shortly after applying topsoil to the site, native grasses and weeds began to reestablish themselves forming a thick ground cover within several weeks. To prepare the site for seeding with the desired mixture of grass types, the site was mowed and disked on October 3. The entire site was then seeded with a mixture of predominantly fescue with small amounts of rye and timothy.

Soil Compaction Performance

Representatives of the consulting engineering firm, Daily and Associates, Inc., of Peoria, Illinois, monitored conditions during construction of the experimental covers to ensure that the desired density and gravimetric moisture content of each lift of compacted soil were achieved. Density was measured in the field by either the volumeter balloon test (ASTM D-2167) using a Humboldt Voluvessel or by using a nuclear moisture-density device (Seaman Nuclear Corporation Model C-75 Density Meter with a radium-beryllium source). Gravimetric moisture content was determined at the field site using the nuclear moisture-density meter and/or by drying in a microwave oven. Table 9 summarizes the results of tests of gravimetric moisture content and density of the upper layer of loess or till, and the lower layer of till within each trench cover.

Most lifts of compacted till and loess achieved at least the specified 90 percent of maximum dry density determined by the Standard Proctor Compaction Test (ASTM D-698). The maximum dry density used for determination of the percent compaction achieved was 1.97 g/cm^3 for the Tiskilwa Till and 1.75 g/cm^3 for the loess. The optimum gravimetric moisture content determined from the Standard Proctor Test was approximately 10.3 percent for the till and 12.7 percent for the loess.

During construction, three lifts of compacted till were rejected initially because of low gravimetric moisture content and low density. These lifts were then scarified, wetted, recompacted, and rechecked prior to acceptance. Nine lifts of loess were rejected because of high gravimetric moisture content and low density; these lifts were reworked and allowed to dry prior to recompaction. Considerable variations in gravimetric moisture content and density were still observed in compacted soils within each cover. While these variations are not extreme or unexpected, the lack of homogeneity and the presence of observable cracks in some lifts suggested that water movement through an individual lift would probably not be uniform.

The average gravimetric moisture content and density of each layer in the experimental trench covers were calculated based on combined data from both the balloon test and the nuclear moisture-density meter. The results (table 9) indicate that the average density achieved for all lifts in both the upper and lower compacted layers in each trench was considerably greater than the minimum specified density for construction. The specified minimum was 90 percent of the maximum density from the Standard Proctor Test. The average gravimetric moisture content of all lifts in the lower layer of compacted till in all four covers was approximately equal to the optimum gravimetric moisture content of 11.6 percent. The original plans specified that this lower layer of till was to be compacted at a gravimetric moisture content approximately 2 percent wet of optimum; however, this was not uniformly achieved because of the low natural gravimetric moisture content of the till. The upper layer of each cover was originally to be compacted at a gravimetric moisture content slightly (2%) dry of optimum to increase moisture storage capacity. This was easily achieved in the upper layer of till in cover 1, which had a relatively low natural gravimetric moisture content. However, because of the relatively high natural gravimetric moisture content of the loess, the gravimetric moisture content of the upper layers of loess in covers 2, 3, and 4 averaged 13.5, 14.1, and 14.2 percent—slightly greater than optimum.

FIELD MONITORING OF EXPERIMENTAL PROTOTYPE COVERS

Phase One: July–November, 1983

- **Instrumentation**

Two procedures were used in the initial phase of the monitoring program for the field prototype covers: tensiometer networks and observation of water flow from the drains. Tensiometer studies yielded most of the data collected at the site.

Monitoring began in July 1983 when tensiometers were installed in the trenches and at a background location. All were standard gauge tensiometers (Model 2725) manufactured by Soil Moisture Equipment Corporation of Santa Barbara, CA. The tensiometers were installed in the northwest quadrant of each trench (fig. 63, Field-Scale Experiments section). The instruments were placed at depths ranging from approximately 30 to 150 cm (1 to 5 ft) in order to monitor each horizon. A typical tensiometer nest is shown in figure 65. Each nest generally consisted of two tensiometers in the upper layer (loess or till), one in the gravel, and one at each interface between gravel and fine-grained material. The actual depths and materials monitored are listed in table 10. Cover 2 has no tensiometer at the gravel till interface because caving of the gravel prevented deeper insertion.

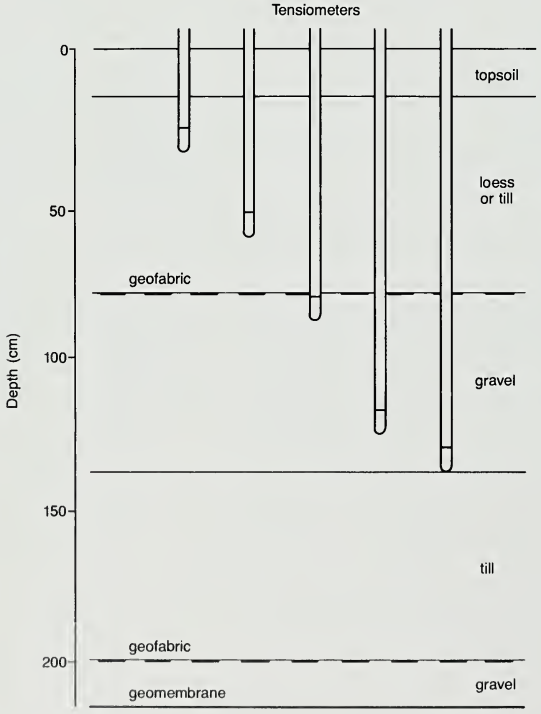

Figure 65 Schematic diagram of tensiometer nest used in the Phase 1 monitoring program.

Table 10. Phase 1 tensiometer installation data

	Tensiometer no.	Depth (cm)	Depth (in)	Material monitored
Cover 1	1-1	30	12	till
	1-2	58	23	till
	1-3	84	33	gravel
	1-4	122	48	gravel
	1-5	135	53	gravel
Cover 2	2-1	33	13	loess
	2-2	61	24	loess
	2-3	91	36	loess/gravel interface
	2-4	124	49	gravel
Cover 3	3-1	25	10	loess
	3-2	33	13	loess
	3-3	64	25	loess
	3-4	81	32	loess
	3-5	124	49	gravel
Cover 4	4-1	30	12	loess
	4-2	61	24	loess
	4-3	91	36	loess
	4-4	122	48	loess
	4-5	152	60	till

The tensiometers were installed by pushing a soil probe slightly larger in diameter than the tensiometer to a depth of 1 ft above the position at which the ceramic tip was to be set. A soil probe slightly smaller in diameter than the tensiometer was then pushed to the desired depth. After filling the tensiometer with water and zeroing the gauge at saturation, the tensiometer was inserted in the hole. By using a smaller soil probe for the bottom of the hole, good contact between the ceramic tip of the tensiometer and the surrounding materials was established. Granular bentonite was used to fill the annular space around the tensiometer tube near the land surface to prevent water from running down the side of the tensiometers. Additional tensiometers were installed in early October as the need for more data became apparent.

Due to the distance to the field site, data were collected at irregular intervals. From mid-September, until early November, however, efforts were made to collect data at least bi-weekly. Hence, the majority of the data were collected in the last six weeks of this phase of the monitoring program.

All tensiometers were removed after the first hard frost in the area—the first phase of the monitoring program ended on November 7, 1983. Since the water-filled gauge tensiometers are destroyed by freezing conditions, they could not be used through the winter. Three of the shallow tensiometers stopped functioning before we were able to remove them, even though they had been covered with straw to insulate them from light freezes.

Perimeter and center drains in each cover sump were checked whenever the tensiometers were read. All center drains began dripping slowly immediately after the trenches were built and this continued into September. No sustained discharge was ever observed from any of the perimeter drains during this period. We believe that the water discharging from the drains during this period originated during trench construction and was not the result of infiltration through the cover.

Daily rainfall data, necessary to interpret the tensiometer results, were obtained from a U.S. Geological Survey rain gauge at the Sheffield low-level radioactive waste disposal site, about 1 km northeast of the cover study site. The rainfall data for the monitoring season are shown in figure 66.

LIBRARY

NOV 22 1989

ILL. STATE GEOLOGICAL SURVEY

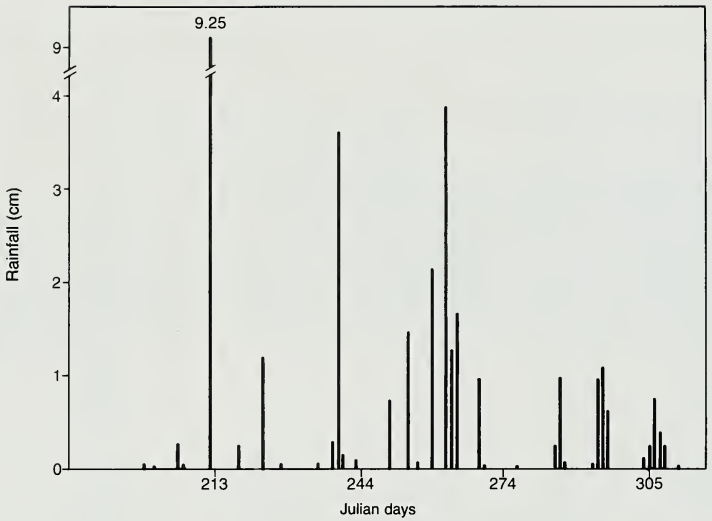

Figure 66 Daily rainfall for the monitoring period July - November, 1983. Data from U.S. Geological Survey rain gauge located 1.0 km from the cover study site.

• Results of Field Monitoring

Total head, h, in centimeters of water is shown for the tensiometer nests in the four covers in figure 67. Total head is calculated using the relationship

$$h = \psi - z$$

where z is depth,
ψ is pressure head.

According to this convention, wetter conditions result in greater values of head. At saturation, ψ becomes zero, and total head increases linearly with decreasing depth.

Variations in total head with time in cover 1 are illustrated in figure 67, which shows a strong correlation of head with rainfall for the upper till layer; total heads rose quite high and were nearly equal by November. For the gravel layer in cover 1, measurements of total head were very stable and significantly greater than in the overlying till immediately after construction. However, as moisture redistribution occurred and the cover responded to precipitation, total head in the gravel began a general decrease which continued through September (day 270). Before September, hydraulic gradients were very erratic. By mid-September (day 260), a generally consistent pattern developed wherein a downward gradient was created in the upper till layer. In the gravel, however, upward hydraulic gradients were maintained throughout the remainder of the monitoring period. Fluctuations in head were apparent at each depth, but total heads in the gravel were consistently lowest at the 84 cm depth. This would appear to indicate that after cover 1 equilibrated following construction significant infiltration into the gravel did not occur.

Calculated values of total head within the loess (tensiometers 2-1, 2-2, 2-3) in cover 2 (fig. 67), also fluctuated widely from July until September, when relatively consistent patterns developed. From mid-September until November, a consistent downward gradient was present down to the loess/gravel interface suggesting that significant moisture might have moved vertically into the gravel. The total head at the base of the gravel, which was also quite similar to the total head at

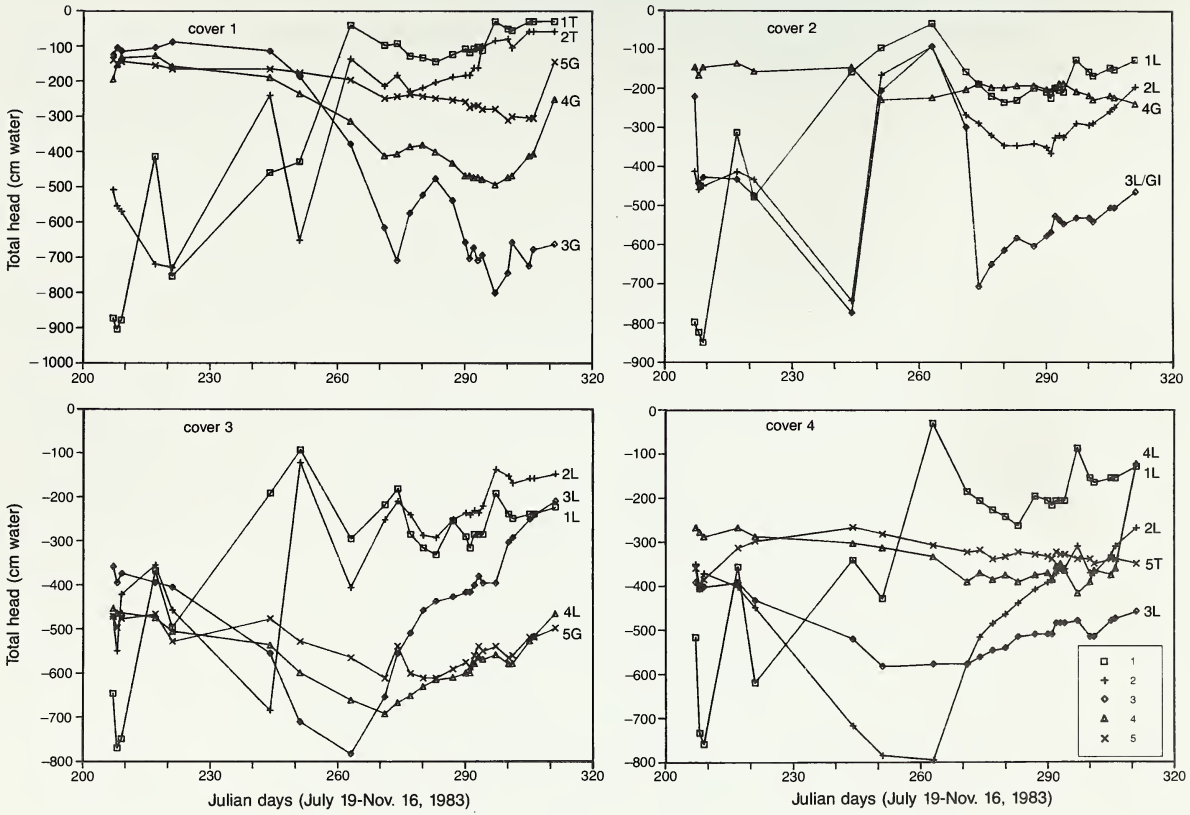

Figure 67 Tensiometer readings from various depths in the four covers plotted as total head for the period July 19 through November 16, 1983.

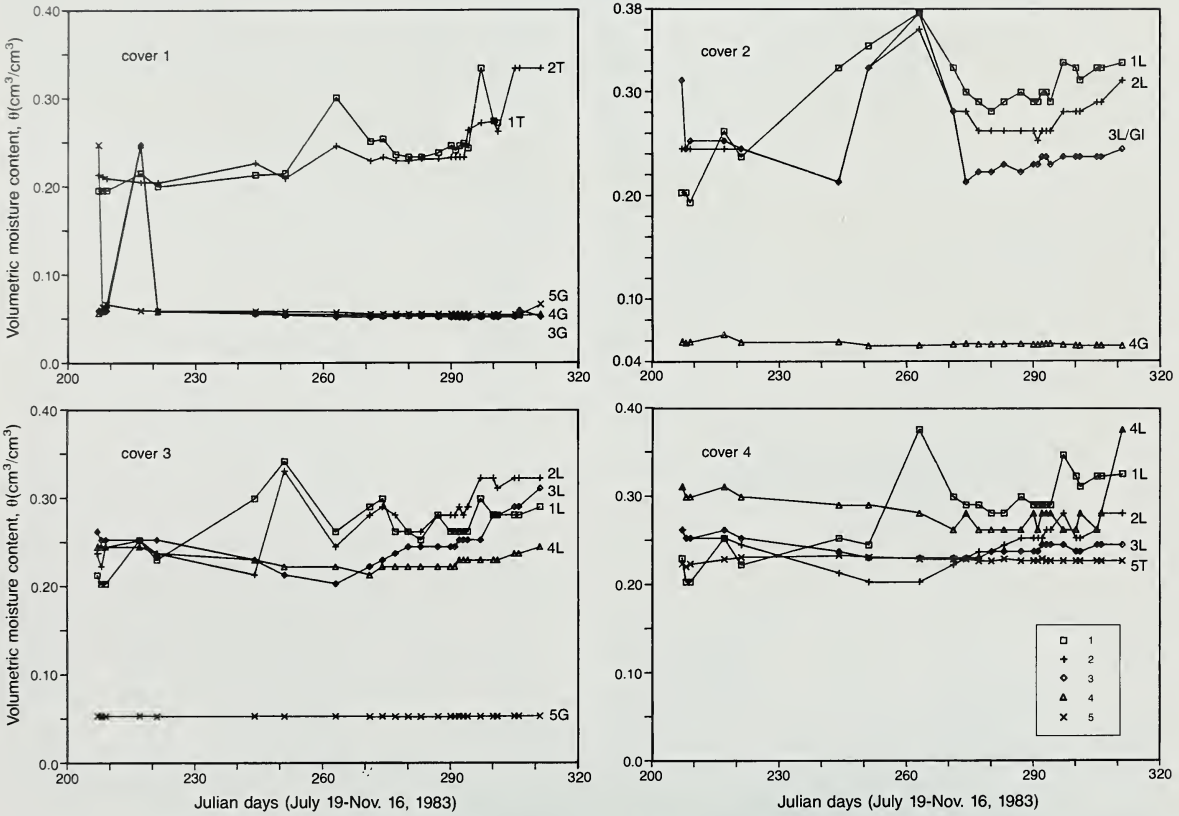

Figure 68 Tensiometer readings from the same instruments shown in figure 67, but plotted as moisture content for the period July 19 through November 16, 1983.

the base of the gravel in cover 1, did not change appreciably throughout the entire period of interest. After September, the total heads measured at the base of the gravel were also significantly higher than those at the overlying loess/gravel interface indicating an upward gradient within the gravel during this portion of the monitoring period. Thus, significant downward infiltration apparently did not reach deeply into the gravel after September.

Changes of total head with time indicated by the tensiometers in cover 3 are shown in figure 67. The distribution of head and the changes that occurred at depths of approximately 30 to 60 cm are very similar to those observed in cover 2, except that there was no increase in head at the 60 cm depth during September as there was in cover 2. A short time after installation, a consistent downward gradient developed and maintained itself at these shallow depths. During the last several weeks of monitoring this downward gradient was apparent to a depth of at least 81 cm. Below that depth, the values of total head indicated by tensiometers in the gravel were quite similar to, and often slightly higher than, the total head at 81 cm, in the overlying loess. This indicates that no appreciable gradients had developed across the gravel, although a significant downward gradient had developed in the loess.

The pattern of total head indicated by the shallow tensiometers in cover 4 (fig. 67) was virtually identical to that observed in cover 3; i.e., a consistent downward gradient developed to a depth of 60 cm, and after September, extended clearly to a depth of 90 cm. This downward gradient was also very similar in magnitude to those measured in covers 2 and 3, although there is no gravel layer in cover 4. Indicated changes in total head at 122 cm in the loess and in the underlying till were quite small; only a slight decrease in head was indicated. The heads at those depths indicated a consistent upward gradient from the till toward the loess.

Estimated volumetric moisture content within the covers during the monitoring period is depicted in figure 68. Volumetric moisture content was estimated using the moisture retention curves (fig. 11, Evaluation of Geologic Materials section) obtained from laboratory analysis of samples taken from the covers. These values are only approximate since hysteresis was ignored in their calculation; however, they give a useful qualitative picture of the moisture profile within the covers.

The most striking feature of figure 68 is the nearly constant volumetric moisture content of the gravel layers. The only exceptions were single, high values measured early in the monitoring period by each instrument in the gravel layer of cover 1. In general, this indicates that no moisture ever accumulated within it, although small amounts of moisture may have been moving through the gravel.

Moisure content fluctuations within the upper, fine-grained layers generally follow fluctuations in total head (fig. 67). Volumetric moisture content changes in the till of cover 1 are more subdued than those in the loess of cover 2 and cover 3. Except for a single reading in September (day 265) and several in November, the volumetric moisture content in the till of cover 1 shows a very gradual increase, indicating steady infiltration into the till. Volumetric moisture content in the loess of cover 2 and the shallower portions of covers 3 and 4 fluctuated rapidly in response to precipitation. The downward moisture gradient within the loess of cover 2 during the later stages of monitoring was very apparent. The gradual increase in volumetric moisture content at each level in the loess of cover 2 indicated a downward flux of moisture toward the gravel. A similar, though more subdued, pattern was apparent in the volumetric moisture content changes within the deeper portions of the loess in cover 3.

The volumetric moisture content of the lower till layer of cover 4 was very steady throughout the period. Although the deeper portion of the loess also maintained a fairly steady volumetric moisture content, the amount was higher than that of both the overlying loess and the underlying till. This might indicate that moisture moved rapidly through the upper portions of the loess, then accumulated in the lower portion above the fine-grained till.

Phase Two: May 1984 - June 1986

- **Instrumentation**

In the period since November 1983, efforts concentrated on the installation of more permanent monitoring instrumentation in each of the covers. This instrumentation included permanently installed tensiometers, thermisters, neutron moisture probe access tubes, and soil-water samplers. The tensiometers were connected to individual pressure transducers; a microprocessor-controlled data-logging system was used to collect nearly continuous data of pressure head and soil temperature on site.

Permanent tensiometers were installed at various depths in a small area immediately northwest of the center of each cover. These tensiometers consisted of porous ceramic cups of ½-inch diameter or less connected to small-diameter nylon tubing or ½-inch diameter PVC pipe. Each tensiometer was connected at the surface to an individual differential pressure transducer (Honeywell Microswitch Model 141PC15D). Wires from each of the transducers extended to the Campbell Scientific, Inc. (CSI) CR-7 data-logging system in the instrument shed.

A total of 26 tensiometers were installed on the four covers. They were placed at depths ranging from approximately 30 to 180 cm in order to monitor each of the layers in the covers. Figures 69 to 72 illustrate the monitoring instrumentation in each of the four covers. At the time, five tensiometers were installed in cover 1, six in cover 2, eight in cover 3, and six in cover 4. In several instances duplicate tensiometers were installed at similar depths to determine the reliability of the data. More detailed information concerning tensiometer installation is included in the Appendix.

Twenty-four thermisters (CSI model 107-B) were emplaced in four 6-instrument nests, one nest per cover. The thermisters are accurate to ± 0.4°C over the range of -33°C to +44°C. The datalogger employs a fifth-order polynomial to linearize the output and convert the reading to temperature in centigrade degrees. Soil temperature was monitored by the thermisters at depths ranging from approximately 15 to 130 cm with measurements in each layer of the covers. The CR-7 datalogger was programmed to take hourly readings from the thermisters immediately following tensiometer measurements.

- **Volumetric Moisture Content**

Measurements of volumetric moisture content were taken in the access tubes with the Troxler probes on May 11 and 25 and July 2, 1984 and on August 27, 1985. Neutron measurements shown in figure 73 indicate a uniform distribution of moisture in the layer overlying the gravel in covers 1, 2, and 3. A slight increase in volumetric moisture content was observed at the interface of the loess and the till in cover 4. This buildup in moisture was related to the somewhat lower saturated hydraulic conductivity of the underlying till and higher natural volumetric moisture content of the loess. Gravimetric measurements of volumetric moisture content supported these observations (fig. 74).

Figure 73 shows that the upper layer in cover 1 consistently had the lowest volumetric moisture content of any of the covers. Values of volumetric moisture content were always about 0.1 cm^3/cm^3 less than those observed in the other covers. Because of the higher density and lower hydraulic conductivity of its upper till layer, cover 1 had a lower infiltrability than the other covers. This was evidenced by the smaller increase in volumetric moisture content in cover 1 than in the other covers after a heavy rain on the night of May 24, 1984. Cover 1 appeared to have limited infiltration best.

Covers 2, 3, and 4 performed in a similar manner to each other with volumetric moisture contents only somewhat higher in cover 4. Although few weather data were available during this period, it is apparent that profiles were drying toward the end of summer 1984 and that the very dry conditions that persisted in 1985 were reflected in the very low values of volumetric moisture content.

Measurements of volumetric moisture content in the access tubes near the land surface were anomalously low and not considered to be very reliable at depths less than 0.3 m.

- **Gravimetric Moisture Content**

Gravimetric measurements of moisture content were made during installation of tensiometers in August 1984. Analysis of samples of topsoil for gravimetric moisture content in covers 2, 3, and 4 indicated that the near-surface values of gravimetric moisture content measured using the neutron probe are much too low to be reliable (fig. 74). Gravimetric moisture contents of these materials at the 0.1 m depth ranged from 0.11 g/g in cover 4 to 0.14 g/g in cover 2. Measurements of gravimetric moisture content from the neutron probe deeper in the profiles, however, were confirmed by the gravimetric data. Gravimetric moisture content was found to increase with depth in all covers. Figure 74 shows a buildup of water at the loess-till interface in cover 4 and a lower gravimetric moisture content in the till. Gravimetric moisture content in cover 2 increased down to the gravel layer and then decreased significantly in the gravel. This condition might have been caused by moisture retention in the loess overlying the gravel—the wick effect—or by the differences in water-holding capacities of the two materials. A buildup of gravimetric moisture content was also observed near the bottom of the gravel at the interface of the underlying lower permeability till layer.

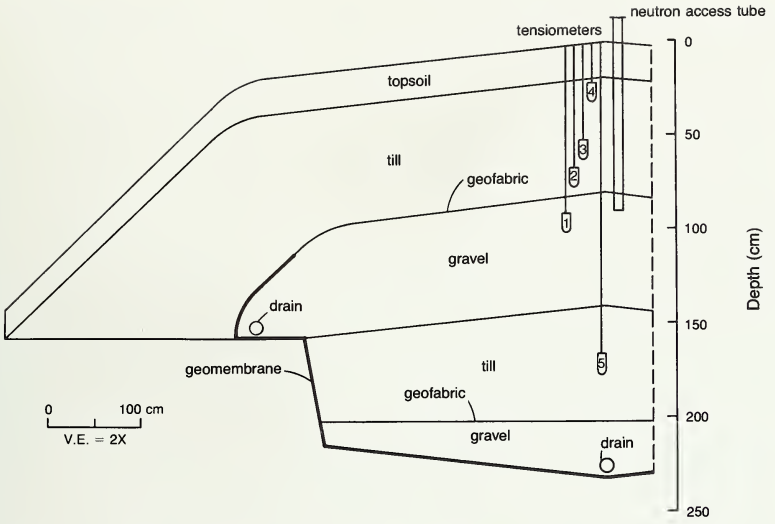

Figure 69 Cross-section of cover 1 depicting Phase Two tensiometers and neutron-probe access tube.

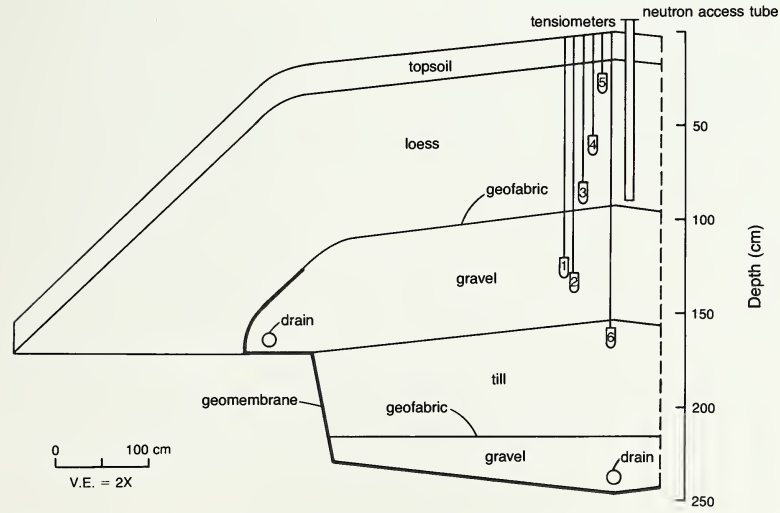

Figure 70 Cross-section of cover 2 depicting Phase Two tensiometers and neutron-probe access tube.

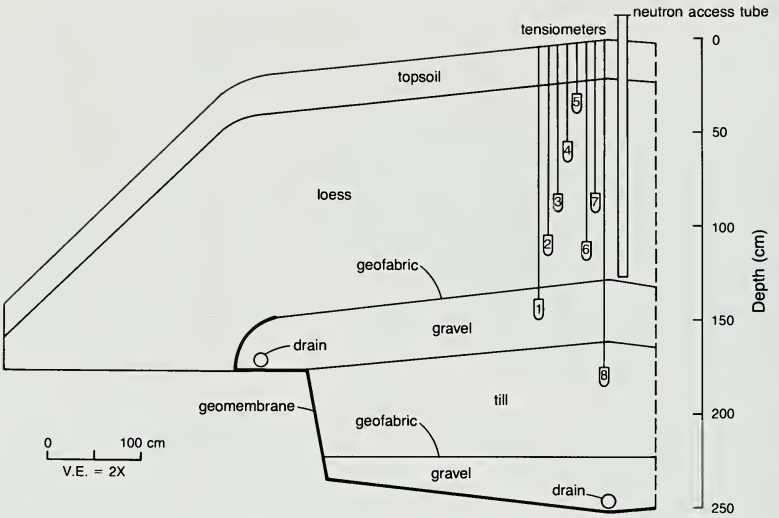

Figure 71 Cross-section of cover 3 depicting Phase Two tensiometers and neutron-probe access tube.

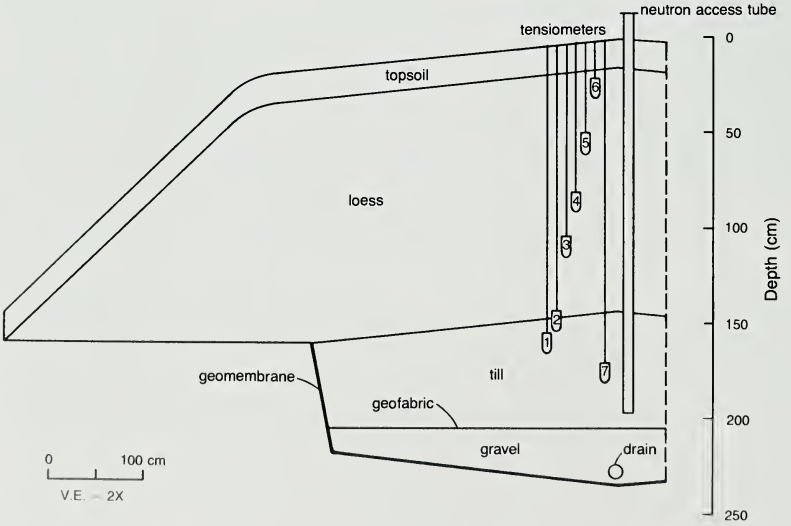

Figure 72 Cross-section of cover 4 depicting Phase Two tensiometers and neutron-probe access tube.

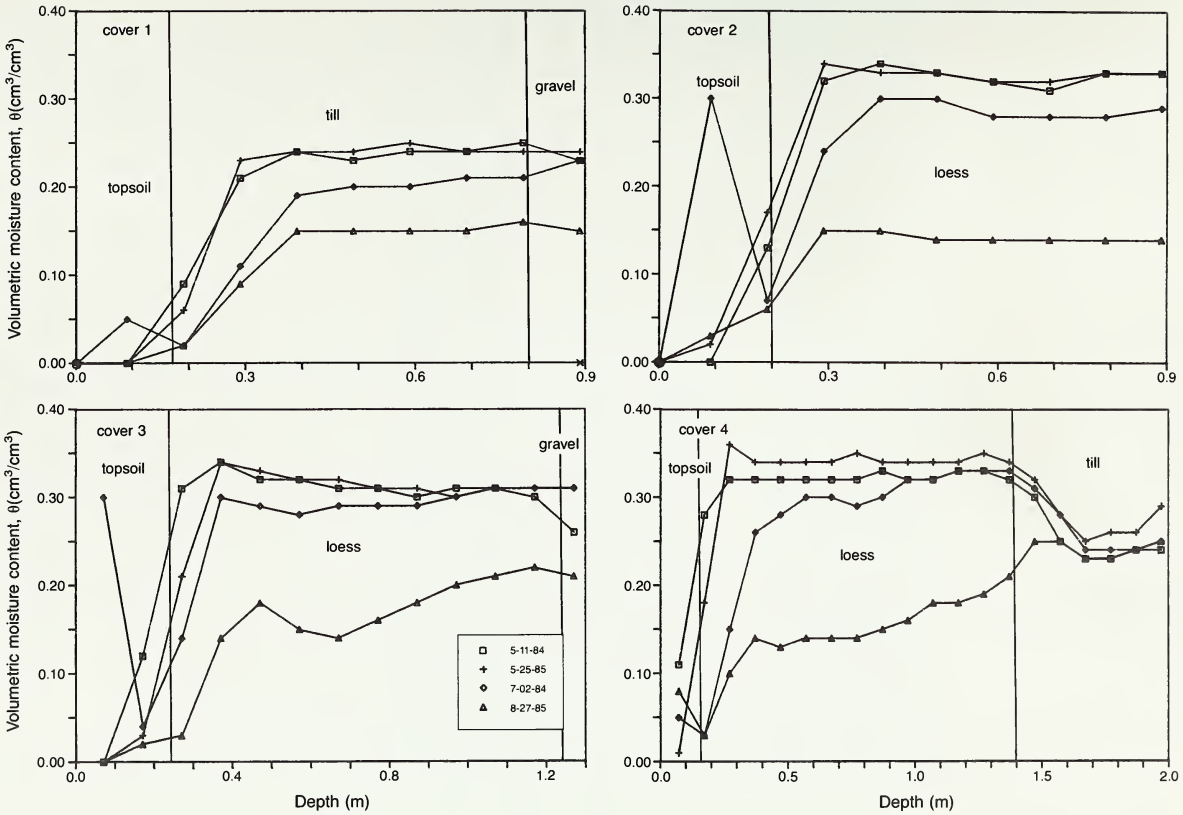

Figure 73 Volumetric moisture content within the experimental covers on four days in 1984 and 1985 as determined with the neutron moisture probe.

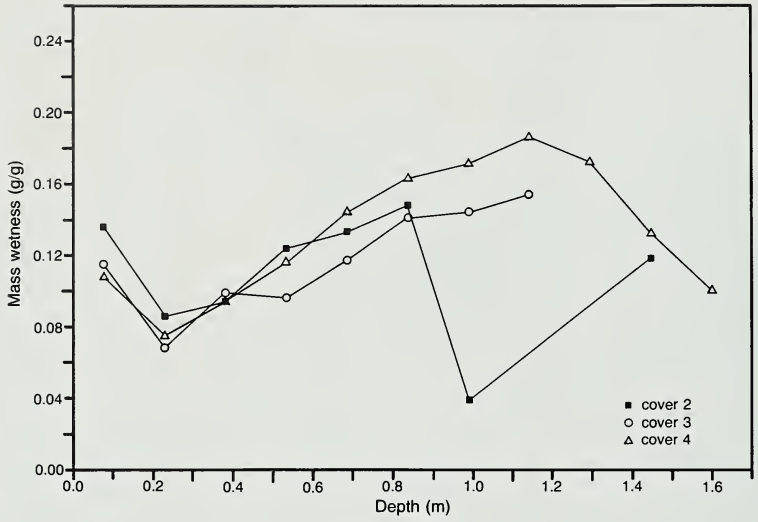

Figure 74 Mass wetness (gravimetric moisture content) of samples from three covers collected in August 1984.

• Soil Tensions

Hourly measurements were made of pressure head from late September, 1985 through June, 1986. Occasional battery failure resulted in some loss of data; however, over 125,000 data points were gathered covering 213 days. For convenience, the monitoring period will be considered in three shorter portions which roughly coincide with the seasons of the year: autumn (September 22 through December 22), winter (January 9 through March 21) and spring (April 3 through June 13). The entire data set is too large to easily present in this report; therefore, we present data from six representative days for each season to illustrate long-term patterns and detailed data from two, significant, individual events. Hourly data often showed pronounced diurnal periodicity. Since we were not concerned with diurnal variations in this study, we removed them by taking daily averages of the hourly data. This simple method of data reduction is an effective low-pass filter, and has the further advantage of reducing the volume of data to a manageable size.

Autumn, 1985 Autumn 1985 was a period of gradual wetting after a dry summer. Total monthly and daily average rainfall (measured at the USGS meteorological station 1 km north) for the months September through December are tabulated in table 11. Rainfall amounts in October and November were unusually large; November was the wettest on record in much of Illinois. In general, this pattern is reflected in the soil data. Each cover exhibited large fluctuations in total head (fig. 75) throughout October, but then all began to decrease in head (especially at shallow depths) in early November. By mid-November, and continuing into December, all covers exhibited low head throughout their entire profiles. Similarly, volumetric moisture content profiles (fig. 76) indicated increasing volumetric moisture content with time.

Cover 1 The shallowmost portion of cover 1 remained moist throughout the autumn. However, the lower portions of the upper fine-grained (till) layer were dry in early October and gradually became wetter until the end of October. The gravel layer (about 105 cm depth) experienced a

Table 11. Rainfall near Sheffield, Illinois during autumn 1985

Month	Rainfall (cm)
September (8 days)	2.77
October	13.06
November	14.66
December	0.36

similar fluctuation in head. The only time that any of the gravel layer was shown to be experiencing saturated conditions was in cover 1 during a few days in early October. Hourly data indicate that this condition persisted for about two days (October 3 and 4) before returning to dryer conditions. Otherwise, the gravel maintained a nearly constant, low volumetric moisture content. Total head in the lower fine-grained (till) layer started out with a lower head, which abruptly increased only after both overlying layers had also increased in head. However, this fluctuation was not large enough to cause significant change in volumetric moisture content of the lower layer. The saturated volumetric moisture content of Tiskilwa Till was measured in the laboratory to be 33.36 percent. Neither layer of till in this cover approached this saturation level during the autumn monitoring season.

Cover 2 Transducers monitoring pressure head in the shallow portions of cover 2 were malfunctioning during early October. Readings available from the upper fine-grained (loess) layer indicated wetting in the shallowest portion and drying, then wetting near the base of the layer (89 cm). The deeper portion became saturated by mid-November, before drying slightly in December. The gravel layer (between approximately 110 and 150 cm) responded in a similar manner to the gravel layer in cover 1. The total head varied throughout the period, but the volumetric moisture content did not. The response of the underlying till layer was somewhat different from that of the lower till layer in cover 1. An initial, moderately low head remained constant until high heads were established in the profile above; only then did the head in the till increase to a higher value. This increase was sufficient to produce a significant rise in the moisture of the till, reaching saturation by mid-November. Total head gradients in cover 2 during this period also show two distinct patterns, fluctuating early in the period and remaining nearly constant later. As infiltration proceeded, a generally downward gradient was present in the upper layer during October and early November. The gradient across the loess-gravel interface and within the gravel fluctuated until mid-November when a nearly constant gradient was established. The head gradient across the gravel-till interface was consistently upward until mid-November when the nearly constant gradient penetrated into the lower layer.

Cover 3 Interpretation of the data from cover 3 was complicated by the failure of several transducers during the autumn. In particular, the single instrument monitoring the gravel layer (approximatley 145 cm) was not operational until the end of October. Other instruments experienced intermittent failures. Despite these difficulties, the two-part pattern, similar to that established in cover 2, was clearly evident. Initially, the deeper portion of the loess layer (approximately 90 to 120 cm) was relatively dry. A downward gradient resulted in infiltration through this layer, until a nearly constant gradient was established in mid-November. Even though relatively high heads were evidenced in the gravel, these were still not enough to increase the volumetric moisture content of the gravel. Pressure head must be less than 5 cm of water before any increase above 5 or 6 percent volumetric moisture content will occur. Total head in the underlying layer of till was relatively high throughout the period. Consequently, only a small increase in head was observed in mid-November. Volumetric moisture content of the till remained nearly constant throughout the autumn, much as the lower till layer in cover 1.

Cover 4 The gradual wetting that occurred during this period was very apparent in the two-layer cover 4. The upper fine-grained loess layer (to depth of approximately 130 cm) exhibited increasing head and volumetric moisture content throughout October and early November. An

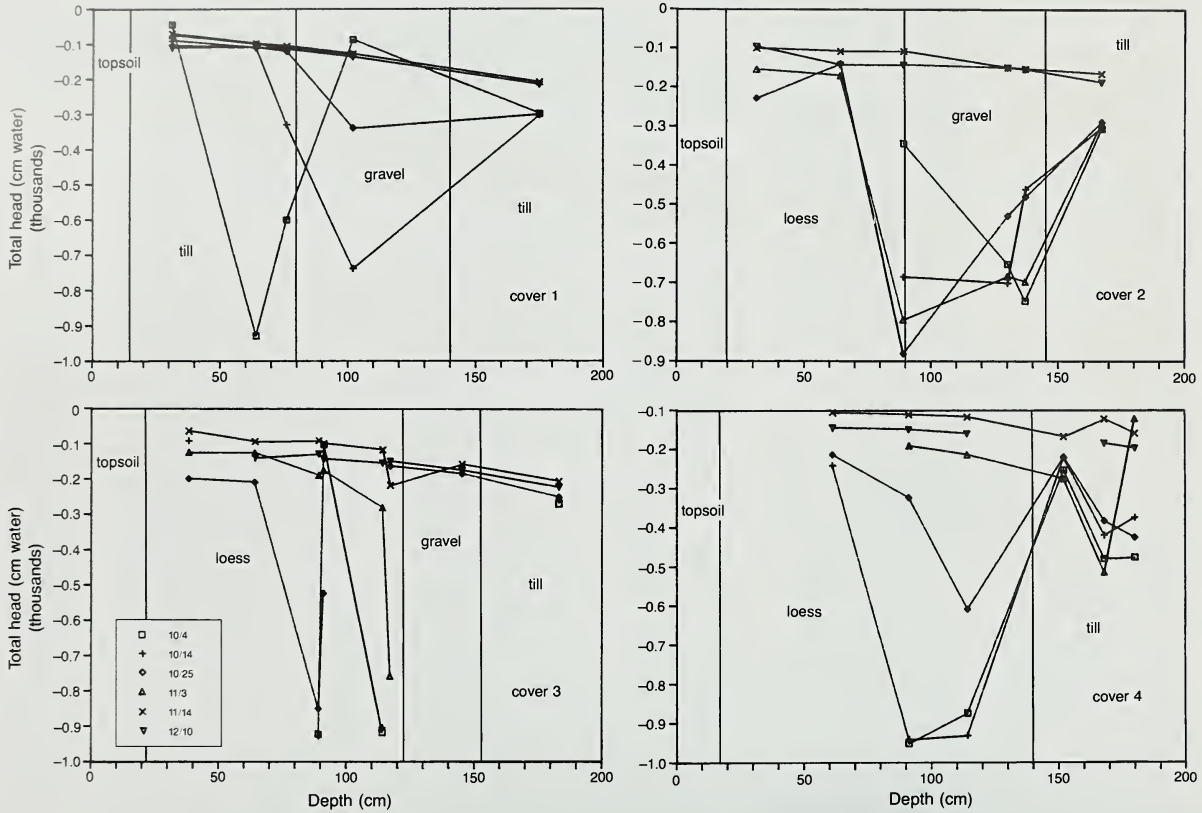

Figure 75 Average daily values of total head determined for 6 days during autumn, 1985 for each of the four experimental covers.

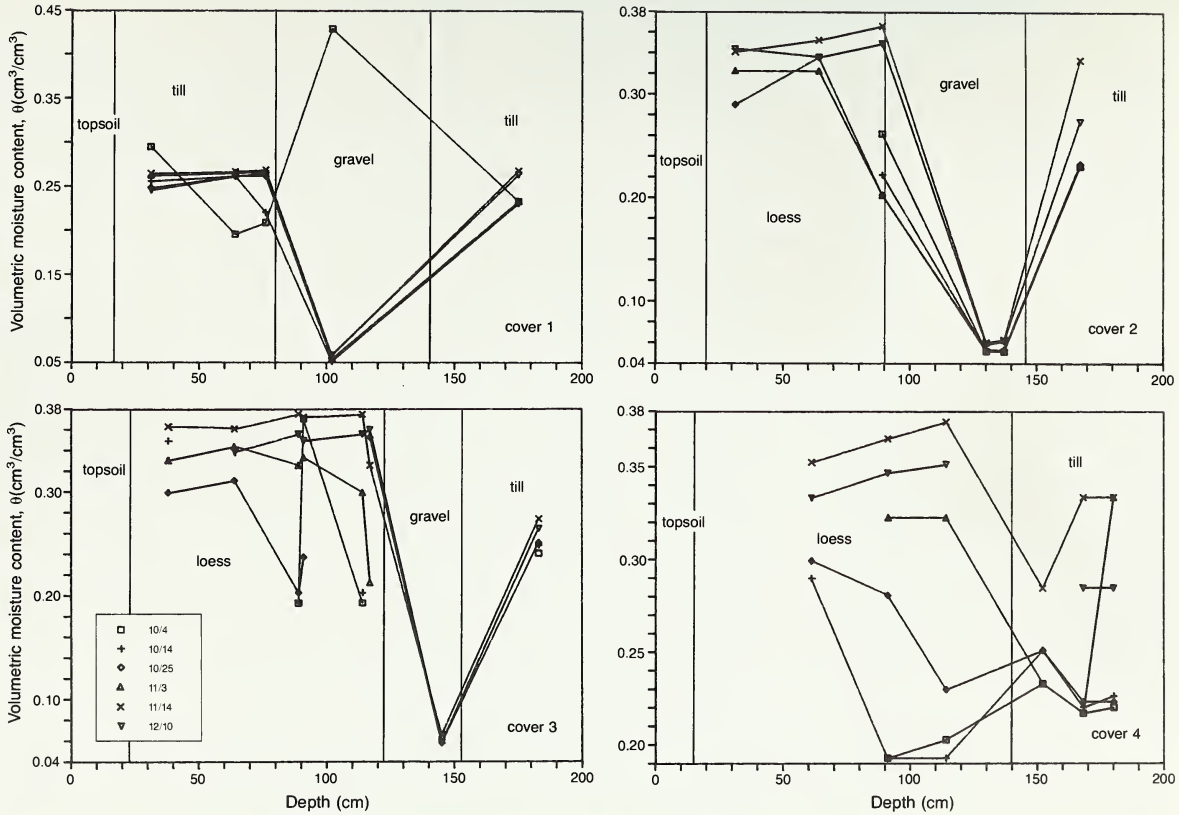

Figure 76 Average daily values of volumetric moisture content determined from tensiometer readings on 6 days during autumn 1985 for each of the four experimental covers.

initially steep downward gradient gradually flattened to nearly constant by mid-November. The underlying fine-grained till layer of cover 4 was monitored in greater detail than any of the other deeper till layers. This is due to the absence of an intermediate gravel layer, which, as noted above, inhibited the placement of instruments in the other covers. The shallowest portion of the till layer in cover 4 responded much as the till on other covers. Initial fluctuations in head were small, until the overlying layer became saturated in mid-November: a significant increase in head was measured, corresponding to an increase in volumetric moisture content to about 28 percent. The deeper portion of the till layer (below approximately 165 cm) exhibited the greatest fluctuation in head and volumetric moisture content measured in any of the lower till layers. Initially at a relatively low value, the total head gradually increased throughout October. The deepest instrument measured an extremely level head in early November, increasing slightly thereafter. However, the intermediate instrument (approximately 165 cm) indicated a drop in head in early November, then an increase to a very high value in mid-November. An overall downward head gradient was evident in the till layer throughout October; frequent reversals between the two deepest instruments may indicate that moisture was accumulating from the bottom upwards as well as infiltrating downward. The high total head condition measured in the deeper portion of the till corresponded to saturated volumetric moisture contents. This lasted throughout November in the deepest portion before a drying episode in December.

Winter, 1986 Very cold weather in late December 1985 and early January 1986 damaged several tensiometers and caused a temporary failure of the electronic data logger resulting in the loss of several weeks of data. The extreme cold was short lived, however, and thermistor measurements indicate that the frost did not penetrate deeply into the covers. This was a dry period; total precipitation (reported as equivalent rainfall) as recorded at the USGS meterological station is shown in table 12. Total head and volumetric moisture content are shown in figures 77 and 78 for six representative winter days.

Cover 1 Plots of total head and volumetric moisture content in cover 1 depict an apparent, dramatic wetting episode at approximately 65 cm deep in the upper fine-grained till layer. We believe that this was a spurious event and the head throughout January was probably much like that shown for early February (day 41). Recalling the consistently high head recorded at the end of autumn, we find it difficult to explain why the middle of the layer would suddenly experience such a decrease in head, without a similar change in the same unit just below. Otherwise, total head measurements in the upper till indicated generally moist conditions with small fluctuations throughout the period.

Only very small total head fluctuations were recorded in the gravel layer, which maintained a nearly constant, low volumetric moisture content. During January, readings in the lower till layer indicated high total head consistent with late autumn. Following several weeks of lost data due to data logger malfunction, this same instrument indicated very low head and significantly lower volumetric moisture contents. Although the lower till might have drained during this period, the indicated change in head was quite large; and we suspected that a persistent malfunction occurred.

Cover 2 Total head in the upper fine-grained loess layer of cover 2 did not change significantly during most of winter, although a uniform increase in head did occur near the end of the period in late March. Not only was there little change with time, there generally was not an appreciable head gradient. A small downward gradient (slightly more pronounced in late January) was observed in the shallower portion, shifting to an even smaller upward gradient in the deeper portion. The volumetric moisture content of this layer was maintained at a fairly constant level of about 30 to 32 percent until becoming wetter in late March. Throughout the period, the deeper portion of the layer tended to be wetter than the middle portion. This seemed to indicate that some moisture was accumulating at the base of the fine-grained layer.

The total head in the gravel layer of cover 2 fluctuated throughout this period. Two cycles of increasing head occurred, one beginning with very low head (high matric suction) in early January and the second reversing a trend of decreasing head in late February. These fluctuations might have been related to two freeze-thaw events that occurred during the winter. Early January and late February had very cold weather, corresponding to the low heads; however, a thaw occurred in early February, which might account for the higher heads observed on day 41. Similarly, the extreme cold weather of late February did not continue long into March when snow cover melted for the rest of the season. No fluctuation of head was sufficient to produce large changes in the

Table 12. Precipitation near Sheffield, Illinois, during winter, 1986

Month	Equivalent rainfall (cm)
January	0.78
February	6.05
March	2.21

volumetric moisture content in the gravel. However, because of the persistent downward gradient from the overlying loess, we presumed that limited moisture movement was occurring.

Total head in the underlying fine-grained till layer remained nearly constant throughout the winter. This corresponded to a fairly high, constant volumetric moisture content. The head gradient across the gravel-till interface was consistently upward throughout this period, indicating that little moisture movement was occurring from the gravel down into the till.

Cover 3 Instruments in cover 3 sustained the most damage during the early winter. Only five of the eight tensiometers functioned consistently. Except for one extremely low measurement in early January, total head measurements in the upper fine-grained loess layer of cover 3 were very similar to those in cover 2. This is not surprising since the recording instruments were at approximately the same depths in both covers. Unfortunately, the deeper instrument installed in cover 3 was not functioning during this period.

Total head measurements in the gravel layer of cover 3 were quite different from those in cover 2. No low head measurements were recorded in cover 3, and the sense of head changes was also different. Relatively high head was observed throughout the first half of the period and this decreased during the second half of the winter. Gradients across the loess-gravel interface appeared to fluctuate throughout this period, although the large separation between the functioning instruments made the interpretation of the observed gradient very tenuous. As in cover 2, the fluctuations in head observed in the gravel layer did not correspond to any appreciable changes in volumetric moisture content.

Total head observed in the underlying fine-grained till layer of cover 3 was similar to those observed in cover 2 during this period. Total head fluctuated slightly more in cover 3, but not significantly more. The gradient in head across the gravel-till boundary was slightly downward or constant during this period, suggesting that some moisture movement might have been occurring. However, very little change in volumetric moisture content was observed.

Cover 4 Tensiometer measurements in the upper loess layer of cover 4 appeared to indicate that wide fluctuations of head occurred during the winter. Although it is characteristic of this material to fluctuate in head (autumn), we caution that at least some of this fluctuation might be apparent and not caused by moisture or pressure changes within the cover. As mentioned above in relation to cover 1, two instruments in cover 4 recorded unusually long periods of low-pressure events, first during January and then later in March. Detailed information not presented in this report also revealed three similar events recorded by the two instruments in cover 4 but not by the single instrument in cover 1. We believe that these events were spurious and probably related to some unknown malfunction of the instrumentation. We report them since they might be real pressure events related to freeze and thaw. The profile established in early February was probably more normative for this layer during this period. Within the profiles for late February through March, we observed in this layer a downward gradient that gradually decreased with time. This appeared to indicate renewed infiltration through the cover, possibly in response to snow melt during the latter stages of winter.

An incomplete record of head was obtained from the three tensiometers in the underlying till layer of cover 4. What was apparent from the available measurements was that the head was fairly stable throughout this period at about the same level it had reached by the end of autumn. Only a very small gradient was apparent either within the layer or between it and the overlying layer. Volumetric moisture content was high, but not at saturation as it had been in early to mid-November.

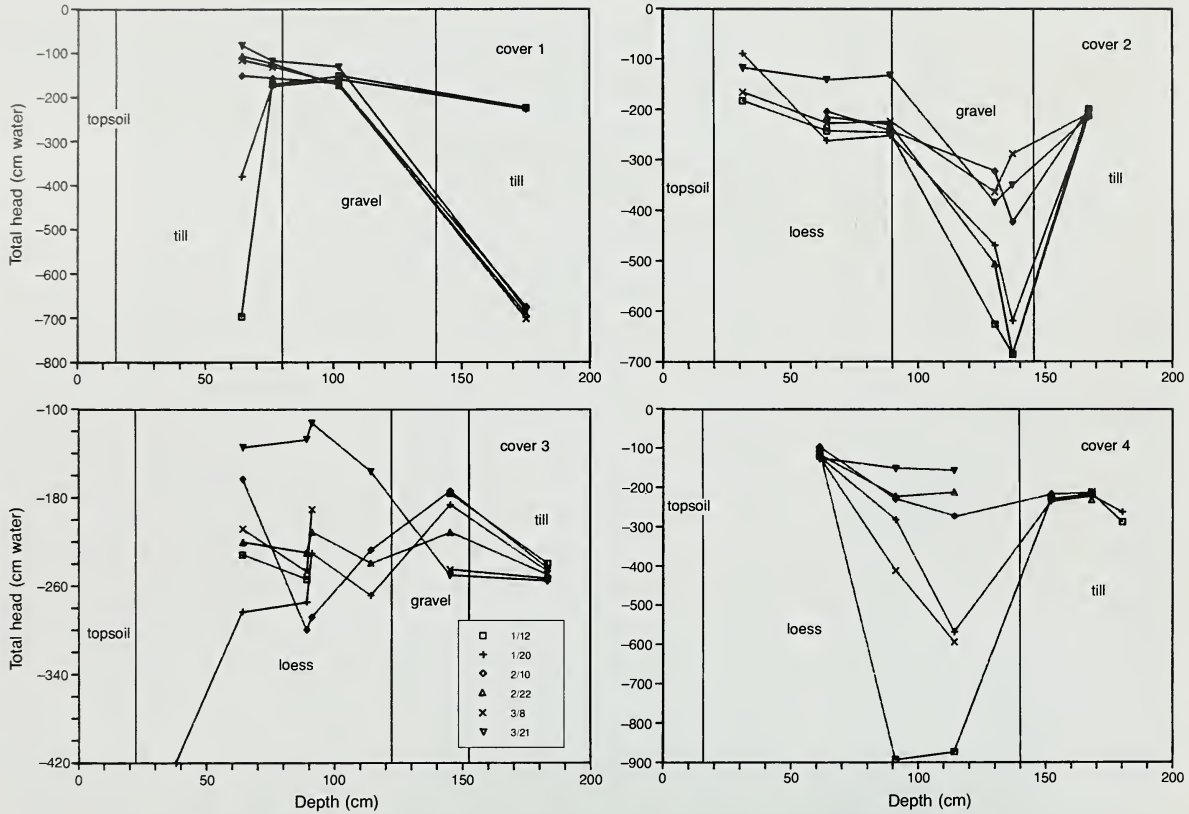

Figure 77 Average daily values of total head determined for 6 days during winter 1986 for each of the four experimental covers.

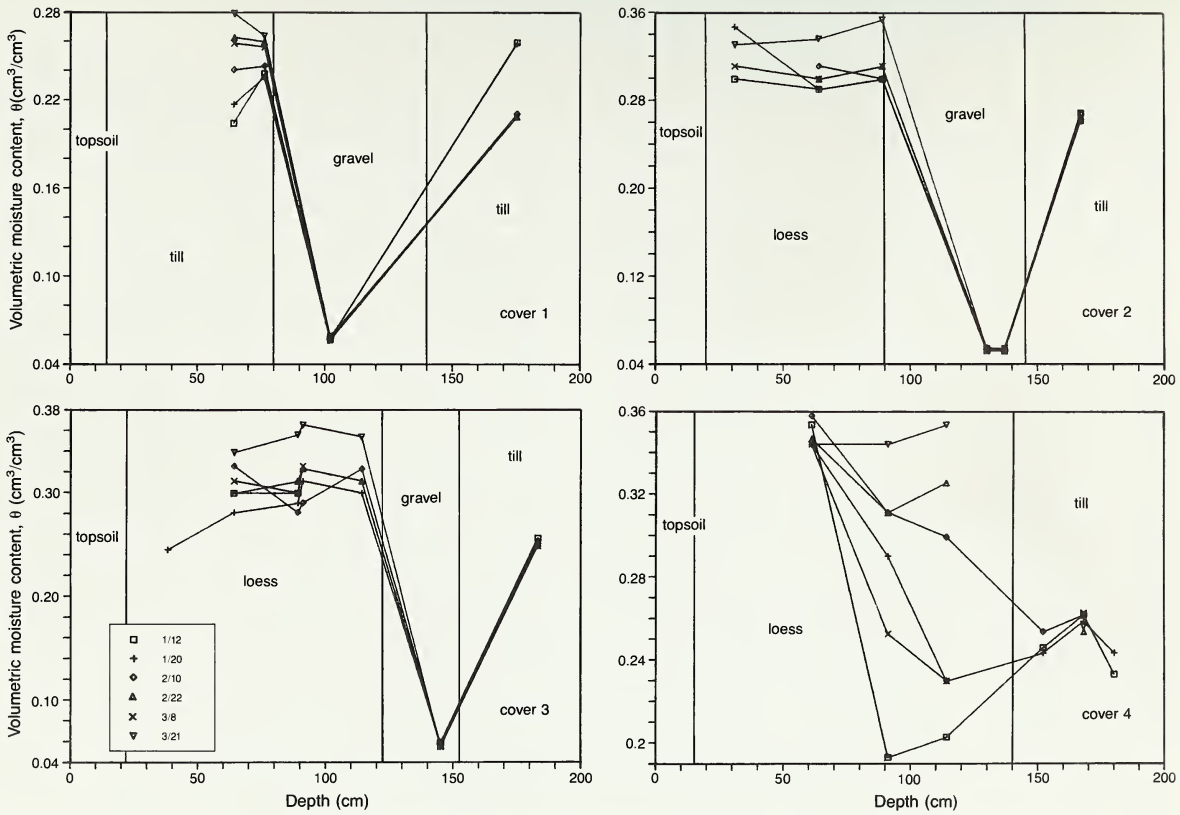

Figure 78 Average daily values of volumetric moisture content determined from tensiometer readings on 6 days during winter 1986 for each of the four experimental covers.

Table 13. Total monthly rainfall near Sheffield, Illinois, during spring, 1986

Month	Rainfall (cm)
April (19 days)	6.38
May (24 days)	14.78
June (12 days)	7.26

Spring, 1986 Observations of soil matric potential were continued through the middle of June 1986. Early spring (late March through mid-May) was relatively dry. The most significant spring rainfall occurred over four days in mid-April when the ISGS rain gauge located on cover 3 recorded a total of 10.03 cm of rainfall. The effects of this heavy rainfall will be analyzed in more detail in the next section of this report. Rainfall for April, May, and June was recorded by the ISGS rain gauge in cover 3 (table 13). Total head and volumetric moisture content measured within the four covers are presented in figures 79 and 80.

Cover 1 The upper fine-grained till layer of cover 1 maintained fairly high total head throughout the spring. Significant departure from this trend occurred during late April and early May prior to the heavy May rains. Gradients were very small except for that unusual drying episode when an upward gradient was established, suggesting that drying was occurring from the surface downward, and not from drainage out the bottom.

Total head within the gravel layer was observed to be nearly constant and approximately the same as in the overlying till. This trend was broken only in mid-May when the till began to dry. The total head within the underlying till layer was consistently low throughout this period, as it was during most of the winter. This suggested that although a strong downward gradient was observed, very little moisture movement was occurring.

Cover 2 Fluctuations of total head in the upper fine-grained loess layer of cover 2 were very apparent during the spring. In general, the magnitude of the fluctuations was greater than in the upper till layer of cover 1. The decrease in total head observed during April and early May in cover 1 was also apparent in cover 2 as was the subsequent increase in total head following the heavy rainfall episode. In spite of these fluctuations over time, the head gradients did not vary appreciably, especially within the deeper portions of the layer. Small upward gradients were evident in this portion of the layer. Downward gradients were observed in the shallower portions following rainfall. This suggested that moisture accumulated at the base of the layer during winter and dried primarily from the surface downward. The increase in head following the heavy May rainfall resulted in an increase in volumetric moisture content throughout the layer.

The pattern of the total head observed in the gravel layer of cover 2 clearly depicted an early time of decreasing total head followed by a dramatic increase in late May. The head gradients were significant because they were strongly downward before the May rainfall and constant or only slightly downward afterward. This was true even though the gradient within the overlying loess was nearly identical in early April and in late May. There was apparently a connection between the times of low head in the gravel and moisture accumulation at the base of the overlying loess. Downward moisture movement appeared to be retarded during these times in comparison to times when the total head in the gravel was nearly the same as in the base of the overlying loess.

Total head within the underlying till layer was nearly constant throughout this period; however, it was at a much higher value than the underlying till layer of cover 1. Unlike the autumn, the total head in the till did not change when the overlying layers showed an increase in late May. This was probably because the till was moist from the autumn. However, the total head gradient in late May was nearly constant over the entire profile.

Cover 3 Total head fluctuations within the upper fine-grained loess layer of cover 3 were similar to the pattern established in cover 2. In general, however, the head was lower in cover 3, partly because it was thicker and could store more moisture. Total head gradients in the deeper

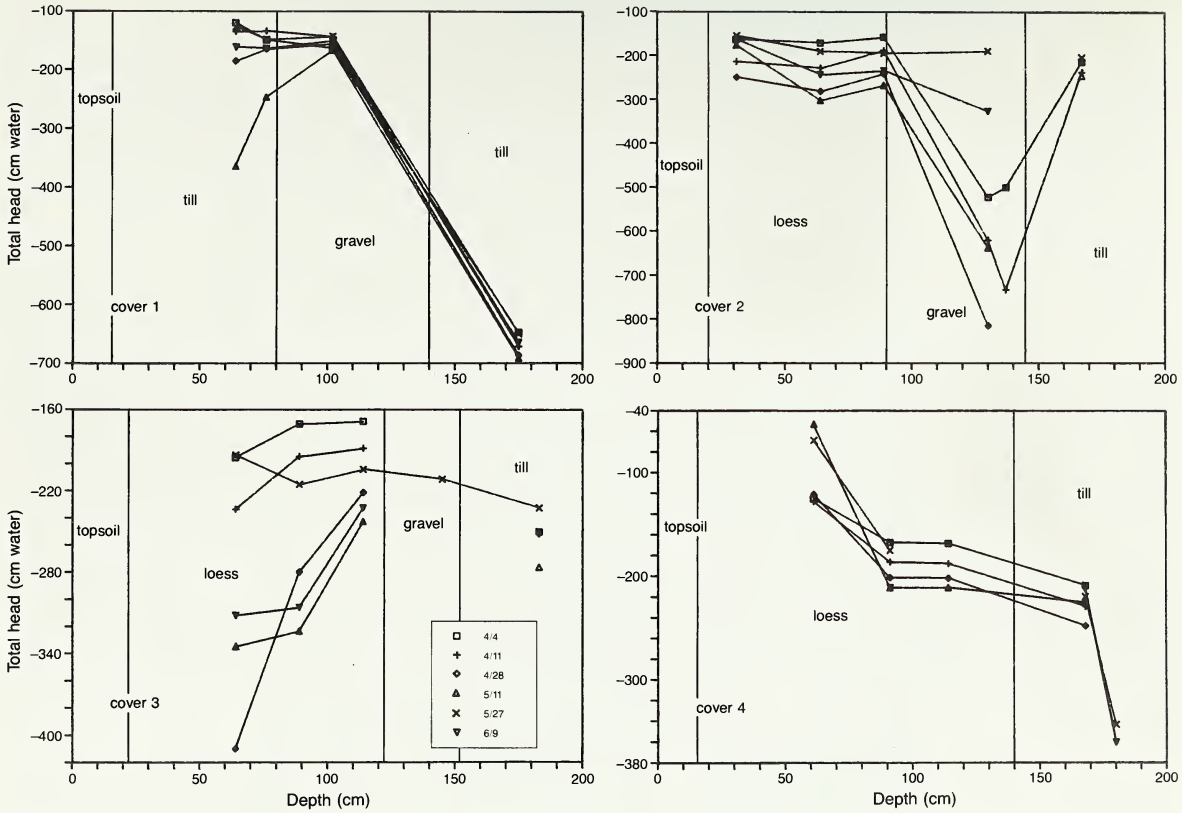

Figure 79 Average daily values of total head determined from tensiometer readings on 6 days during spring 1986 for each of the four experimental covers.

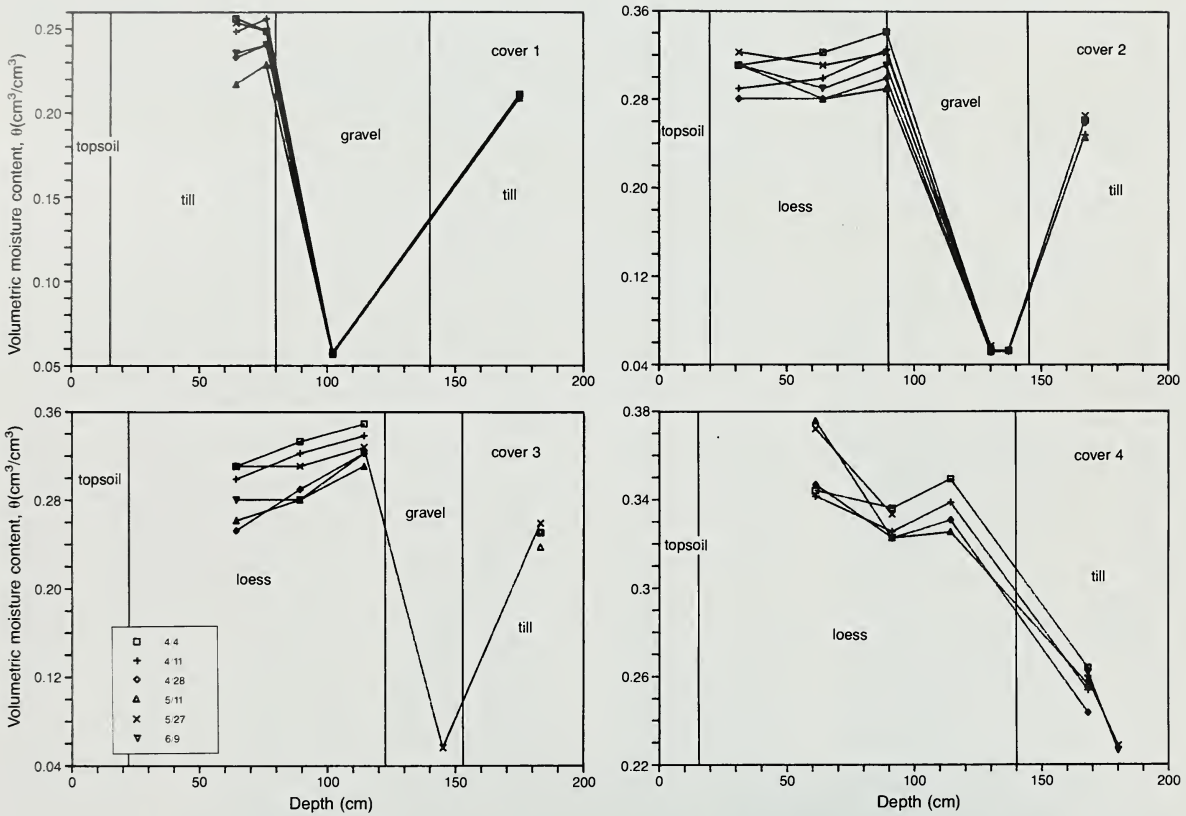

Figure 80 Average daily values of volumetric moisture content determined from tensiometer readings for six days during spring 1986 for each of the four experimental covers.

portion (the only portion with functioning tensiometers) were nearly constant or slightly upward. This indicated that moisture accumulated at the base of the layer and drying (when it occurred) proceeded from the surface downward. The volumetric moisture content at the base was consistently higher than the overlying material.

Unfortunately, the transducer monitoring pressure head in the gravel layer was malfunctioning during most of this period. Measured suction was probably too great to be recorded by the transducer except for the short period following the May rainfall event. This reading represented a minimum suction (maximum total head) for the gravel during this period.

Total head within the underlying fine-grained till layer of cover 3 during spring was similar to comparable layers of covers 1 and 2. Only small fluctuations were observed, and the volumetric moisture content remained between 24 and 28 percent.

Cover 4 Total head within the upper (loess) layer of cover 4 was relatively high throughout the spring. Some decrease in head was apparent in the deeper portion during April and early May, but not to the extent of decrease in the other covers. Total head within the shallower portion remained high, creating a continuous downward gradient. Figure 79 does not indicate a significant response to the heavy May rainfall. However, more detailed information presented in the following section does show that the upper layer did become saturated for a short time between May 11 and 27. This is not as apparent in figure 79 because the preceding decrease in head was very minor so that the increase following the rainfall was not very large.

Total head within the underlying till layer was nearly constant throughout the spring and very similar to levels observed in covers 2 and 3. The deepest instrument (180 cm) in cover 4 was brought back into service at the end of May, at which time it indicated relatively low total head in the deeper portion of the layer.

Detailed Analysis of Two Infiltration Events Two unusual events, which occurred during this monitoring period, deserve closer analysis. The first is the conclusion of the long series of autumn infiltration episodes with subsequent drying. We chose one representative monitoring instrument in each layer of each cover and calculated daily average volumetric moisture content (presented as percent saturation in fig. 81) from November 9 (day 313) through November 20 (day 324) and December 5 (day 338) through December 9 (day 342). The instruments were chosen to monitor approximately the same depths in each cover and to provide as continuous and reliable a record as possible over this period. The second event chosen for closer analysis was the heavy rainfall that occurred in mid-May 1986. Daily average volumetric moisture content (presented as percent saturation in fig. 82) was calculated for May 10 through May 29 (days 130-149). Whenever possible, we chose readings from instruments at similar depths in each cover for analysis. Most of the instruments were also the same as those used in the analysis of the autumn event.

November-December, 1985 The long period of infiltration culminating in record-setting amounts of rainfall during November 1985 produced the most severe test of the Sheffield prototype covers. Responses of the covers to this infiltration should be a measure of their relative effectiveness. The upper layers of loess on covers 2, 3, and 4 became saturated (or nearly saturated) by November 10 and remained saturated until at least November 20, when we experienced temporary failure of the monitoring system. By early December each was beginning to dry. The upper layer of till on cover 1 remained at a nearly constant volumetric moisture content (approximately 80% saturation) throughout November and December.

Very little change in volumetric moisture content of the gravel layers was detected during this period. Small increases were apparent in cover 1 between November 10 and 11 and in cover 2 between November 14 and 15. The small increase in volumetric moisture content in cover 2 was associated with a very large increase in head (approximately 500 cm) that occurred on that day. Even though the volumetric moisture content was nearly constant, moisture movement may still have occurred both into and through the gravel. However, the peripheral drains maintained low volumetric moisture content by removing most of the moisture that passed through the gravel. The effect of the drains in maintaining the low volumetric moisture content was probably most important when the head was very high; then the moisture moved into the drains and was not available to accumulate within the gravel.

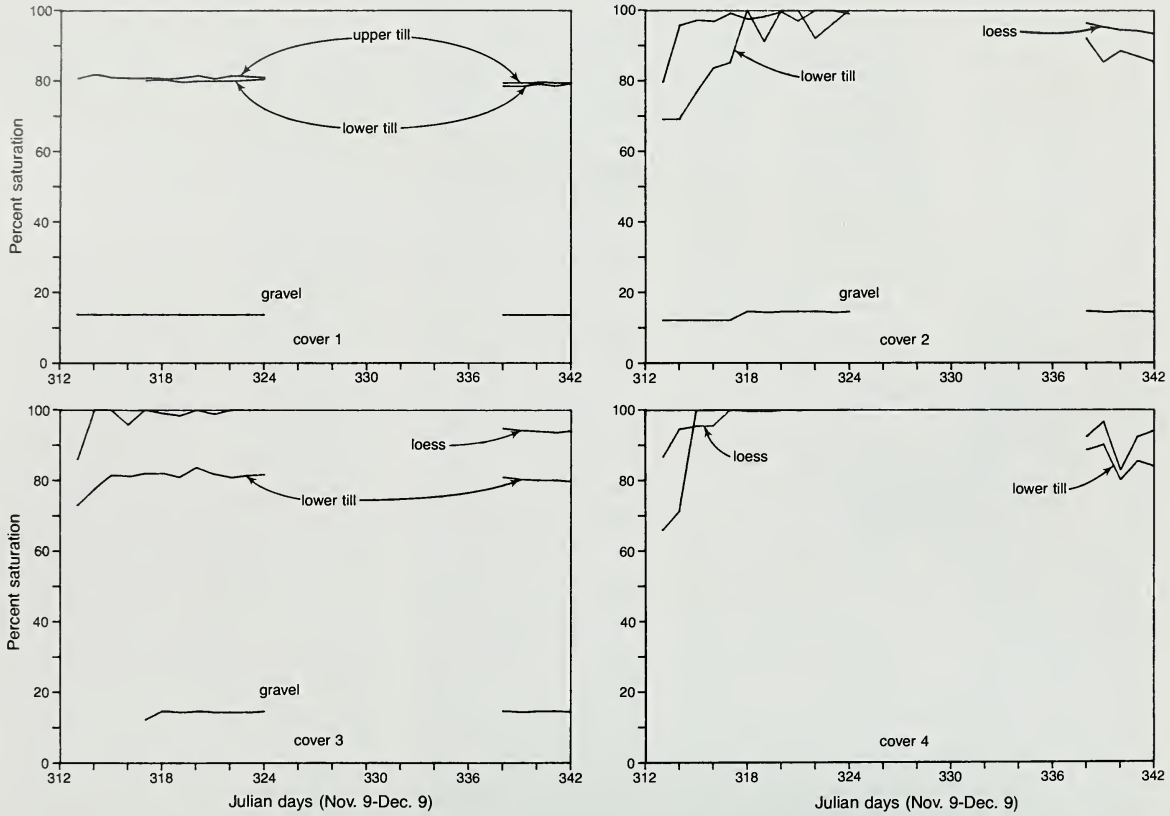

Figure 81 Average daily values of moisture content plotted as percent saturation for the period November 9 through December 9, 1986 in each of the four experimental covers. Measurements were taken from one representative instrument in each layer.

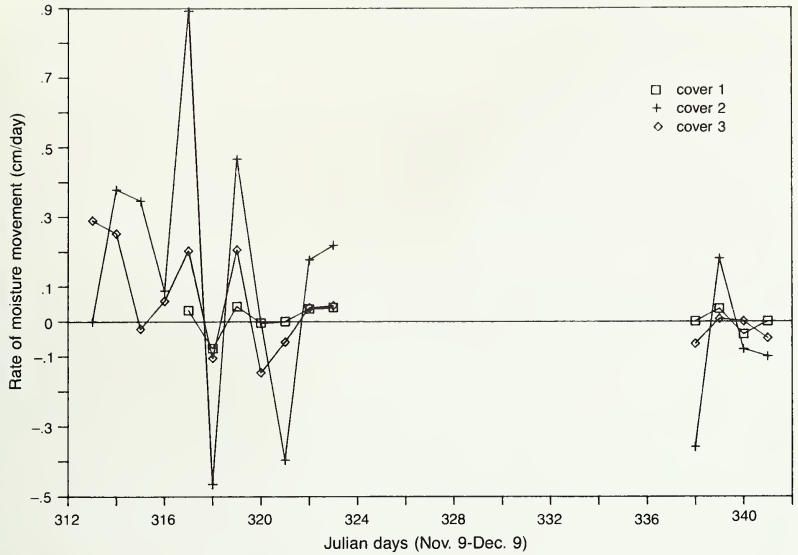

Figure 82 Rate of moisture movement into the lower layers of experimental covers 1, 2, and 3 is shown for the period November 9 through December 9, 1985.

That moisture movement did occur through the gravel layers was evidenced by the increase in volumetric moisture content within the underlying till in covers 2 and 3. This was not as apparent in cover 1, which did not show an increase in volumetric moisture content in the underlying till layer. In fact, the volumetric moisture content of both till layers of cover 1 remained nearly constant and nearly identical throughout this period. Cover 4 had no intermediate gravel layers; the volumetric moisture content in the underlying till increased sharply in early November and remained at or near saturation as long as the overlying loess was also saturated.

Assuming that maximum flux would occur when the till was saturated, the performance of covers could be roughly compared using the number of days under saturated conditions. Cover 4 became saturated quickly and remained saturated for at least 10 days. Cover 2 reached saturation somewhat later and remained at or near saturation for at least 7 days. Cover 3 exhibited some increase in volumetric moisture content but did not approach saturation. Cover 1 did not even exhibit an increase in volumetric moisture content. This simple test showed that while under severe stress, cover 1 performed the best, followed by covers 3 and 2. Cover 4 showed the poorest performance under these conditions.

A second perspective on cover performance can be obtained by considering the rate of moisture movement into the lower layer. Making a conservative estimate, we assumed that all moisture moved downward from the gravel into the till below. A simple calculation based on volumetric moisture content measured on each side of the interface was used to give an approximate indication of moisture movement. We took the rate of moisture movement, q_z, defined as

$$q_z = \int_{z_1}^{z_2} \frac{d\theta}{dt} \, dz$$

Table 14. Average rate of moisture movement across coarse-grained/fine-grained interface

Cover	Moisture movement (cm/day)
Cover 1	6.6×10^{-3}
Cover 2	9.0×10^{-2}
Cover 3	4.4×10^{-2}

where q_z is the rate of moisture movement through the depth interval;
Z is the interval of measurement;
Z_1 and Z_2 are the upper and lower boundaries of Z;
$\frac{d\theta}{dt}$ is the rate of moisture change.

Values obtained by this calculation were not fluxes, since no account was made for moisture movement in the soil profile above the zone of interest. Positive values implied moisture accumulation (using our assumptions) while negative values implied drainage.

Results of this analysis are presented in figure 82 for data from covers 1, 2, and 3 during parts of November and December 1985. (This calculation is not pertinent for cover 4, which lacked the intervening gravel layer. A Darcian approach might be useful in that case, but not easily comparable to the present analysis.) Average rates for this period are presented in table 14. Rates of moisture movement oscillated between positive and negative values indicating that moisture accumulated and then moved through the zone of interest. We assumed that all the movement was downward and eventually left the covers. All the moisture that accumulated was available for drainage, and we took this to indicate the relative performance of the covers. Movement into the lower layer of cover 1 was about one order of magnitude less than for either of the other two covers. Movement through cover 3 appeared to be half the rate of movement through cover 2.

May 1986 Heavy spring rains combined with high soil volumetric moisture content following winter snowmelt can be expected to stress the infiltration-reducing performance of trench covers. The spring of 1986 was not a severe test at the prototype cover site. Snow cover was not deep and it melted during winter. Early spring was relatively dry, giving the soil time to drain before the large rainfall in mid-May. Nonetheless, the response of the covers to this event was indicative of their performance in general. The heaviest rainfall (8 cm) occurred on May 16 (day 136). We have chosen to examine several days preceeding and following this event, specifically May 10 (day 130) through May 29 (day 149). Figure 83 depicts the average daily response of single tensiometers located in each layer of each cover. For comparison purposes, we have converted head data to percent saturation using soil moisture retention curves for these materials obtained in our laboratory (fig. 11, Evaluation of Geologic Materials section).

Except for the three gravel layers, the response of the covers to the single, large May rainfall was much different than their response to the extensive period of rainfall the previous autumn. Gravel layers were maintained at nearly constant moisture values of 12 to 15 percent saturation. A slight increase was observed in cover 2 on day 138, possibly in response to the rainstorm on day 136. It was not surprising that the gravel layers all behaved in this manner, since the drainage system was designed to maintain a low volumetric moisture content in the gravel. Low volumetric moisture content in the gravel did not imply that moisture moved through it, only that moisture did accumulate in this layer. Pressure head in the gravel fluctuated widely, but never dropped below the level required for water to fill the pores.

The upper layer in each cover exhibited a pronounced response to the May 16 rainfall. For several days preceding the rainfall, each had a constant or slightly decreasing volumetric moisture content. Each peaked in volumetric moisture content on May 18 before decreasing during the following days. The three covers containing loess as an upper fine-grained material, exhibited

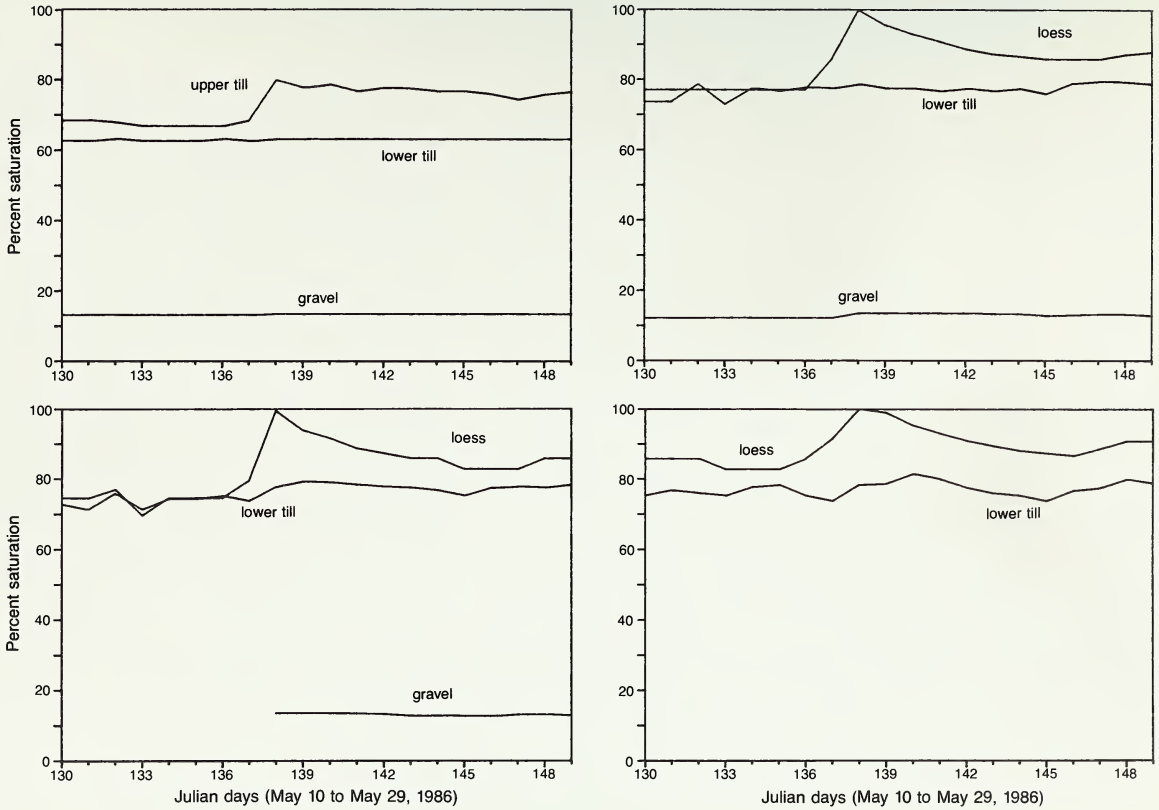

Figure 83 Average daily values of moisture content, plotted as percent saturation, for the period May 10 through May 29, 1986, are shown for each of the four experimental covers. Infiltration can be seen following an intense rainstorm which occurred on day 136. Measurements are shown from one representative instrument in each layer.

sharp peaks, reaching saturation on May 18, then decreasing rapidly in volumetric moisture content to approximately 80 to 85 percent saturation by May 27. Cover 1, which contained till as an upper fine-grained material exhibited a slightly different pattern. It also reached peak volumetric moisture content on May 18, but the peak was only at approximately 80 percent saturation and the volumetric moisture content within the layer decreased very slowly in the next few days to approximately 75 percent saturation on May 27.

None of the underlying fine-grained till layers showed any significant response to the May 16 infiltration event. Slight increases could be observed in covers 3 and 4, peaking at 2 to 3 percent saturation greater than background levels. The volumetric moisture content in the underlying layer of cover 2 increased only 1 or 2 percent, and no increase was observed in cover 1. This suggested that the amount of moisture eventually penetrating the entire cover system as a result of this large infiltration event was very small.

Progress of the moisture front through the upper layers is shown in greater detail in figure 84, which includes data from all functioning tensiometers in those layers. Only two instruments in cover 1 were recording during the entire sequence, and they were only separated in depth by 12 cm. Prior to the May 16 event, the shallowest instrument was indicating drier conditions. The instruments were too close together to resolve the passage of the moisture front through them. Instead we detected a slight response of both on May 17 (day 137) and a coincident peak on May 18. Drying was nearly the same for both, although the deeper instrument exhibited less uniformity. A shallower instrument began to function late in the sequence (May 22) indicating higher volumetric moisture content at that level of the cover. The continual downward flux implied by this relationship may be part of the reason that the entire layer did not dry very rapidly, or the conductivity was so low that the moisture drained very slowly.

A definite downward progression of the moisture front could be resolved in both covers 2 and 3. Response at the shallowest levels was apparent already on May 16, but delayed until May 17 at intermediate depths and until May 18 at the deepest recorded depth (cover 3). In general, the decrease in volumetric moisture content in covers 2 and 3, proceeded from the surface downward.

The response of cover 4 was similar in many respects to covers 2 and 3. The shallowest recording instrument in cover 4 indicated saturated or nearly saturated conditions throughout this sequence. More likely this instrument was not functioning. The deepest instrument responded to the infiltration event much as instruments at comparable depths in covers 2 and 3. However, it indicated a slight increase in moisture at the 91 cm depth on May 16, a day earlier than instruments at similar depths in the other covers. The decline in volumetric moisture content was also slightly slower than in covers 2 and 3.

Comparison These two examples illustrate the response of the prototype covers to two distinctly different infiltration events. The May event is an example of response to a typical, high intensity, isolated rainfall. All four covers responded satisfactorily to this type of event: little, if any, moisture was allowed to penetrate through the lower layers of the systems. Although the finer grained till in the upper layer of cover 1 did not increase as much in volumetric moisture content as the coarser grained loess in the other three covers, the elevated level of volumetric moisture content was maintained longer in cover 1 than in the other covers. This suggests the possibility that cover 1 may be more susceptible to influx from subsequent infiltration events.

The November-December record illustrates response to more long-term infiltration. This type of infiltration is more stressful because the systems are not allowed time to recover from individual events. Differences in performance of the four systems are more apparent than the response to a single event. Cover 1, containing the finer grained till material in both the upper and lower layers, exhibited superior performance. Volumetric moisture content in both of its fine-grained layers was maintained at approximately 80 percent saturation, the peak value in the May response to single infiltration events. Moisture influx during this period was sufficient to maintain saturation in the upper layers consisting of loess. This apparently produced more severe stress in the lower layers of those systems. The two covers containing intermediate gravel layers performed better than cover 4, which had no gravel layer to provide drainage of excess moisture. The underlying till layer in cover 4 also became saturated and remained in that condition for a considerable time. Although saturated conditions were indicated in the upper layers of both covers 2 and 3, the underlying till layers of cover 3 never approached saturation. We suggest that the greater thickness of cover 3 offered greater storage capacity, allowing less cumulative moisture penetration into the gravel. Therefore, less moisture was available to enter the underlying till.

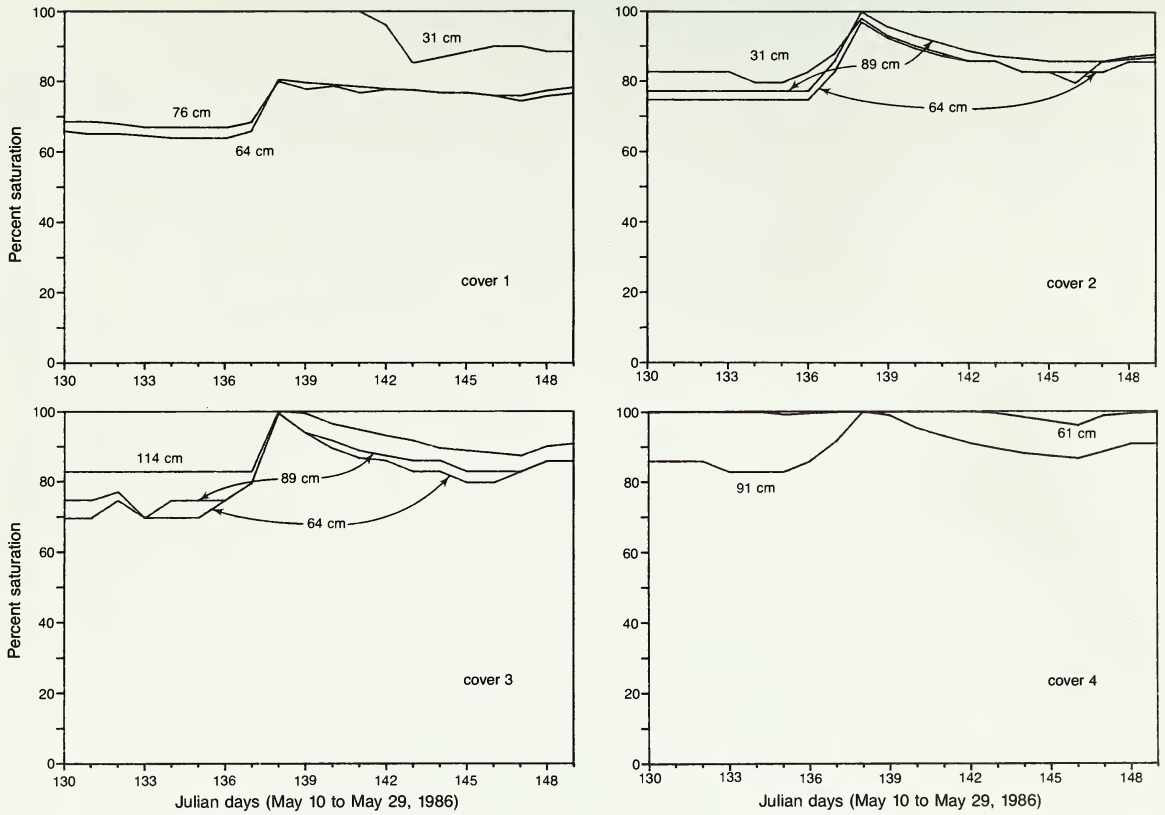

Figure 84 Average daily values of moisture content, plotted as percent saturation, for the period May 10 through May 29, 1986 are shown for each of the four experimental covers. All measurements are from instruments in the upper layers and show infiltration following a rainstorm on day 136.

- **Soil Temperatures**

Soil temperatures (fig. 85) were monitored for two purposes: to investigate frost penetration into the covers, and to determine if moisture fronts moving through the covers could be detected by a temperature signature. Neither of these objectives has been perfectly met by the present study; however, the information obtained provides preliminary results. In order to investigate frost penetration, average daily temperatures were examined for six days during winter 1986. (These are the same six winter days discussed in the previous section on soil tensions.) The temperature effects of a moisture front will be illustrated using the same May storm examined previously.

Winter, 1986 Thermister nests were emplaced along the medial line of each cover immediately north of the tensiometer nests. This region of the cover was less likely to be affected by frost than the edges. Therefore, our winter measurements were probably maximum values for the covers as a whole, indicating maximum frost penetration. Figure 85 depicts the average daily temperatures for six days during winter 1986 at several depths in each cover. Only cover 3 registered below-freezing average daily temperature and that was by only the shallowest instrument on one day. A cold period in February depressed the temperature at all levels on each cover. Although there were no below-freezing, average daily temperatures on February 10, some instruments did record subfreezing temperatures during parts of this day.

The winter temperatures within the loess layers were very similar from cover to cover. Temperatures within the gravel layers were slightly elevated (especially in cover 3) with respect to temperatures at a similar depth within the loess of cover 4. Temperature profiles within the till layer of cover 1 differed somewhat from those in the loess layers. In general, they exhibited steeper gradients and a wider range of temperatures at any particular depth.

In summary, our data indicate that frost penetration into these prototype covers was minimal. No frost was detected from average daily temperatures below a depth of 15 cm. However, these data are by no means conclusive: we considered only a small sample of winter days; our measurements were taken along the median of the covers; and the winter of 1986 was relatively mild.

May, 1986 The primary mechanism of heat flow in soils is conduction. Changes in subsurface temperatures should grossly reflect variations in air temperature. Due to its relatively high specific heat, however, moving water will also transport heat through soil by means of convection. If this were to result in a detectable change in temperature, then moisture movement within the covers could be qualitatively monitored by thermisters. To investigate this phenomenon, we chose to study the effects of the spring rainstorm that occurred on day 136. Moisture movement resulting from this event is depicted in figures 83 and 84. As discussed in the previous section, the moisture front moved through each cover within two days.

Average daily temperatures for the period of May 10 through May 29 (days 130 to 149) at various depths in each cover are shown in figure 86. Superimposed on the soil temperatures is the average daily air temperature as recorded at 1 m height over cover 3.

All the instruments showed a gradual increase in temperature through this period with the deeper instruments recording lower temperatures with less fluctuation than the shallower instruments. (The large apparent fluctuations recorded by the instrument at the 130-cm depth in cover 2 are spurious.) These general trends are expected during mid-spring at this latitude. A major decrease in air temperature occurred from day 136 through day 143 with the passage of the weather system that brought the rain on day 136. Resulting depression of the shallow soil temperature was easily detectable in each of the covers down to at least 76 cm. This could be attributed to thermal conduction and not to moisture movement. A small, but significant temperature increase was recorded on day 138 in each of the instruments at 60 cm depth and below. The increase was recorded by instruments in each of the materials—loess, till, and gravel. We believe that this temperature increase resulted from moisture movement, which also peaked on day 138 (fig. 83). The coincidence of the temperature change and the moisture movement is striking. However, we cannot unequivocally conclude that the temperature change was caused by convective transport of heat without more detailed analysis of the data. In any case, the temperature signature of the moisture movement was too small to be readily detected at shallow depths.

In summary, initial analysis of this data suggests that moisture movement following a high-intensity rainfall can be detected by soil thermometry. The effect was small (approximately 1.0°C) in comparison to shallow conductive effects and was not easily detectable above the 50-cm depth.

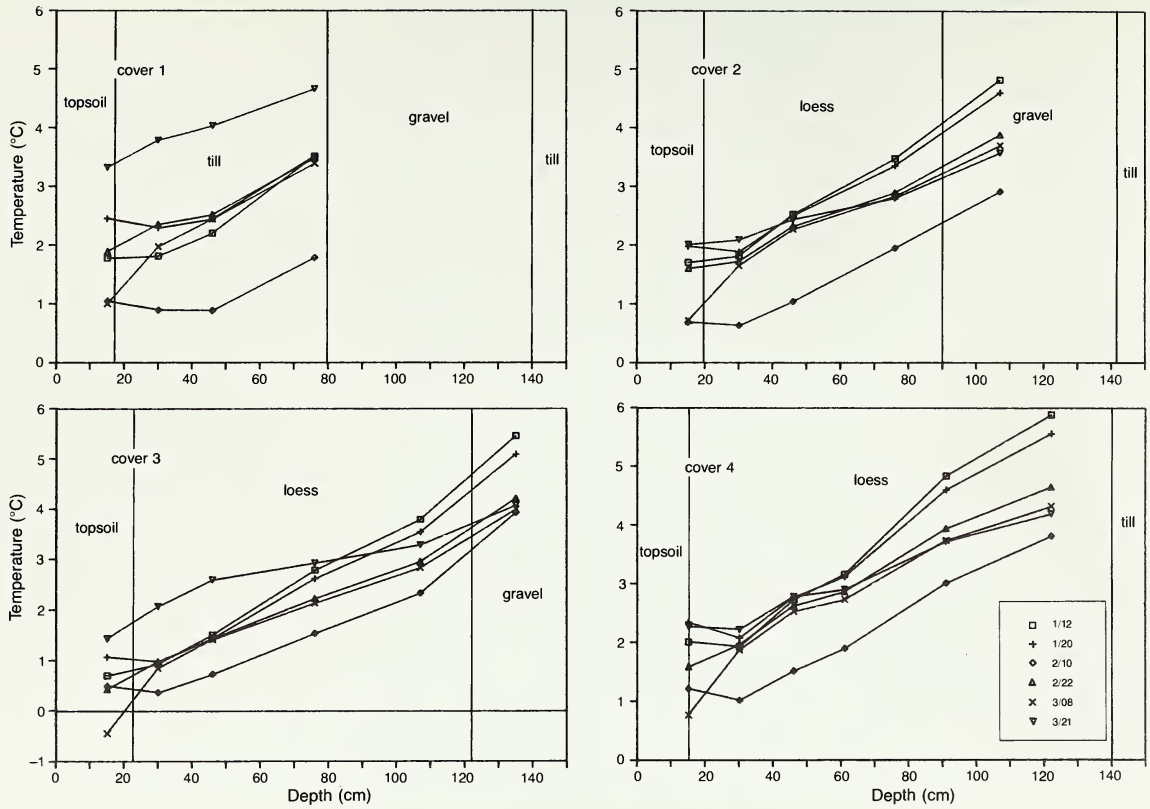

Figure 85 Average daily soil temperatures are plotted for six days during winter 1986 for each of the four experimental covers.

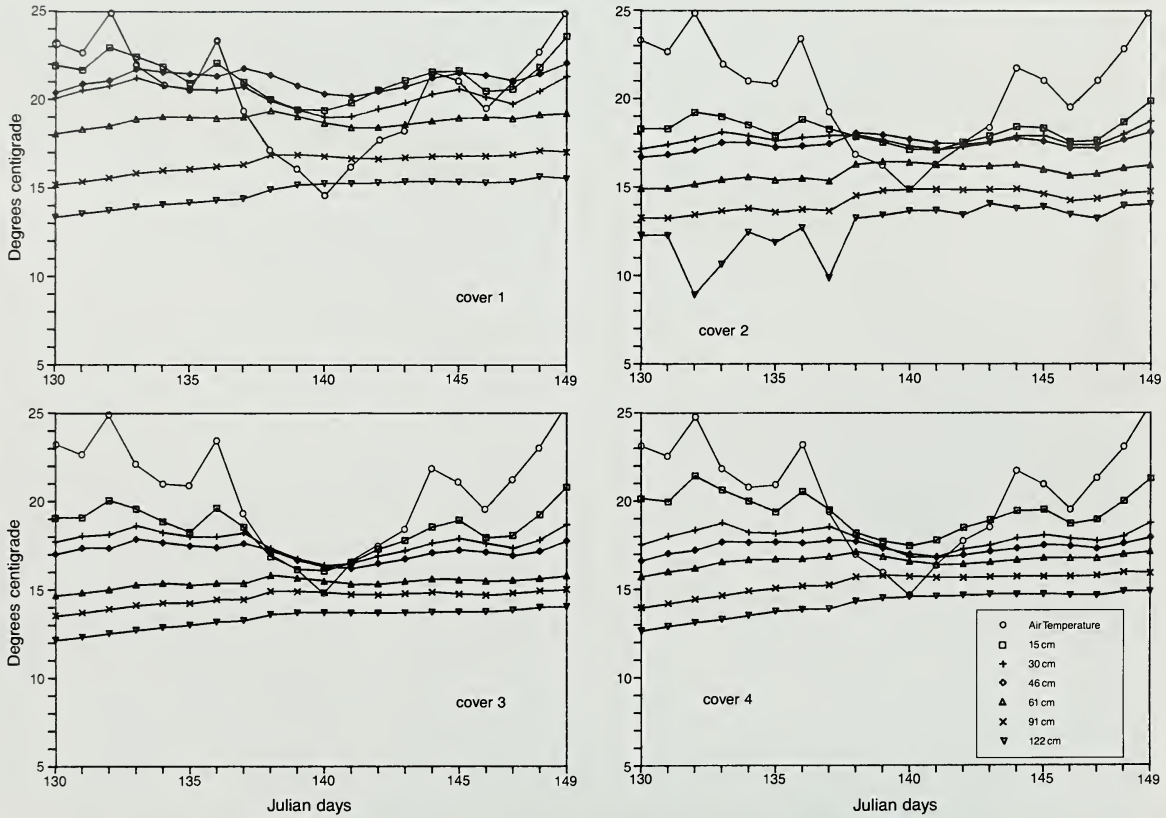

Figure 86 Average daily soil temperatures at various depths within the four experimental covers and average daily air temperature are plotted for the period May 10 through May 29, 1986. A rainstorm, associated with a cold front, passed through this area on day 136.

CONCLUSIONS

Layered covers are superior to thick, nonlayered, fine-grained covers for retarding the downward movement of moisture through waste-disposal trenches. The four prototype covers constructed as part of this study have been in place about 4.5 years. Volumetric and gravimetric moisture content, soil tension, and temperature have been monitored during much of the period. Monitoring techniques have been upgraded, automated, and "winterized" in the process. The best reference data were obtained in the 1985-86 season from automated instruments.

The relative overall performance of the experimental prototype covers is shown in table 15. The difference in performance between covers 2 and 3 was slight, each performing better at different times. This performance ranking is based solely on the ability of the covers to retard moisture movement. Performance of real trench covers was also affected by other factors, including the operational integrity of cover layers. Our experimental design did not allow us to test this important factor; we assumed that integrity would be maintained. Loss of integrity, such as sagging caused by consolidation of underlying waste, would probably have a greater detrimental effect on a layered cover than a nonlayered cover. It is our opinion, however, that as long as the gravel layer is capable of some drainage, the layered cover should still out-perform the nonlayered cover.

The covers with a coarse-grained intermediate layer between two fine-grained layers had two distinct advantages. First, this layering sequence results in the development of a wick effect so that moisture was retained in the upper fine-grained layer, making it more available for evapotranspiration. We found the wick effect difficult to quantify; however, our data suggest that the effect occurred on several occasions (figs. 81 and 83). The second advantage was that moisture penetrating into the coarse-grained layer could be removed from the system by drains placed at the base of the coarse-grained layer. The drain tiles placed in covers 1, 2, and 3 appeared to have been very effective; the volumetric moisture content within the gravel remained very low, rising to 15 percent of saturation only when moisture fronts reached the lower till layer.

One measure of overall performance is the rate of moisture movement into the lower layer. Using data from the November-December wet period, we calculated the rate of moisture movement into the lower layer of cover 1 at 0.0066 cm per day or 2.4 cm per year. The actual yearly rate of moisture movement was probably much less since recharge only occurs for relatively short periods of the year. In this region, our experience suggests that natural recharge occurs between 60 and 90 days per year. The wick effect should reduce this still further to an estimated 45 days of recharge per year. Thus, cover 1 would allow approximately 0.3 cm of moisture movement per year, or is approximately 4 percent of the regional recharge rate of 7.6 cm per year.

Relative cover performance can be estimated by making similar calculations for the other three covers and comparing the results to cover 1. If we use the value of 0.3 cm of moisture movement per year as normal, then the relative performances are 1:14:7:25 for covers 1, 2, 3, and 4, respectively. These figures suggest that the infiltration through covers with a layer of coarse-grained materials between layers of fine-grained materials ranged from less than one-tenth to one-half of the infiltration through covers without the coarse-grained intermediate layer—a significant reduction.

Table 15. Performance ranking of experimental trench covers

Rank	Cover	Upper layer	Intermediate layer	Base layer
First	1	till-65 cm	gravel-65 cm	till-65 cm
Second	3	loess-100 cm	gravel-32 cm	till-65 cm
Third	2	loess-65 cm	gravel-65 cm	till-65 cm
Fourth	4	loess-135 cm	—	till-65 cm

REFERENCES

Abeele, W. V., G. L. DePoorter, and J. W. Nyhan, 1983, Shallow land burial technology — Arid: Proceedings of the Fifth Annual DOE LLWMP Participants' Information Meeting, August, 1983, Denver, CO, Oak Ridge National Laboratory, Oak Ridge, TN.

Alway, F. J., and G. R. McDole, 1917, Relation of water-retaining capacity of a soil to its hydroscopic coefficient: Journal of Agriculture Research, v. 9, p. 27-71.

Arora, H. S., 1980, Infiltration control for low-level radioactive solid wastes disposal areas: An assessment: Oak Ridge National Laboratory, ORNL/TM-6473, Oak Ridge, TN, 66 p.

Arora, H. S., D. D. Huff, D. S. Ward, and O. M. Sealand, 1981. An assessment of the effect of a bentonite seal on groundwater storage in underlying waste disposal trenches at Oak Ridge National Laboratory: Oak Ridge National Laboratory, Environmental Sciences Division, Publication No. 1560, ORNL/TM-7416, Oak Ridge, TN, 41 p.

Barraclough, J. T., J. B. Robertson, and V. J. Janzer, 1979, Geohydrologic study of a burial site for solid radioactive wastes at the Idaho National Engineering Laboratory, *in* M. W. Carter, A. A. Maghissi, and B. Kahn (eds.) Management of Low-Level Radioactive Waste, v. 2, Pergamon Press, p. 795-822.

Battelle Pacific Northwest Labs, 1976, Alternatives for managing wastes from reactors and post-fission operations in the LWR fuel cycle. Volume 4—Alternative for waste isolation and disposal: ERDA-76-43, 199 p.

Bell, J., 1980, Evaluation of test methods and use criteria for geotechnical fabrics in highway application: Interim report. Federal Highway Administration, Washington, DC.

Brunner, D. R., and D. J. Keller, 1972, Sanitary landfill design and operation: U.S. Environmental Protection Agency, Report SW-65ts, Washington, DC, 59 p.

Cherry, J. A., R.W. Gillham, G. E. Grisak, and D. L. Lush, 1979, A concept for long-term isolation of solid radioactive waste in fine-grained deposits, *in* M. W. Carter, A. A. Maghissi, and B. Kahn (eds.) Management of Low-Level Radioactive Waste, v. 2, Pergamon Press, p. 1021-1039.

Cherry, J. A., G. E., Grisak, and W. E. Clister, 1973, Hydrogeologic studies at a subsurface radioactive-waste-management site in west-central Canada, *in* Underground Waste Management and Artificial Recharge, v. 1, International Association of Petroleum Geologists, p. 436-467.

Collins, T. G., and D. D. Newkirk, 1982, The use of geotextile fabrics in pond construction beneath an impermeable membrane (geomembrane): Second International Conference on Geotextiles, Las Vegas, NV, August 1-6, 1982.

Corey, J. C., and J. H. Horton, 1969, Influence of gravel layers on soil moisture content and flow: E. I. DuPont de Nemours & Co., Savannah River Laboratory, DP-1160, Savannah, GA, 23 p.

Das, D. K., and C. Dakshinamurti, 1975, Bentonite as a soil conditioner, *in* Soil Conditioners: Soil Science Society of America, Special Publication No. 7, p. 65-76.

Davis, L. A., and S. P. Neuman, 1983, Documentation and user's guide: UNSAT2-variably saturated flow model (including 4 example problems): U.S. Nuclear Regulatory Commission, NUREG/CR-3390, Washington, D.C., 206 p.

Dragonette, K., J. Blackburn, and K. Cartwright, 1979, Interagency task force report on the proposed decommissioning of the Sheffield nuclear waste disposal site: Illinois State Geological Survey, Open-File Report, 121 p.

Duguid, J. O., 1976, Annual progress report of burial ground studies at Oak Ridge National Laboratory: Period ending September 30, 1975: Oak Ridge National Laboratory, 62 p.

Eagleman, J. R., and V. C. Jamison, 1962, Soil layering and compaction effects on unsaturated moisture movement: Soil Science Society of America Proceedings, v. 26, p. 519-522.

Elzeftawy, A. and B. J. Dempsey, 1976, Unsaturated transient and steady-state flow of moisture in subgrade soil, in Transportation Research Record, No. 612, p. 56-61.

Farb, D. G., 1978, Upgrading hazardous waste disposal sites: Remedial approaches: U.S. Environmental Protection Agency, Report EPA/500/SW-667, Cincinnati, OH, 40 p.

Feddes, R. A., S. P. Neuman, and E. Bresler, 1975, Finite element analysis of two-dimensional flow in soils considering water uptake by roots: II. Field applications: Soil Science Society of America Proceedings, v. 39, p. 231-237.

Fenn, D., K. J. Hanley, and T. V. DeGeare, 1975, Use of the water balance method for predicting leachate generation from solid waste disposal sites: U.S. Environmental Protection Agency, Report SW-l68, Cincinnati, OH, 40 p.

Ferraz, E. S. B., and R. S. Mansell, 1979, Determining water content and bulk density of soil by gamma ray attenuation methods. University of Florida, Gainesville, Agricultural Experiment Station, Bulletin 807 (Technical), 51 p.

Frind, E. O., W. Gillham, and J. P. Pickens, 1977, Application of unsaturated flow properties in the design of geologic environments for radioactive waste storage facilities, *in* W. G. Gray, G. F. Pinder, and C. A. Brebbia (eds.), Finite Elements in Water Resources: Pentech Press Ltd., Plymouth, England, p. 3.133-3.163.

Fowler, Jack, 1982, Personal communication.

Fritton, D. D., 1969, Resolving time, mass absorption coefficient and water content with gamma-ray attenuation: Soil Science Society of America Proceedings, v. 33, p. 651-655.
Green, R. E., and J. C. Corey, 1971, Calculation of hydraulic conductivity: a further evaluation of some predictive methods: Soil Science Society of America Proceedings, v. 35, p. 3-8.
Hanks, R. J., and S. A. Bowers, 1962, Numerical solution of the moisture flow equation for infiltration into layered soils: Soil Science Society of America Proceedings, v. 26, p. 530-534.
Hawkins, R. H., and J. H. Horton, 1967, Bentonite as a protective cover for buried radioactive waste: Health Physics, v. 13, p. 287-292.
Herzog, B. L., K. Cartwright, T. M. Johnson, and H.J.H. Harris, 1982. A study of trench covers to minimize infiltration at waste disposal sites: Review of present practices and annotated bibliography: U.S. Nuclear Regulatory Commission, NUREG/CR-2478, v. 1, 245 p.
Hill, D. E., and J.-Y. Parlange, 1972, Wetting front instability in layered soils: Soil Science Society of America Proceedings, v. 36, p. 697-702.
Hillel, D., and H. Talpaz, 1977, Simulation of soil water dynamics in layered soils: Soil Science, v. 234, no. 1, p. 54-62.
Hittman Nuclear Development Corporation (HNDC), 1983, Decommissioning plan for the Maxey Flats disposal sites: Prepared for Department of Environmental Protection, Kentucky Natural Resources and Environmental Protection Cabinet, Frankfort, KY: Hittman Nuclear and Development Corporation, Columbia, MD.
Johnson, T. M., T. H. Larson, B. L. Herzog, K. Cartwright, C. J. Stohr, and S. J. Klein, 1983, A study of trench covers to minimize infiltration at waste disposal sites: Laboratory evaluation and computer modeling of trench cover design: U.S. Nuclear Regulatory Commission, NUREG/CR-2478, v. 2, 94 p.
Kelleher, W. J., 1979, Water problems at the West Valley burial site, *in* M. W. Carter, A. A. Moghissi, and B. Kahn (eds.), Management of Low-Level Radioactive Waste, v. 2: Pergamon Press, NY, p. 843-850.
King, L. B., 1965, Description of soil characteristics for partially saturated flow: Soil Science Society of America Journal, v. 29, p. 359-362.
Klein, S., T. M. Johnson, and K. Cartwright, 1982, Soil-moisture characteristics and hydraulic conductivity of compacted fine-grained soils for use in covers at waste disposal sites: Transactions American Geophysical Union, EOS, v. 63, no. 19, p. 328.
Klute, A., and D. F. Heermann, 1978, Water movement in uranium mill tailings profiles: U.S. Environmental Protection Agency, Office of Radiation Programs, Technical Note ORP/LV-78-8, Las Vegas, NV.
Lappala, E. G., 1980, Modeling of water and solute transport under variably saturated conditions: State of the art, *in* Modeling and Low-Level Waste Management: An Interagency Workshop, Denver, CO: Oak Ridge National Lab., Oak Ridge, TN, 57 p.
Launtz, B. W., 1982, Intra-Company Memo to D. D. Newkirk, Subject: Geotextile Protection of Plastic Pad LMembrane During Aggregate Compression Loading, February 25, 1982: Crown-Zellerbach, Inc.
Lindsay, L. E., R. W. Gillham, and E. D. Frind, 1979, Studies of the wick effect as a means of waste isolation in the unsaturated zone: Transactions of the American Geophysical Union, EOS, v. 60, no. 18, p. 258.
Lutton, R. J., G. L. Regan, and L. W. Jones, 1979, Design and construction of covers for solid waste landfills: U.S. Environmental Protection Agency, Report EPA-600/2-79-165. Cincinnati, OH, 249 p.
Matuszek, J. M., L. Husain, A. H. Lu, J. F. Davis, R. H. Fakundiny, and J. W. Pferd, 1979, Application of radionuclide pathways studies to short- and long-term management insights for shallow, low-level radioactive waste burial facilities, *in* Management of Low-Level Radioactive Waste, v. 2, Pergamon Press, p. 901-914.
Meyer, G. Lewis and Michael O'Connell, 1973, Potential impact of commercial low-level radioactive-waste disposal practices on hydrogeologic environment, *in* Underground Waste Management and Artificial Recharge, v. 2, International Association of Petroleum Geology, p. 795.
Moore, R. E., 1939, Water conduction from shallow water tables: Hilgardia, v. 12, no. 6, p. 383-426.
Mualem, Y., 1976, A new model for predicting the hydraulic conductivity of unsaturated porous media: Water Resources Research, v. 12, p. 513-522.
Murphy, E. S., and G. M. Holter, 1980, Technology, safety and costs of decommissioning a reference, low-level waste burial ground: v. 1 and 2, U.S. Nuclear Regulatory Commission, NUREG/CR-0570; Batelle-Pacific Northwest Laboratory, 619 p.
National Research Council, Panel on Land Burial, 1976, The shallow land burial of low-level radioactively contaminated solid waste: National Academy of Sciences, 150 p.
Nelson, D. L., K. Cartwright, and R. A. Griffin, 1980, A landfill design for a sensitive environment, *in* The Proceedings of the Third Madison Conference of Applied Research and Practice on Municipal and Industrial Waste: Madison, WI, p. 286-301.
Neuman, S. P., 1973, Saturated-unsaturated seepage by finite elements: Journal of Hydraulics Division of the American Society of Civil Engineers, v. 99, no. 12, p. 2233-2250.
Neuman, S. P., R. A. Feddes, and E. Bresler, 1975, Finite element analysis of two-dimensional flow in soils considering water uptake by roots: I. Theory: Soil Science Society of America Proceedings, v. 39, p. 244-230.

Green, R. E., and J. C. Corey, 1971, Calculation of hydraulic conductivity: a further evaluation of some predictive methods: Soil Science Society of America Proceedings, v. 35, p. 3-8.
Hanks, R. J., and S. A. Bowers, 1962, Numerical solution of the moisture flow equation for infiltration into layered soils: Soil Science Society of America Proceedings, v. 26, p. 530-534.
Hawkins, R. H., and J. H. Horton, 1967, Bentonite as a protective cover for buried radioactive waste: Health Physics, v. 13, p. 287-292.
Herzog, B. L., K. Cartwright, T. M. Johnson, and H.J.H. Harris, 1982. A study of trench covers to minimize infiltration at waste disposal sites: Review of present practices and annotated bibliography: U.S. Nuclear Regulatory Commission, NUREG/CR-2478, v. 1, 245 p.
Hill, D. E., and J.-Y. Parlange, 1972, Wetting front instability in layered soils: Soil Science Society of America Proceedings, v. 36, p. 697-702.
Hillel, D., and H. Talpaz, 1977, Simulation of soil water dynamics in layered soils: Soil Science, v. 234, no. 1, p. 54-62.
Hittman Nuclear Development Corporation (HNDC), 1983, Decommissioning plan for the Maxey Flats disposal sites: Prepared for Department of Environmental Protection, Kentucky Natural Resources and Environmental Protection Cabinet, Frankfort, KY: Hittman Nuclear and Development Corporation, Columbia, MD.
Johnson, T. M., T. H. Larson, B. L. Herzog, K. Cartwright, C. J. Stohr, and S. J. Klein, 1983, A study of trench covers to minimize infiltration at waste disposal sites: Laboratory evaluation and computer modeling of trench cover design: U.S. Nuclear Regulatory Commission, NUREG/CR-2478, v. 2, 94 p.
Kelleher, W. J., 1979, Water problems at the West Valley burial site, *in* M. W. Carter, A. A. Moghissi, and B. Kahn (eds.), Management of Low-Level Radioactive Waste, v. 2: Pergamon Press, NY, p. 843-850.
King, L. B., 1965, Description of soil characteristics for partially saturated flow: Soil Science Society of America Journal, v. 29, p. 359-362.
Klein, S., T. M. Johnson, and K. Cartwright, 1982, Soil-moisture characteristics and hydraulic conductivity of compacted fine-grained soils for use in covers at waste disposal sites: Transactions American Geophysical Union, EOS, v. 63, no. 19, p. 328.
Klute, A., and D. F. Heermann, 1978, Water movement in uranium mill tailings profiles: U.S. Environmental Protection Agency, Office of Radiation Programs, Technical Note ORP/LV-78-8, Las Vegas, NV.
Lappala, E. G., 1980, Modeling of water and solute transport under variably saturated conditions: State of the art, *in* Modeling and Low-Level Waste Management: An Interagency Workshop, Denver, CO: Oak Ridge National Lab., Oak Ridge, TN, 57 p.
Launtz, B. W., 1982, Intra-Company Memo to D. D. Newkirk, Subject: Geotextile Protection of Plastic Pad LMembrane During Aggregate Compression Loading, February 25, 1982: Crown-Zellerbach, Inc.
Lindsay, L. E., R. W. Gillham, and E. D. Frind, 1979, Studies of the wick effect as a means of waste isolation in the unsaturated zone: Transactions of the American Geophysical Union, EOS, v. 60, no. 18, p. 258.
Lutton, R. J., G. L. Regan, and L. W. Jones, 1979, Design and construction of covers for solid waste landfills: U.S. Environmental Protection Agency, Report EPA-600/2-79-165. Cincinnati, OH, 249 p.
Matuszek, J. M., L. Husain, A. H. Lu, J. F. Davis, R. H. Fakundiny, and J. W. Pferd, 1979, Application of radionuclide pathways studies to short- and long-term management insights for shallow, low-level radioactive waste burial facilities, *in* Management of Low-Level Radioactive Waste, v. 2, Pergamon Press, p. 901-914.
Meyer, G. Lewis and Michael O'Connell, 1973, Potential impact of commercial low-level radioactive-waste disposal practices on hydrogeologic environment, *in* Underground Waste Management and Artificial Recharge, v. 2, International Association of Petroleum Geology, p. 795.
Moore, R. E., 1939, Water conduction from shallow water tables: Hilgardia, v. 12, no. 6, p. 383-426.
Mualem, Y., 1976, A new model for predicting the hydraulic conductivity of unsaturated porous media: Water Resources Research, v. 12, p. 513-522.
Murphy, E. S., and G. M. Holter, 1980, Technology, safety and costs of decommissioning a reference, low-level waste burial ground: v. 1 and 2, U.S. Nuclear Regulatory Commission, NUREG/CR-0570; Batelle-Pacific Northwest Laboratory, 619 p.
National Research Council, Panel on Land Burial, 1976, The shallow land burial of low-level radioactively contaminated solid waste: National Academy of Sciences, 150 p.
Nelson, D. L., K. Cartwright, and R. A. Griffin, 1980, A landfill design for a sensitive environment, *in* The Proceedings of the Third Madison Conference of Applied Research and Practice on Municipal and Industrial Waste: Madison, WI, p. 286-301.
Neuman, S. P., 1973, Saturated-unsaturated seepage by finite elements: Journal of Hydraulics Division of the American Society of Civil Engineers, v. 99, no. 12, p. 2233-2250.
Neuman, S. P., R. A. Feddes, and E. Bresler, 1975, Finite element analysis of two-dimensional flow in soils considering water uptake by roots: I. Theory: Soil Science Society of America Proceedings, v. 39, p. 244-230.
Nowatzki, E. A., and J. G. McGray, 1983, An application of soil arch and soil beam concepts to the construction of shallow land burial trench covers, *in* Proceedings of Symposium on Low-Level Waste Disposal:

Facility Design, Construction and Operating Practices: U.S. Nuclear Regulatory Commission, NUREG/CP-0028, v. 3, Washington, DC, 18 p.
Oakes, T. W., and K. E. Shank, 1979, Review of environmental surveillance data around low-level waste disposal areas at Oak Ridge National Laboratory: Oak Ridge National Laboratory, CONF-790209-5, Oak Ridge, TN, 26 p.
Oster, C. A., 1982, Review of ground-water flow and transport models in the unsaturated zone: U.S. Nuclear Regulatory Commission, NUREG/CR-2917, PNL-4427, Washington, DC.
Parlange, J.-Y., 1972, Theory of water movement in soils: 8. One-dimensional infiltration with constant flux at the surface: Soil Science, v. 114, p. 1-4.
Peck, A. J., 1965, Moisture profile development and air compression during water uptake by bounded porous bodies. 3. Vertical columns: Soil Science, v. 100, p. 44-51.
Philips, J. R., 1969, Theory of infiltration: Advances in Hydroscience, v. 5, p. 215-305.
Philips, J. R., 1975, Stability analysis of infiltration: Soil Science Society of America Proceedings, v. 39, p. 1042-1049.
Prudic, D. E., and A. D. Randall, 1979, Ground-water hydrogeology and sub-surface migration of radioisotopes at low-level solid radioactive waste disposal site, West Valley, New York, *in* Management of Low-Level Radioactive Waste, v. 2, Pergamon Press, p. 853-881.
Raats, P. A. C., 1973, Unstable wetting fronts in uniform and nonuniform soils: Soil Science Society of America Proceedings, v. 37, p. 681-685.
Rancon, D., 1980, Application de la technique des barrieres capillaires aux stockages en tranchees, *in* Underground Disposal of Radioactive Waste, v. 1: International Atomic Energy, Vienna, p. 241-265.
Rojstaczer, S. A., 1981, Moisture movement through layered soils of highly contrasting texture: Master's thesis, Department of Geology, University of Illinois at Urbana-Champaign, 86 p.
Saffman, P. G., and G. I. Taylor, 1958, The penetration of a fluid into a porous medium or Hele-Shaw cell containing a more viscous liquid: Proceedings of Royal Society of London, A245, p. 312-329.
Santo, L. T., and G. Y. Tsuji, 1977, Soil bulk density and water content measurements by gamma-ray attenuation techniques: Hawaii Agricultural Experiment Station, University of Hawaii, Technical Bulletin 98.
SCS Engineers, 1978, Study of engineering and water management practices that will minimize the infiltration of precipitation into trenches containing radioactive waste: U.S. Environmental Protection Agency, Report ORPLV-78-5, Las Vegas, NV, 85 p.
Sherard, J. L., L. P. Dunnigan, R. S. Decker, and E. F. Steele, 1976, Pinhole test for identifying dispersive soils: Journal of Geotechnical Engineering Division, American Society of Civil Engineers, v. 102, p. 69-85.
Stroosnijder, L., H. van Keulan, and G. Vachaud, 1972, Water movement in layered soils. 2. Experimental confirmation of a simulation model: Netherlands Journal of Agricultural Science, v. 20, p. 67-72.
Tabuchi, T., 1961, Infiltration and ensuing percolation in columns of layered glass particles packed in laboratory (in Japanese, with a summary in English): Nogyo dobuku kenkyn, Bessatsu (Trans. Agr. Eng. Soc., Japan) 1, p. 13-19.
Tolman, A. L., A. P. Ballestero, Jr., W. W. Beck, Jr., and G. H. Emrich, 1980, Guidance manual for minimizing pollution from waste disposal sites: U.S. Environmental Protection Agency, Report EPA-600/2-78-142, Cincinnati, OH, 82 p.
Topp, G. C., 1969, Soil-water hysteresis measured in a sandy loam and compared with the hysteretic domain model: Soil Science Society of America Journal, v. 33, p. 646-651.
U.S. Environmental Protection Agency, Office of Solid Waste, 1978, Draft Environmental Impact Statement on the Proposed Guidelines for the Landfill Disposal of Solid Waste: U.S. Environmental Protection Agency, 186 p.
U.S. Government Accounting Office (U.S. GAO), 1976, Improvements needed in the land disposal of radioactive wastes—A problem of centuries: U.S. Government Accounting Office Report RED-76-54, 57 p.
Vachaud, G., M. Vauclin, D. Khanji, and M. Wakil, 1973, Effects of air pressure on water flow in an unsaturated stratified vertical column of sand: Water Resources Research, v. 9, no. 1, p. 160-173.
van Keulen, H., and C.G.E.M. van Beek, 1971, Water movement in layered soils—a simulation model: Netherlands Journal of Agricultural Science, v. 19, p. 138-153.
Volclay Soil Laboratory, 1975, Use of Bentonite as a Soil Sealant for Leachate Control in Sanitary Landfills, 35 p.
Webster, D. A., 1979, Land burial of solid radioactive waste at Oak Ridge National Laboratory, Tennessee: A case history, *in* M. W. Carter, A. A. Moghissi, and B. Kahn (eds.), Management of Low-Level Radioactive Waste, v. 2; Pergamon Press, NY, p. 731-745.
Whisler, F. D., and A. Klute, 1969, Analysis of infiltration into stratified soil columns, *in* P. E. Rijtema and H. Wassink (eds.) Water in the Unsaturated Zone, Proceedings of the Wageningen Symposium: International Association of Scientific Hydrology—UNESCO, v. 1, Ceuterick, Inc. Belgium, p. 451-470.
White, I., P. M. Colombera, and J. R. Philip, 1977, Experimental studies of wetting front instability induced by gradual change in pressure gradient and by heterogeneous porous media: Soil Science Society of America Journal, v. 41, p. 483-489.
Yeh, G. T., and D. S. Ward, 1980, FEMWATER: A finite-element model of water flow through saturated-unsaturated porous media: Oak Ridge National Laboratory, Environmental Sciences Division, Publication No. 1370, Oak Ridge, TN, 153 p.

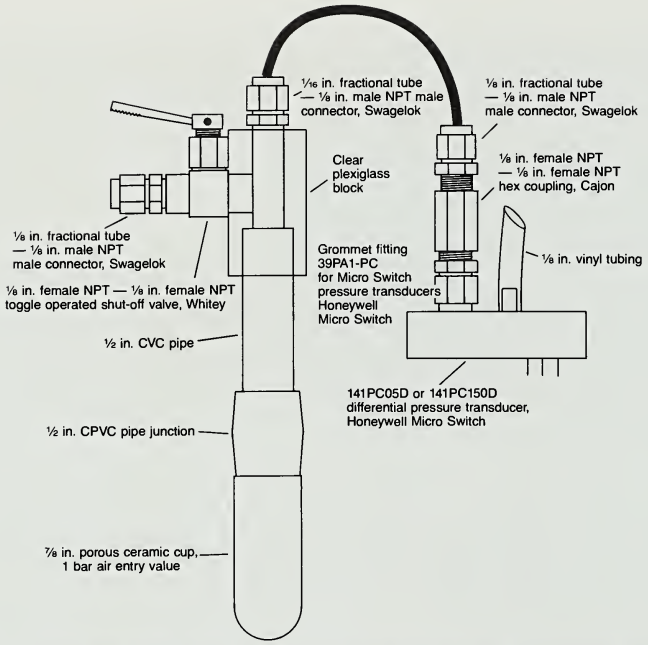

Figure 87 Original tensiometer design using 7/8-inch ceramic cup and rigid 1/2-inch plastic pipe.

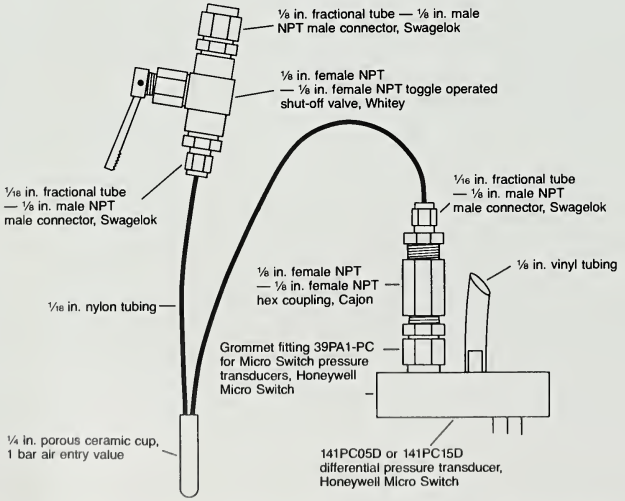

Figure 88 Modified tensiometer design utilizing very small (1/4-inch) ceramic cup and 1/16-inch tubing.

APPENDIX: TENSIOMETRY

At the beginning of this study, no satisfactory electronic tensiometer systems were directly available from manufacturers. We decided to construct our own tensiometers in the laboratory. Most of the components used to construct tensiometers (such as porous ceramic cups, tubing, and epoxy) are inexpensive. Pressure transducers, however, can involve a major expenditure. In some previous studies such as that by Elzeftawy and Dempsey (1976, p. 58) a single relatively expensive pressure transducer was used in conjunction with a rotary switching valve to monitor a number of tensiometers, thus avoiding the expense of a multiple transducer system. We tested a similar system in the laboratory and found it unsatisfactory. We opted for lower cost pressure transducers (Microswitch models 141PC05D and 141PC15D) so that each tensiometer would have its own transducer. These transducers have excellent characteristics such as a short response time, temperature compensation, good linearity, and minimal hysteresis.

Output voltage from these transducers is readily converted to units of pressure as

$$\frac{V_o/V_S - K_o}{K_1} = P$$

where V_o = transducer output voltage,
V_s = supply voltage,
K_o = 0.1250,
K_1 = 0.0417/psi for 15 psi transducers,
K_1 = 0.1250/psi for 5 psi transducers,
or P = negative pressure (suction in psi).

Then if V_s is held constant at 8.0 volts by a voltage regulator, the equation simplifies to

$P = 3\ (V_o - 1)$ for 15 psi transducers
and $P = V_o - 1$ for 5 psi transducers.

Since soil-matric suction is usually desired in units of cm H_2O:

$P_1 = P\ (70.3\ \text{cm}\ H_2O/\text{psi})$
where P_1 = soil-matric suction in cm H_2O measured at the transducer port.

The column of water between the transducer port and the ceramic cup must be removed from the equation. Therefore:

$P_2 = P_1 - (Z_1 - Z_2)$,
where P_2 = soil-matric suction in cm H_2O measured at the cup,
Z_1 = elevation of transducer port in cm above or below some reference datum,
Z_2 = elevation of center of ceramic cup in cm above or below some reference datum.

We experimented with three different tensiometer configurations illustrated in figures 87, 88, and 89. The initial configuration (fig. 87) featured a 7/8-inch-diameter porous cup attached to a 1/2-inch PVC pipe. This was simple to construct and install, but we found that the large volume of water required to fill and flush these instruments was cumbersome to haul into the field. Subsequent configurations have used smaller diameter cups and tubing. Our second style, illustrated in figure 88, was a 1/4-inch-diameter cup attached to two pieces of 1/16-inch tubing. This, we found, was too small. The tubing, especially, is difficult to handle and is easily damaged. Finally, we decided on an intermediate size (fig. 89) using 3/8-inch porous cups and 1/8-inch tubing. We found this configuration to be most satisfactory, although care must be taken during installation to achieve correct placement depth. We were able to manipulate the cups inside the auger hole by including the quick disconnect. The tubing was passed into a piece of 1/2-inch PVC pipe which we used as an insertion probe; the disconnect acted as a stopper at the bottom.

[1]Mention of trade names is for comparison only and does not constitute endorsement by the Illinois State Geological Survey.

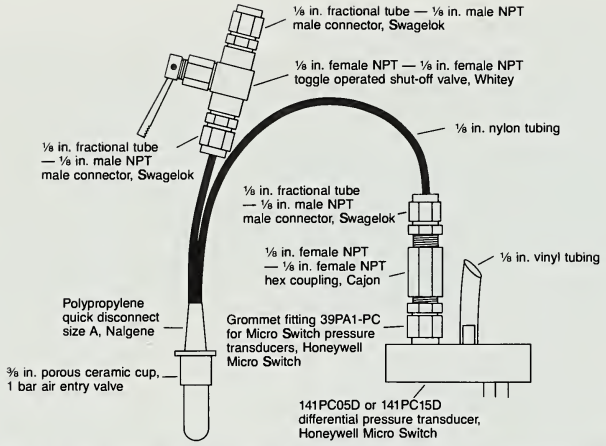

Figure 89 Final tensiometer design features intermediate-sized ceramic cups and nylon tubing.

Tensiometers have been installed using several methods. Generally, a boring was made with a hand auger or soil probe to the desired depth. For the 7/8-inch-diameter tensiometers, a soil probe slightly smaller in diameter than the tensiometer was then pushed somewhat deeper and the tensiometer inserted directly into the smaller hole. This established good contact between the ceramic cup and the surrounding materials. Smaller tensiometers were installed in a slurry of water and soil at the bottom of the hole. The hole was backfilled with compacted materials and a bentonite seal was placed in the annular space near the surface.

Initially, great difficulty was encountered in emplacing tensiometers beneath the gravel layer in covers 1, 2, and 3 due to caving of the gravel into the open hole during the installation process. However, a method was developed to drive a double-wall casing through the gravel into the underlying till. When the inner casing was removed, tensiometers could be installed in the materials at the bottom of the hole inside the outer casing. The outer casing was then withdrawn and the hole is backfilled. Tensiometers were installed through the gravel using this method in each of the covers.

The Campbell Scientific CR7 datalogger monitors and records data from field instruments, including soil-moisture blocks, tensiometers, and thermistors. It also turns on power to these devices at user-set intervals. The thermistors and soil-moisture blocks are switched on momentarily by the 725 excitation card on the CR7 before each hourly reading is taken. The analog ports on the 725 excitation card can each supply a user selectable output of up to 5 volts DC at 25 mA per port, sufficient to power the thermistors and soil-moisture blocks. The transducers connected to tensiometers, however, draw considerable current (approximately 20 mA each), and require an 8-volt optimum voltage source. Therefore, an external 12-volt battery is wired to an 8-volt regulator in order to supply the higher current (and voltage) which the CR7 is unable to provide to the transducers. This 8-volt regulated supply is turned on 1 minute prior to hourly readings through a 12-volt DC relay driver (Campbell Scientific model A21) switched by a digital excitation port on the 725 excitation card. The CR7 datalogger has a built-in rechargable 12-volt battery pack that will power the CR7 for a maximum period of about nine days. Therefore, the 12-volt external marine battery is connected directly to the CR7 as well, thus allowing continual charging of the internal battery pack of the CR7.